Paired NLR receptors: Interplay of RPS4 and RRS1 in *Arabidopsis* immunity

Inaugural-Dissertation

zur
Erlangung des Doktorgrades
der Mathematisch-Naturwissenschaftlichen Fakultät
der Universität zu Köln

vorgelegt von

Anne Coerdt

aus Aachen

Köln, 2015

Die vorliegende Arbeit wurde angefertigt am
Max-Planck-Institut für Pflanzenzüchtungsforschung in Köln
in der Abteilung für Pflanze-Mikroben Interaktionen
(Direktor: Prof. Dr. Schulze-Lefert).

Berichterstatter:	Prof. Dr. Paul Schulze-Lefert
	Prof. Dr. Ulf-Ingo Flügge
	Prof. Dr. Aska Goverse
Prüfungsvorsitz:	Prof. Dr. Ute Höcker

Tag der Disputation: 01. Dezember 2014

Knowledge rests not upon truth alone,
but upon error also.

Carl Jung

Publication

Williams, S.J., Sohn, K.H., Wan, L., Bernoux, M., Sarris, P.F., Segonzac, C., Ve, T., Ma, Y., Saucet, S.B., Ericsson, D.J., Casey, L.W., Lonhienne, T., Winzor, D.J., Zhang, X., Coerdt, A., Parker, J.E., Dodds, P.N., Kobe, B. and Jones, J.D.G. (2014) Structural Basis for Assembly and Function of a Heterodimeric Plant Immune Receptor. *Science*, **344**, 299-303.

Abstract

Plants have evolved intracellular NLR receptors to recognize pathogen effectors and trigger a robust immune response (ETI). The *Arabidopsis NLR* gene pair *RPS4* (*Resistance to Pseudomonas syringae 4*) and *RRS1* (*Resistance to Ralstonia solanacearum 1*) cooperates genetically and physically to recognize, amongst others, the *Pseudomonas syringae* effector AvrRps4. A second *RPS4*/*RRS1-like* gene pair (*RPS4b*/*RRS1b*) contributes to AvrRps4 recognition.

Transient or stable overexpression of *RPS4*, but not *RRS1* induces immunity, and RPS4, but not RRS1 depends on a canonical ATP-binding pocket for its function. Also, RRS1 interacts with both RPS4 and pathogen effectors, suggesting a model where RRS1 as a sensor recognizes effectors and conveys the information to the executor RPS4, releasing it from RRS1 negative regulation to trigger immunity. However, *RRS1* contributes to effector-independent autoimmunity in *RPS4* overexpressing *Arabidopsis*, indicating an additional positive regulatory function apart from the suggested effector sensing.

The work presented here re-evaluates the role of *RRS1* in *RPS4* induced signaling. In the absence of both RRS1a and RRS1b, *RPS4* autoimmunity such as plant stunting and transcriptional reprogramming is decreased. Also, RPS4 protein accumulation is substantially reduced without RRS1, suggesting RRS1 positively contributes to RPS4 induced signaling by stabilizing RPS4 to allow sufficient immune complex formation.

To gain insight into these RPS4-associated immune complexes and to connect RPS4 activation with defense outputs like cell death and transcriptional reprogramming, RPS4 co-purified proteins in pre- and post-activation complexes were analyzed by mass-spectrometry. Identified candidates are involved in processes such as protein synthesis and stability control, redox regulation and secretion. Their potential roles in immunity are discussed in this study.

For several NLR receptors, nuclear localization is necessary for defense activation, and recently direct interactions between NLRs and transcription factors were reported, pointing at a close connection of these NLRs, including RPS4, to the chromatin. RRS1 contains a C-terminal WRKY transcription factor domain, and disruption of its DNA binding causes autoimmunity in the *Arabidopsis slh1* mutant. To unravel the importance and dynamics of RRS1 DNA-association in plant immunity, transgenic *RRS1* lines were

characterized and used for chromatin-immunoprecipitation (ChIP). To allow conclusive evaluation of ChIP results, targeted mutations were inserted into RRS1 to generate loss- or gain-of-function alleles as ChIP controls.

Summarizing published information and data obtained from this work, a new model of RPS4 and RRS1 interaction is discussed where distinct immune complexes are formed in different cellular compartments to mediate cell death in the cytoplasm and transcriptional reprogramming in the nucleus.

Zusammenfassung

Pflanzen besitzen intrazelluläre Rezeptoren, die von Pathogenen injizierte Effektoren wahrnehmen und eine starke Immunreaktion auslösen. Ein gekoppeltes Rezeptorenpaar in *Arabidopsis*, RPS4 (Resistance to *Pseudomonas syringae* 4) und RRS1 (Resistance to *Ralstonia solanacearum* 1), kooperiert genetisch und physisch bei der Abwehr eines bakteriellen Pathogens, *Pseudomonas syringae*, das den Effektor AvrRps4 produziert. Ein zweites, ähnliches Rezeptorenpaar (RPS4b und RRS1b) trägt ebenfalls zur Erkennung von AvrRps4 bei.

Überexpression von *RPS4*, aber nicht *RRS1* induziert pflanzliche Immunreaktionen. Für die Funktion von RPS4, aber nicht RRS1 ist eine intakte ATP-Bindetasche nötig. RRS1 interagiert sowohl mit RPS4, als auch mit Effektoren von Pathogenen. Aus diesen Daten wurde ein Modell entwickelt, bei dem RRS1 als Sensor Effektoren wahrnimmt und diese Information an den Exekutor RPS4 weiterleitet. Dadurch löst sich RPS4 aus der Inhibition durch RRS1 und stimuliert die pflanzliche Abwehr. Darüber hinaus trägt RRS1 auch zur Effektor-unabhängigen Induktion des pflanzlichen Immunsystems durch Überexpression von RPS4 bei. Dies deutet, neben der Funktion als Sensor für Effektoren, auf eine zusätzliche positive Rolle von RRS1 hin.

In der vorliegenden Arbeit wurde der Beitrag von RRS1 zu RPS4-induzierten Immunreaktionen genauer untersucht. Das Fehlen von sowohl *RRS1a*, als auch *RRS1b* verringert die Stärke RPS4-induzierter Autoimmunreaktionen, wie Zwergwuchs und die Expression von Abwehrgenen. Zudem ist ohne RRS1 der Gehalt an RPS4 Protein deutlich reduziert. RRS1 könnte demnach für die Stabilisierung von RPS4 in Immunkomplexen nötig sein.

Um diese Immunkomplexe genauer zu erforschen und die Verbindung zwischen der Aktivierung von RPS4 und der Induktion von Abwehrreaktionen wie Zelltod und veränderter Genexpression herzustellen, wurden RPS4-enthaltende Immunkomplexe vor und nach Aktivierung des Immunsystems aufgereinigt und analysiert. Die dabei detektierten Komponenten, unter anderem aus Proteinsynthese und –stabilitätskontrolle, Redoxregulation und Sekretion, werden in dieser Arbeit vorgestellt und ihre mögliche Funktion im pflanzlichen Immunsystem diskutiert.

Einige intrazelluläre Rezeptoren lösen nur eine effektive Immunreaktion aus, wenn sich zumindest ein Teil ihres zellulären Proteinvorrats im Zellkern befindet. Zudem wurden

für mache Rezeptoren Interaktionen mit Transkriptionsfaktoren gezeigt, was auf eine enge Verbindung dieser Rezeptoren, darunter auch RPS4, mit Chromatin hindeutet. RRS1 beinhaltet eine DNA-bindende WRKY-Domäne, die typischerweise in WRKY Transkriptionsfaktoren vorkommt, und gestörte DNA-Bindung ruft Autoimmunreaktionen in der *Arabidopsis* RRS1-Mutante *slh1* hervor. Um die Relevanz und die Dynamik von RRS1-DNA-Assoziationen in pflanzlichen Abwehrreaktionen besser zu verstehen, wurden RRS1-produzierende transgene Linien charakterisiert und für Chromatin-Immunoprezipitation genutzt. Als Kontrollen für die Spezifität möglicher identifizierter RRS1 Chromatin-Bindestellen wurde *RRS1* gezielt mutiert, um Allele mit erhöhter oder verringerter Aktivität herzustellen.

Zusammenfassend werden publizierte und in dieser Arbeit generierte Daten in ein neues Modell für die Zusammenarbeit von RPS4 und RRS1 integriert, in dem je nach zellulärer Lokalisation verschiedene Immunkomplexe gebildet werden, welche wiederum Zellkompartment-spezifische Immunantworten vermitteln.

Table of Contents

Abbreviations

ANOVA	analysis of variance
ARC	APAF-1, R proteins and CED-4
Avr	avirulence
C-terminal	carboxy-terminal
CC	coiled-coil
CNL	CC-NLR
ETI	effector-triggered immunity
GOF	gain-of-function
HR	hypersensitive response
LOF	loss-of-function
LRR	leucine-rich repeats
MAMP	microbe-associated molecular pattern
N-terminal	amino-terminal
NB	nucleotide binding
NLR	NB-LRR receptor
NLS	nuclear localization signal
p value	probability value
PTI	pattern-triggered immunity
pv.	pathovar
TIR	Toll/Interleukin-1 receptor like
TNL	TIR-NLR
TTSS	type three secretion system
wt	wild-type

Genes

-	fused to (in the context of gene/protein fusion constructs)
35S	*35S* promoter from Cauliflower mosaic virus
opRRS1	native *RRS1* promoter
EDS1	*Enhanced disease susceptibility 1*
NPR1	*Nonexpressor of PR genes1*
PAD4	*Phytoalexin deficient 4*
PEPC	*Phosphoenolpyruvate carboxylase*
PR	*Pathogenesis related*
R	*Resistance*
RPM	*Resistance to P. syringae pv. maculicola*
RPP	*Resistance to Peronospora parasitica*

X

RPS	*Resistance to P. syringae*
RRS1	*Resistance to Ralstonia solanacearum 1*
SAG101	*Senescence associated gene 101*
SNC1	*Suppressor of npr1, constitutive 1*
SRFR1	*Suppressor of rps4-RLD 1*
YFP	*yellow fluorescent protein*

Pathogens

C.	*Colletotrichum*
C.h.	*Colletotrichum higginsianum*
Hpa	*Hyaloperonospora arabidopsidis*
P.	*Pseudomonas*
Pst	*Pseudomonas syringae* pv. *tomato*
R.s.	*Ralstonia solanacearum*

Methods

coIP	co-immunoprecipitation
PAGE	polyacrylamide gel-electrophoresis
PCR	polymerase chain reaction
RT-PCR	reverse transcription-polymerase chain reaction
Y2H	yeast-two-hybrid

Compounds and chemicals

cDNA	complementary DNA
dATP	desoxyadenosinetriphosphate
dH_2O	deionised water
ddH_2O	deionised distilled water
dNTP	desoxynucleosidetriphosphate
DMF	dimethylformamide
DMSO	dimethylsulfoxide
DNA	desoxyribonucleic acid
DNase	desoxyribonuclease
EDTA	ethylenediaminetetraacetic acid
EtOH	ethanol
gDNA	genomic DNA
HRP	horseradish peroxidase
mRNA	messenger RNA
PAA	polyacrylamide
RNA	ribonucleic acid

ROS	reactive oxygen species
SA	salicylic acid
SDS	sodium dodecyl sulphate
T-DNA	transfer DNA
TBS	Tris buffered saline
Tris	Tris-(hydroxymethyl)-aminomethane

Measuring units

°C	degrees Celsius
bp	basepair
cfu	colony forming unit
d	day
dpi	days post infection
FW	fresh weight
g	gram
h	hour
hpi	hours post infection
kb	kilobasepair
kDa	kilodalton
L	liter
M	molar (mol/L)
m	milli
µ	micro
min	minute
mM	millimolar
MW	molecular weight
ng	nanogram
nm	nanometer
OD	optical density
pH	negative decimal logarithm of the H^+ concentration
rpm	rounds per minute
RT	room temperature
sec	second
U	unit
V	Volt
v/v	volume per volume
w/v	weight per volume

1. Introduction

Plants are continuously exposed to a wide range of microbial pathogens such as viruses, bacteria, fungi and oomycetes that can damage plant health and impair quality and amount of yield (Dangl and Jones, 2001; Jones and Dangl, 2006). Even though pathogens attack with a variety of different strategies, sickness is the exception rather than the rule as plants successfully fend off most pathogens by their sophisticated multi-layered innate immunity. In contrast to the mammalian immune system, plant immunity lacks an adaptive branch but relies on two major layers of innate immunity: Pattern-triggered immunity (PTI) is effective against non-adapted pathogens and is induced by pattern-recognition receptors (PRR) on the cell surface upon recognition of conserved microbe-associated molecular patterns (MAMPs) (Jones and Dangl, 2006). To suppress PTI, virulent pathogens deliver many effector proteins into plant cells to interfere with host defense pathways and promote infection (Jones and Dangl, 2006). Certain plant genotypes protect themselves from virulent pathogens by effector recognition through intracellular resistance (R) proteins, thereby converting effector-mediated disease susceptibility to effector-triggered immunity (ETI), a strong defense response leading to plant resistance (Dodds and Rathjen, 2010). While a lot is known about the initiation and the outputs of plant resistance responses, research is just starting to unravel the detailed signaling mechanisms and interconnections between different layers of plant immunity.

1.1. Effector-triggered immunity (ETI)

R proteins are encoded by the most divergent gene family in plants (Meyers et al., 2003; Jacob et al., 2013). Still, most R proteins share a canonical modular domain structure consisting of a central nucleotide binding (NB) and a C-terminal leucine-rich repeat (LRR) domain, and are therefore referred to as NLR proteins. Two main *R* protein classes have been subdivided based broadly on their N-terminal domain of either a coiled coil (CC) or Toll/Interleukin-1 receptor like (TIR) domain into CNLs and TNLs, respectively. In a current model, activation of TNLs and CNLs by direct or indirect effector recognition causes an ATP-dependent conformational change rendering the NLR open for altered or additional interaction (Qi and Innes, 2013). This leads to resistance activation culminating

in defense gene reprogramming and local programmed cell death often referred to as hypersensitive response (HR) (Lamb et al., 1989; Jones and Dangl, 2006; Dodds and Rathjen, 2010).

This study focusses on the *Arabidopsis TNL* gene pair *RPS4* (*Resistance to Pseudomonas syringae 4*) and *RRS1* (*Resistance to Ralstonia solanacearum 1*, see section 1.4), which acts cooperatively to confer resistance to the leaf-infecting bacterium *Pseudomonas syringae* pv. *tomato* DC3000 expressing the effector AvrRps4 (*Pst* AvrRps4), the soil-borne bacterial pathogen *Ralstonia solanacearum* expressing the effector PopP2 (*R.s.* PopP2) and the hemibiotrophic fungus *Colletotrichum higginsianum* (*C.h.*) delivering an unknown effector (Birker et al., 2009; Narusaka et al., 2009a; Narusaka et al., 2009b).

1.2. Structure of TNLs

1.2.1. Toll-/interleukin-1 receptor domain

By analogy with known functions in mammalian innate immunity, the TIR domains of plant NLRs have been implicated in the mediation of downstream signaling responses. Most information available in plants comes from analysis of the flax L6 flax rust resistance protein TIR domain structure. It forms a compact globular structure consisting of a five-stranded parallel β-sheet surrounded by five α-helices (Bernoux et al., 2011). The L6 TIR domain includes an additional α-helix compared to animal TIR domains, the αD3-helix (Bernoux et al., 2011). Moreover, the L6 TIR domain self-associates, and transiently expressed L6 TIR induced cell-death in tobacco, as was shown for other TIR domains (Frost et al., 2004; Michael Weaver et al., 2006; Swiderski et al., 2009; Krasileva et al., 2010; Bao et al., 2014), implicating TIR domains function in immune signaling leading to cell death.

More recently, the crystal structures of the *Arabidopsis* RPS4 and RRS1 TIR domains were solved as homo- and heterodimers, revealing a common interaction interface used for homo- and heterodimerization (Williams et al., 2014). Multiple sequence alignment of 150 plant TIR domains showed the conservation of several amino acid residues also found to be important for RPS4 and RRS1 dimerization events (Williams et al., 2014). The conserved amino acid patch includes an SH- (serine-histidine)-motif in the αA-helix which formes stacking interactions and hydrogen-bonds in the RPS4-RRS1

homo- and heterodimers (Williams et al., 2014). Mutations in the SH-motif disrupted TIR dimerization and abolished RPS4 TIR-induced effector-independent cell death in tobacco as well as effector-triggered cell death by transiently expressed RPS4 with RRS1 full-length proteins (Williams et al., 2014).

1.2.2. Nucleotide-binding domain

Plant NLR receptors belong to the superfamily of STAND (signal transduction ATPases with numerous domains) ATPases. Their nucleotide-binding domain consists of three subdomains: (1) the NB catalytic core forming a classical NTPase fold of a five-stranded parallel β-sheet surrounded by seven α-helices, (2) the four-helix-bundle ARC1 (APAF-1, R proteins and CED-4) functioning as a scaffold for intramolecular interactions with the LRR domain and (3) the ARC2 forming a winged-helix fold, working as a regulatory element interacting with the LRR domain and transducing pathogen perception by ARC2 dislocation and thus subdomain reorganization (Takken et al., 2006; van Ooijen et al., 2008; Lukasik and Takken, 2009; Bonardi et al., 2012; Takken and Goverse, 2012).

The NB-ARC domain is thought to be the molecular switch for NLR activation, with its ADP-bound form being inactive while ATP binding causes a conformational change and thereby activates the NLR. Support for this model came from tomato NLR I2, which was shown to bind and hydrolyse ATP in vitro (Tameling et al., 2002). I2 autoactive alleles are preferentially bound to ATP, while native I2 bound to ADP was more stable than the ATP-bound form and thus likely represents the inactive state of the protein (Tameling et al., 2006). Also, an autoactive mutant of flax rust NLR M co-purified with more ATP than ADP, while the wildtype M mostly bound ADP (Williams et al., 2011). Crystallization of the mouse NLR NLRC4 (NLR family, CARD containing 4) revealed its structure in an ADP-bound, closed conformation and showed that ADP-mediated interactions in the NB-ARC subdomains stabilized the inactive conformation (Hu et al., 2013).

The NB-ARC subdomains contain numerous conserved, well-characterized motifs that are involved in nucleotide binding and NLR activation, some of which are discussed in detail below. In the NB domain, the Walker A (P-loop) motif GxxxxGKS/T includes a conserved, positively charged K (lysine) which binds the β-/γ-phosphate of ADP or ATP, respectively. The adjacent S (serine) or T (threonine) binds a magnesium ion (Mg^{2+}) which is needed as a co-factor for ATP hydrolysis (Takken et al., 2006; van Ooijen et al., 2008; Bonardi et al., 2012; Takken and Goverse, 2012). In the Walker B motif hhhhDD/E, the

invariant D (aspartic acid) is involved in indirect coordination of Mg^{2+}, whereas the second acidic residue D or E (glutamic acid) is the catalytic module for ATP hydrolysis (Takken et al., 2006; Tameling et al., 2006; van Ooijen et al., 2008; Bonardi et al., 2012; Takken and Goverse, 2012). The NB domain RNBS-B (Sensor I) motif hhhhToR is thought to interact via the conserved R (arginine) with the ARC2 MHD motif (see below) to support the closed, ADP-bound NB-ARC conformation. In *Caenorhabditis* CED4 (Cell death protein 4), interaction of the conserved positive R with the negative charge of the ATP γ-phosphate transmits to the other protein parts, causing protein activation (Yan et al., 2005; Takken et al., 2006). Apart from the described motifs in the NB subdomain, the ARC2 contains a highly conserved MHD motif hxhHD. The basic H (histidine) is localized in the ADP-binding pocket and binds and positions the β-phosphate of ADP, stabilizing the compact ADP-bound (closed) conformation of the NB-ARC domain (Takken et al., 2006; van Ooijen et al., 2008; Bonardi et al., 2012).

1.2.3. Leucine-rich repeats (LRRs)

The LRR domain is the most variable part of NLRs, containing many hypervariable amino acids which are under positive selection (Takken and Goverse, 2012). It is highly irregular, being comprised of varying numbers and lengths of repeats, sometimes also including non-canonical LRR motifs. Generally, a plant LRR consists of 24 to 28 residues with a core set of 14 amino acids sharing the consensus sequence LxxLxxLxLxxC/Nxx forming a β-strand, which then forms a horseshoe-like superhelical parallel β-sheet together with the other LRRs which are connected through more variable amino acid sequences (Kobe and Kajava, 2001; Enkhbayar et al., 2004; van Ooijen et al., 2007; Padmanabhan et al., 2009).

LRR domains are considered to carry out a dual function: NLR autoinhibition is mediated by an N-terminal cluster of positively charged residues which cover the signaling competent NB-ARC through electrostatic interactions, which was shown for the potato NLR Rx and is supported by analysis of the mouse NLRC4 crystal structure (Rairdan and Moffett, 2006; Hu et al., 2013; Slootweg et al., 2013; Takken and Goverse, 2012). Pathogen recognition specificity is often determined via the LRR C-terminus which in a folded NLR protein lies in close proximity of the NLR N-terminal domain (i.e. TIR) and is able to sense changes in the environment due to pathogen effector disruptions of host proteins or direct effector binding (Takken and Goverse, 2012). For example, flax L receptors L5 and L6 directly interact with their cognate AvrL5 and AvrL6 effectors, respectively, and the

effector recognition specificity is determined by the L5 and L6 LRR domains (Dodds et al., 2006; Ravensdale et al., 2012). Interestingly, while flax L6 and L11 differ only in the LRR, L6 and L7 differ in their TIR domains only, but yet all show different effector recognition specificities (Ellis et al., 1999), thus supporting a role of both the TIR and LRR domains in effector recognition.

1.3. NLR modes of action

1.3.1. Gene-for-gene hypothesis

Based on studies of the genetic inheritance of resistance and susceptibility in flax interactions with flax rust fungus (*Melampsora lini*), Harold Flor proposed the gene-for-gene hypothesis in which one plant *R* gene is necessary and sufficient to confer resistance to a pathogen carrying one specific avirulence (Avr) gene (Flor, 1971). The gene-for-gene complementary described in this model suggested direct R protein interaction with its respective avirulence protein. However, direct interaction of NLRs with effectors was reported for a few cases only (Jia et al., 2000; Deslandes et al., 2003; Dodds et al., 2006; Krasileva et al., 2010; Kanzaki et al., 2012; Ravensdale et al., 2012). Also, the presence of ~150 *R* genes in *Arabidopsis* (Meyers et al., 2003) would be unlikely to combat the plethora of multiple and rapidly evolving effectors from different pathogens (Deslandes and Rivas, 2012).

1.3.2. Guard hypothesis

The guard hypothesis was developed to explain indirect NLR-mediated effector recognition. In the guard model, an NLR is guarding a plant protein, the guardee. Interference with the guardee structure or function by one or several pathogen effectors is recognized by the NLR, causing its activation and triggering of immunity (van der Hoorn and Kamoun, 2008). Extending this model, a guardee constitutively associated with its NLR guard can function as a bait to draw over effectors and facilitate their recognition by the NLR (Collier and Moffett, 2009). Because effectors are delivered to promote pathogen virulence, their targeting of host proteins implies that the guardee plays a role in plant basal resistance or PTI. This was described for *Arabidopsis* host protein RIN4 (RPM1 interacting protein 4),

a negative regulator of basal immunity (Kim et al., 2005; Liu et al., 2009). RIN4 is guarded by the two CNLs RPM1 (Resistance to *P. syringae* pv. *maculicola* 1) and RPS2 (Resistance to *P. syringae* 2) against interference by *Pseudomonas* effectors AvrRpm1, AvrRpt2 and AvrB, which then triggers ETI (Axtell and Staskawicz, 2003; Mackey et al., 2003; Kim et al., 2005; Liu et al., 2009).

1.3.3. Decoy model

In some cases of ETI, the guardee is not (or no longer) involved in plant immunity. In other words, NLRs can monitor decoy proteins that are not actively involved in defense, but share similarity with active defense components to intercept effector virulence activities (van der Hoorn and Kamoun, 2008). Supporting this model, *Arabidopsis* protein kinase PBS1 (AvrPphB susceptible 1) has no known function in immunity (Zhang et al., 2010a), but is cleaved by the *Pseudomonas* effector AvrPphB, which then activates a PBS1-guarding NLR, RPS5 (Ade et al., 2007). Interestingly, other PBS1-like plant protein kinases are AvrPphB operational targets (Zhang et al., 2010a), among which the kinase BIK1 (*Botrytis*-induced kinase 1) positively regulates PTI (Kadota et al., 2014; Li et al., 2014b). In this model, while the real effector target is involved in host defense (i.e. BIK1) and might change structurally to enhance its resistance function or avoid pathogen interference, the decoy (PBS1) can still intercept effector tampering with the host cell and trigger resistance through its NLR guard.

1.3.4. Paired NLR functions

An emerging plant resistance strategy is the action of paired NLR receptors. The first published example of two *NLR* genes functioning cooperatively in plant resistance to the oomycete *Hyaloperonospora arabidopsidis* was the TNL pair *RPP2A* (Resistance to *Peronospora parasitica* 2A) and *RPP2B*, encoded by closely linked genes orientated in a head-to-tail manner with an intergenic spacer of about 3kb only (Sinapidou et al., 2004). In rice, a number of NLR pairs cooperate genetically to confer resistance to rice blast disease (*Magnaporthe oryzae*) (Ashikawa et al., 2008; Lee et al., 2009; Okuyama et al., 2011; Zhai et al., 2011; Kanzaki et al., 2012; Césari et al., 2014; Zhai et al., 2014). Recently, two studies on paired rice CNLs provided important insights into the molecular functions of paired NLR receptors. For the *NLR* gene pair *Pikh-1* and *Pikh-2*, it was shown that Pikh-1 interacts with both the recognized *M. oryzae* effector AvrPik-h and with Pikh-2 through its

CC domain (Zhai et al., 2014). *Pikh-2* (but not *Pikh-1*) triggered cell death when transiently overexpressed in tobacco independently of both *AvrPik-h* and *Pikh-1*, whereas in native promoter studies in rice protoplasts all three proteins were needed to trigger cell death (Zhai et al., 2014). Similarly, the head-to-head oriented NLR pair *RGA4 (R* gene analog 4) and *RGA5* is required for recognition of Avr-Pia and Avr-PiCO39 rice blast effectors (Okuyama et al., 2011; Cesari et al., 2013). While *RGA4* encodes a classical CNL, the CNL-like *RGA5* N-terminus is dissimilar to other known domains and the protein comprises an additional C-terminal RATX1 (Related to ATX1) domain with significant homology to a heavy-metal-associated domain containing copper chaperone ATX1 (Anti-Oxidant 1) from yeast (Okuyama et al., 2011). RGA5 associated with the effectors Avr-Pia or Avr-PiCO39 via its C-terminal RATX1 domain, with two RGA5 alternate splicing variants showing different affinities to each effector (Cesari et al., 2013). No effector association was detected for RGA4 (Cesari et al., 2013). RGA4 and RGA5 were shown to localize to the cytoplasm and were able to form homomeric and heteromeric complexes (Césari et al., 2014). RGA5 suppressed the effector-independent cell death induced by overexpressed RGA4 in transient tobacco assays, and this RGA5 inhibitory effect was released by co-expression of Avr-Pia (Césari et al., 2014). RGA4 resistance and cell death-triggering activity depended on a functional nucleotide-binding pocket (Césari et al., 2014). Moreover, the usually highly conserved MHD motif is degenerated in RGA4, and this degeneration was necessary for RGA4 cell death inducing activities (Césari et al., 2014). This suggests that RGA4 carries a gain-of-function mutation in its MHD motif, allowing enhanced ATP binding and leading to RGA4 autoactivity in tobacco (Césari et al., 2014). By contrast, RGA5 repressive function on RGA4 activity, as well as the effector-triggered release of this RGA5 repression was independent of a functional nucleotide-binding or MHD motif (Césari et al., 2014). Taken together, these data suggest a new model of paired NLR action (compare Figure 1). An “executor” protein responsible for downstream signaling activation (*here:* RGA4) is held in check by the effector-sensing “sensor” protein (*here:* RGA5). A conformational change upon effector recognition by the sensor releases or activates the executor for defense activation.

The close linkage of functional NLR pairs and a frequent arrangement in head-to-head orientation on the chromosome suggests shared promoter elements and thus tightly linked regulation and well-matched gene expression (Li et al., 2006; Chen et al., 2010; Chen et al., 2014). However, *Pikh-1* and *Pikh-2* transcripts showed distinct expression patterns upon pathogen treatment, because *Pikh-2* transcript levels increased compared to

the mock control whereas *Pikh-1* levels did not (Zhai et al., 2014). The same trend was described for another rice CNL gene pair, *Pi5-1* and *Pi5-2*, where only the former responded to pathogen challenge (Lee et al., 2009). Certainly, regulation of closely linked *R* gene pairs in plants requires more detailed research. If not for equal expression of NLR pairs, the conserved close linkage might protect functionally interdependent *R* genes from recombination or genome re-arrangement events that might cause the loss of one signaling partner, leading to a loss of resistance or autoimmunity impairing plant growth.

1.4. RPS4 and RRS1

1.4.1. Together we stand… a functional TNL receptor pair in *Arabidopsis* immunity

The *Arabidopsis* TNL pair *RRS1* and *RPS4* cooperates genetically to confer resistance to the *Pst* AvrRps4, *R.s.* PopP2 and *C.h.* (Birker et al., 2009; Narusaka et al., 2009a; Narusaka et al., 2009b). This study focusses on the interaction of *Arabidopsis RPS4* and *RRS1* with *Pst* AvrRps4. However, knowledge on PopP2 recognition and functions will be integrated in the evaluation of generated data.

RPS4 was mapped based on *Pst* AvrRps4 resistance and HR induction in a cross of *Arabidopsis* resistant ecotype Ws-0 with the susceptible ecotype RLD, and segregated as a single dominant locus in the F_2 generation (Hinsch and Staskawicz, 1996). *RPS4* encodes a classical TNL protein with TIR, NB-ARC and LRR domains, while a 318 amino acid C-terminal extension shows no homology to other known proteins (Gassmann et al., 1999). *RPS4* alternative splicing variants were induced upon AvrRps4 recognition and required for *RPS4*-mediated resistance to *Pst* AvrRps4, and *RPS4* splicing variants code for potential truncated proteins correspond mainly to the TIR-NB portion of the protein (Gassmann et al., 1999; Zhang and Gassmann, 2003). RPS4 localization is mainly endomembrane-associated in the cytoplasm, but nuclear accumulation of an RPS4 sub-pool driven by a bipartite nuclear localization signal (NLS) in the C-terminal extension was necessary to confer *Pst* AvrRps4 resistance (Wirthmueller et al., 2007).

RRS1 was identified as the recognition determinant for *R.s.* PopP2 in resistance of *Arabidopsis* ecotype Niederzenz (Nd-1) compared to susceptible Columbia (Col-5) (Deslandes et al., 1998). The alleles *RRS-R* (in Nd-1, resistant) or *RRS1-S* (in Col-5, susceptible) were named in accordance with their contrasting responses to *R.s.* PopP2

(Deslandes et al., 2002). Notably, both RRS1-R and RRS1-S interacted directly with PopP2, indicating that effector binding is not sufficient to trigger immunity (Deslandes et al., 2003). The same allele specific resistance described for *R.s.* PopP2, in which only *RRS1-R* confers resistance, holds true for immunity towards *C. higginsianum*, whereas both *RRS1-R* and *RRS1-S* are functional in conferring resistance to *Pst* AvrRps4 (Birker et al., 2009; Narusaka et al., 2009a; Narusaka et al., 2009b). Interestingly, a cross between Nd-1 and Col-5 resulted in a susceptible F_1 generation, and segregation in the F_2 generation was consistent with *RRS1-R* inheritance as a recessive resistance locus (Deslandes et al., 1998). By contrast, transgenic expression of *RRS1-R* in Col-5 established *R.s.* resistance, while resistant Nd-1 expressing transgenic *RRS1-S* retained *R.s.* resistance, supporting a dominant role of *RRS1-R* independent of transgene expression levels (Deslandes et al., 2002).

RRS1 is an atypical TNL protein carrying a C-terminal WRKY domain (Deslandes et al., 2002) which defines a large plant-specific family of WRKY transcription factors. The WRKY domain forms a 4- to 5-stranded antiparallel β-sheet structure and is able to directly bind DNA at a cognate DNA sequence C/TTGACT/C, the W-box (Yamasaki et al., 2012; Yamasaki et al., 2013). WRKY DNA binding is mediated by the highly conserved N-terminal WRKYGQK motif and a C-terminal zinc finger signature (Yamasaki et al., 2012; Yamasaki et al., 2013). Even though *RRS1-R* and *RRS1-S* share 98% nucleotide sequence identity and the WRKY domain is complete in both allelic forms, the difference in pathogen recognition between *RRS1-R* and *RRS1-S* suggests disparate modes of actions (Deslandes et al., 2002). These might be due to distinct properties of the respective C-termini, which differ by a 90 amino acid extension of RRS1-R compared to RRS1-S (Deslandes et al., 2002). An amino acid insertion in the conserved WRKY domain of RRS1-R in the *slh1* (*sensitive to low humidity 1*) mutant disrupted RRS1-R W-box binding in gel filtration assays and caused an *in vivo* autoactive phenotype in *Arabidopsis* Nd-1, which was associated with plant growth inhibition, cell death and necrotic lesion development, accumulation of SA and activation of defense genes (Noutoshi et al., 2005). These data suggest that RRS1-R is bound to the DNA in its resting state and disruption or alteration DNA binding initiates a resistance response. In line with its predicted function at the chromatin, RRS1 contains a predicted NLS (Deslandes et al., 2002) and could be detected upon co-expression with PopP2 both in the cytoplasm and the nucleus (Deslandes et al., 2003).

Like the rice CNL gene pairs described above, RPS4 and RRS1 are tightly linked at the chromosome and arranged in a head-to-head orientation with an intergenic region of only 254bp in Col-0 (Gassmann et al., 1999). Strikingly, their cooperative resistance function is not only achieved in *Arabidopsis* (Birker et al., 2009; Narusaka et al., 2009a; Narusaka et al., 2009b), but also in other plant genera or families. Co-expression of *RPS4* and *RRS1-R* conferred resistance to *R. s.* PopP2 in tomato (*Solanum lycopersicum*) and japanese mustard spinach (*Brassica rapa* var. *perviridis*) or resistance to *C. higginsianum* in japanese mustard spinach and rapeseed (*Brassica napus*) or *C. orbiculare* in cucumber (Narusaka et al., 2013b, a; Narusaka et al., 2014). This indicates a conservation of *RPS4* and *RRS1* downstream signaling mechanisms among the different plant taxonomic groups. Since resistance is achieved only by co-expression of *RPS4* and *RRS1-R*, this supports the idea that genetic NLR linkage is due to functional co-dependency of NLR pairs as introduced above (see section 1.3.4).

Besides their genetic cooperation in resistance, RPS4 and RRS1 TIR domains formed homomeric and heteromeric dimers as recombinant proteins purified from *E. coli* and in yeast-two-hybrid (Y2H) (Williams et al., 2014). Full length RPS4 and RRS1 proteins interacted in tobacco transient expression independently of an intact TIR domain dimerization interface, suggesting the involvement of other domains in the dimerization (Williams et al., 2014). However, disruption of the TIR-TIR dimerization interface abolished RPS4 and RRS1 immune functions. Most notably, overexpression of RPS4 TIR alone in tobacco induced cell death, and this was abolished in the TIR^{H24A} dimerization-disabled mutant. Also, RRS1 TIR suppression RPS4 TIR-induced cell death depended on a genuine heterodimerization interface, as it was lost in the RRS1 TIR^{H26A} heterodimer-disabled mutant. Furthermore, expression of full length *RRS1-R* in *Arabidopsis* Col-0 stable transgenic lines conferred PopP2 recognition and induction of HR, while expression of the TIR-dimerization disabled *RRS1-*$R^{S25A/H26A}$ allele did not (Williams et al., 2014). Based on these data, RRS1 was proposed to negatively regulate RPS4 defense induction by preventing the formation of a signaling-competent RPS4 TIR homodimer. The repression of RPS4 by RRS1 is released upon effector sensing by RRS1 (Figure 1).

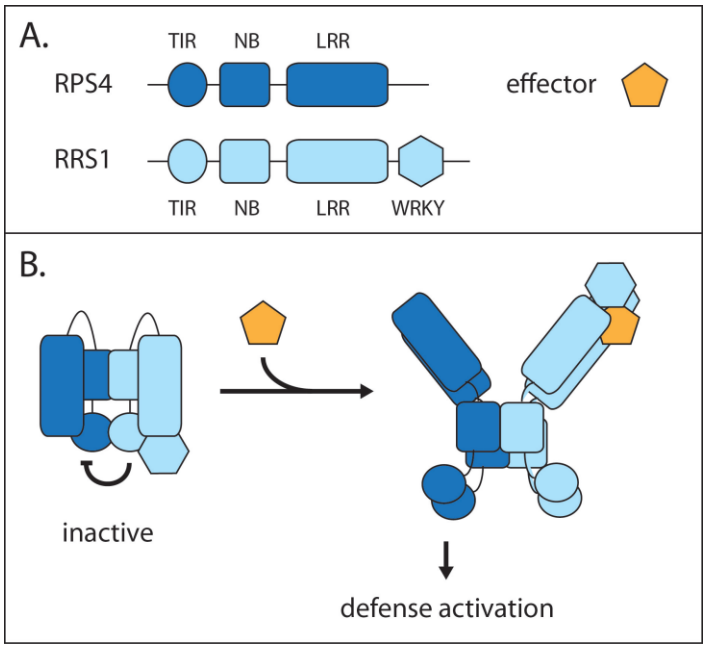

Figure 1: Current model of pairwise NLR activation.

(A) Domain structure of RPS4 and RRS1. TIR, Toll-/interleukin-1 receptor; NB, nucleotide-binding; LRR, leucine-rich repeat; WRKY, transcription factor DNA binding domain. **(B)** In a pre-activation complex, RPS4 activity is repressed by RRS1. Effector recognition of the sensor RRS1 induces conformational changes to allow executor RPS4 homodimerization and downstream signaling activation. Modified from Nishimura and Dangl, 2014.

In accordance with this model, besides RRS1 direct interaction with PopP2 both RRS1-S and RRS1-R were found to co-immunoprecipitate (coIP) with AvrRps4 in tobacco leaf extracts (Williams et al., 2014), supporting the role of RRS1 as a sensor modifying activity of its executor partner RPS4.

However, instead of releasing RRS1 inhibitory effects on RPS4, disruption of the RPS4-RRS1 TIR-TIR interface in RRS1-R$^{S25A/H26A}$ prevented PopP2-induced cell death (Williams et al., 2014). Interestingly, the full length RRS1-R$^{S25A/H26A}$ still associated with RPS4 *in planta* (Williams et al., 2014), thus forming interaction surfaces that potentially enable proper complex formation. While in this complex RRS1$^{S25A/H26A}$-RPS4 TIR-TIR interaction would be disabled, the proposed signaling active RPS4 TIR homodimeric interaction should be retained to initiate defense signaling. The RRS1-R$^{S25A/H26A}$ loss of PopP2-induced cell death therefore indicates that an intact RPS4-RRS1 TIR domain interface is indispensable for their resistance function.

Also, if RRS1 acted only as a negative regulator of RPS4 by inhibiting RPS4 TIR homo-dimerization, a knock-out mutation of *RRS1* would release RPS4 inhibition and lead to an

autoimmune phenotype. This was reported for the rice CNL pair *RGA4* and *RGA5*, in which silencing of *RGA5* in rice protoplasts caused effector-independent *RGA4*-induced cell death (Césari et al., 2014). By contrast, the *rrs1* null mutant impaired defense to the same extent as *rps4* (Birker et al., 2009; Narusaka et al., 2009a), suggesting a positive contribution of RRS1 to RPS4 immunity.

Notably, a K (lysine) to A (alanine) mutation in the conserved RRS1 P-loop motif (K185A) did not alter effector-dependent *RPS4*-*RRS1*-mediated cell death induction in tobacco (Williams et al., 2014). This points towards an RRS1 function independent of ATP binding and/or hydrolysis, usually a crucial step in NLR activity control (Qi and Innes, 2013). The same ATP-independent function holds true for *RGA5* in rice as well (Césari et al., 2014), thus pointing towards a novel mechanism of sensor NLRs acting in cooperation with a paired signaling partner to induce or regulate plant immunity.

1.4.2. One for all, all for one: *Arabidopsis RPS4b* and *RRS1b*

Single or double mutations of *RPS4* and *RRS1* enhanced *Arabidopsis* susceptibility to *Pst* AvrRps4, but retained *RPS4*/*RRS1*-independent resistance (RRIR) (Wirthmueller et al., 2007; Birker et al., 2009). Recently this RRIR was cloned and revealed a second *NLR* gene pair on chromosome 5, which is arranged in a head-to-head orientation with an intergenic spacer of 232bp and contributes to *Pst* AvrRps4 resistance in addition to *RPS4* and *RRS1* (Saucet, 2013). This NLR pair was designated *RPS4b* and *RRS1b* due to its highly similar gene architecture with shared exon/intron and domain structures, and a high amino acid identity of TNL *RPS4b* and TNL-WRKY *RRS1b* to *RPS4* and *RRS1*, respectively (Saucet, 2013). As with RRS1, transiently expressed RRS1b interacted with both AvrRps4 and PopP2 in co-IPs from tobacco (Saucet, 2013). Interestingly, the TIR domains of the four NLRs were able to self- and cross-associate with each other *in planta* (Saucet, 2013), so that in principle the formation of hetero-complexes assembled by combinations of all four NLRs is possible. With the emerging role of NLR pairs in disease resistance, the involvement of a further NLR pair in AvrRps4 recognition and resistance signaling opens up new opportunities to unravel the complexity of NLR receptor interactions and resistance signaling mechanisms.

1.4.3. Know your enemy: the effectors AvrRps4 and PopP2

Many bacterial effectors are delivered directly into the host cell via the bacterial type-III-secretion system (TTSS) (Alfano and Collmer, 2004; Burkinshaw and Strynadka, 2014), where some have been shown to mediate virulence functions by suppressing host immune responses (Guo et al., 2009; Deslandes and Rivas, 2012). AvrRps4 and PopP2 are TTSS-secreted effectors and can be recognized by the plant depending on the presence of the respective *RPS4* and *RRS1* alleles discussed above (see sections 1.4.1, 1.4.2).

R. solanacearum effector PopP2 belongs to the conserved YopJ/AvrRxv effector family (Deslandes et al., 2003; Lewis et al., 2011). PopP2 is targeted to the plant nucleus by an N-terminal NLS, where it interacted with and stabilized both RRS1-S and RRS1-R, likely by inhibiting their proteasome-mediated degradation (Deslandes et al., 2003; Tasset et al., 2010). Besides its effects on RRS1, PopP2 was reported to re-localize the *Arabidopsis* cysteine protease RD19 (Responsive to dehydration 19) involved in *RRS1-R*-mediated resistance from vacuole-associated vesicles/lytic vacuole to the nucleus, where they physically interacted (Bernoux et al., 2008). PopP2 is a functional acetyl-transferase with autoacetylation activity, and both effector enzymatic function and effector recognition by the resistant allele *RRS1-R* are necessary for resistance (Tasset *et al.*, 2010).

AvrRps4 is a TTSS-secreted effector originally identified in *P. syringae* pv *pisi* (Hinsch and Staskawicz, 1996). It is a 221 amino acid protein cleaved in the plant cell between two glycines G133 and G134 just before the KRVY motif (Sohn et al., 2009). Recognition of AvrRps4 by *RPS4/RRS1* activated ETI, whereas in recognition-deficient *Arabidopsis* backgrounds AvrRps4 promoted *Pst* DC3000 growth and suppressed PTI outputs (Sohn et al., 2009). While the KRVY motif is required for both AvrRps4 virulence and avirulence functions, AvrRps4 virulence, but not its avirulence function depends on the *in planta* processing, even though the cleaved C-terminal part of AvrRps4 is sufficient for ETI activation (Sohn et al., 2009). For this defense activation, nuclear accumulation of the nucleo-cytoplasmic proteins RPS4 and AvrRps4 together with the key immune regulator EDS1 (Enhanced disease susceptibility 1, see section 1.5.1) is necessary (Wirthmueller et al., 2007; Heidrich et al., 2011).

Although defense activation by both AvrRps4 and PopP2 requires cooperative function of *RPS4* and *RRS1*, there need to be distinct mechanisms for effector recognition due to differential requirements of *RRS1a-S* and *RRS1a-R* for PopP2 recognition as well as contribution of *RPS4b* and *RRS1b* to AvrRps4, but not PopP2 recognition. Elucidation of

these differences in effector sensing and signaling activation mechanisms will help to gain a detailed comprehension of cooperative NLR functions.

1.5. Components of TNL-mediated resistance

1.5.1. EDS1 – PAD4 – SAG101

The nucleo-cytoplasmic lipase-like protein EDS1 interacts with its nucleo-cytoplasmic signaling partner PAD4 (Phytoalexin deficient 4) to confer basal resistance against virulent pathogens (Jirage et al., 1999; Feys et al., 2001; Rietz et al., 2011), while EDS1 heterodimer formation with its signaling partners PAD4 and nuclear SAG101 (Senescence associated gene 101) is required for TNL-mediated ETI including transcriptional defense gene reprogramming and localized cell death (Wiermer et al., 2005; Wirthmueller et al., 2007; García et al., 2010; Rietz et al., 2011; Wagner et al., 2013). Opposing former beliefs attributing CNL and TNL downstream signaling to either NDR1 (Non race specific disease resistance 1) (Knepper et al., 2011) or EDS1, respectively, EDS1 also contributed to resistance mediated by CNLs (Venugopal et al., 2009). EDS1 interacted with autoactivated overexpressed RPS4 in *Arabidopsis* and other TNLs (Bhattacharjee et al., 2011; Heidrich et al., 2011; Kim et al., 2012). Also, association of EDS1 with AvrRps4 and another *Pst* effector, HopA1, was shown (Bhattacharjee et al., 2011; Heidrich et al., 2011). Together with the lack of direct interaction between RPS4 and AvrRps4, this led to the hypothesis that EDS1 is a TNL guardee due to its functions in basal resistance and acts as a molecular bridge between effector and TNL to allow effector recognition and facilitate downstream signaling (Heidrich *et al.*, 2011; Bhattacharjee *et al.*, 2011).

1.5.2. SRFR1

The tetratricopeptide repeat (TPR) domain containing protein SRFR1 (Suppressor of *rps4*-RLD 1) was identified as a recessive negative regulator of *Pst* AvrRps4 resistance in the susceptible *Arabidopsis* accession RLD, since mutation of *srfr1* could partially restore resistance to *Pst* AvrRps4 compared to Col-0 (Kwon et al., 2004; Kwon et al., 2009; Li et al., 2010). SRFR1 localization is nucleo-cytoplasmic/endomembrane-asscociated and its TPR domain has sequence similarities to transcriptional repressors in other eukaryotes

(Kim et al., 2009; Kwon et al., 2009; Kim et al., 2010; Bhattacharjee et al., 2011). In RLD, apart from AvrRps4-triggered resistance, mutations in SRFR1 enhanced *Pst* HopA1 resistance in the absence of TNL RPS6 (Kim et al., 2009), whereas *srfr1* alleles in Col-0 caused constitutive immune activation revealed by plant stunting, constitutive *PR1* (*Pathogenesis related 1*) gene expression, SA (salicylic acid) accumulation and enhanced resistance to virulent and avirulent pathogens (Kim et al., 2010; Li et al., 2010). These immune outputs in Col-0 are dependent on the presence of the TNL SNC1 (Suppressor of *npr1*, constitutive 1, see below) (Kim et al., 2010; Li et al., 2010). SRFR1 associated with the TNLs RPS4, SNC1 and RPS6 and the immune regulator EDS1, but also with SGT1a and SGT1b, which are involved in NLR stabilization and degradation (see section 1.6; Kim et al., 2010; Li et al., 2010; Bhattacharjee et al., 2011). Intriguingly, *srfr1* mutants accumulated higher levels of SNC1, RPS4 and RPS2 proteins, and SNC1 protein amounts were also increased in *sgt1b* (Li et al., 2010). Together with the enhanced disease resistance phenotypes in *srfr1* mutants, this suggests a negative regulatory role of SRFR1 in TNL mediated resistance likely by facilitating proteasome-mediated TNL degradation. Furthermore, the association of SRFR1 with EDS1, as well as EDS1-RPS4 and EDS1-RPS6 interactions at the endomembrane were disrupted upon co-expression of effectors AvrRps4 and HopA1 in transient tobacco assays (Bhattacharjee et al., 2011), whereas RPS4-EDS1 complexes were found in the soluble cytoplasmic fraction upon RPS4 activation (Heidrich et al., 2011). This led to a model in which SRFR1 retains TNLs at the endomembranes in preformed inactive complexes with EDS1 and potentially other plant immunity components, and restricts TNL activity by promoting their degradation. Upon recognition of pathogen effectors, active signaling complexes are released for relocalization and immune signaling. However, a subpool of nuclear SRFR1 was required for its function, because nuclear excluded transgenic SRFR1 fails to complement the *srfr1* phenotype of enhanced *Pst* AvrRps4 resistance in RLD (Kim et al., 2014). Moreover, SRFR1 interacted with TCP (Teosinte branched1/cycloidea/PCF) transcription factors which positively contribute to ETI mediated by several NLRs, including RPS4 (Kim et al., 2014). These results suggest another layer of SRFR1 negative defense regulation by antagonizing positive functions of TCP at the chromatin.

1.5.3. SNC1

SNC1 is a TNL identified in a forward genetic screen for NPR1 (Non-expressor of *PR* genes 1)- independent resistance (Li et al., 2001). A mutation in the linker region between NB and LRR domains of *snc1* led to *EDS1*- and *PAD4*-dependent constitutive autoimmunity causing plant stunting, expression of *PR* genes, accumulation of SA and enhanced pathogen resistance, including *Pst* AvrRps4 (Li et al., 2001; Zhang et al., 2003; Kim et al., 2010). Mutation of the conserved P-loop motif abolished *snc1* autoimmune phenotypes (Xu et al., 2014a). The stunted growth phenotype of *snc1* rendered these plants an excellent tool for suppressor screens to identify components of TNL signaling, which has extensively been done resulting in MOS (Modifier of *snc1*) genes involved in the regulation of transcription, RNA processing, protein modification and nucleo-cytoplasmic trafficking (Johnson et al., 2012; Copeland et al., 2013; Xia et al., 2013).

Interestingly, SNC1 associates with the transcriptional co-repressor TPR1 (Topless-related 1) via its TIR domain (Zhu et al., 2010b). TPR1 targets and represses two negative defense regulator genes, *DND1* (*Defense no death 1*) and *DND2*, and mutations of *TPR1* and its homologs impaired *snc1* autoimmunity as well as basal and TNL-mediated resistance (Zhu et al., 2010b). Two SRFR1-interacting TCP transcription factors were identified as interactors of TPL (Topless) family proteins in a high throughput Y2H study (Causier et al., 2012), hinting at a complex, sophisticated interaction network of positive and negative defense regulators in the nucleus to fine-tune plant defense activation and balance pathogen resistance against plant growth and development.

1.5.4. NLR-transcription factor interactions – a direct link to defense gene expression?

Various NLR-induced ETI outputs such as ROS (reactive oxygen species) burst, calcium signaling and MAP (mitogen-activated protein) kinase cascade activation, SA (salicylic acid) production and transcriptional reprogramming of defense genes have been characterized (Buscaill and Rivas, 2014). However, little is known about immediate NLR downstream signaling processes in defense. Besides EDS1 and NDR1, NLR downstream components remain elusive, suggesting a short NLR signaling pathway. Several NLRs need to be localized to the nucleus for the activation of defense responses, including *Arabidopsis* RPS4 and SNC1, but also tobacco TNL N and the CNLs MLA10 (Mildew A locus 10) or Pb1 (Panicle blast 1) from barley and rice, respectively (Shen et al., 2007; Wirthmueller et al., 2007; Cheng et al., 2009; Bai et al., 2012; Inoue et al., 2013; Padmanabhan et al., 2013).

Notably, several interactions of NLRs with transcription factors have been reported, providing increasing evidence for a close connection between NLRs and events at the chromatin: Tobacco TNL N interacted with the SPL6 (Squamosa promoter binding protein 6) transcription factor which was needed for N-mediated resistance to tobacco mosaic virus (TMV), and an *Arabidopsis SPL6* ortholog contributed to *RPS4/RRS1* resistance to *Pst* AvrRps4 (Padmanabhan et al., 2013). Barley powdery mildew resistance was antagonistically regulated by the repressive transcription factors WRKY1 and WRKY2 and the activating transcription factor MYB6. The CNL MLA10 interacted with all three transcription factors and was shown to release MYB6 from WRKY1 suppression to allow defense gene expression (Chang et al., 2013). Furthermore, WRKY46 is a component of rice blast defense. Interaction with rice CNL Pb1 protected WRKY46 from proteasome-mediated degradation, thereby allowing its accumulation (Inoue et al., 2013). Interaction of SRFR1 with TCP transcription factors and of SNC1 with the transcriptional co-repressor TPR1 has been described already (see section 1.5.2; Zhu et al., 2010b; Kim et al., 2014). Moreover, SNC1 and RPS4 associated with the bHLH84 (basic helix-loop-helix) transcriptional activator which contributed to both *snc1* induced autoimmunity and *Pst* AvrRps4 resistance (Xu et al., 2014b).

Taken together, these data suggest that a number of NLRs reside in nuclear complexes with transcription factors and other immune signaling components. Upon pathogen recognition, recruitment of new proteins or rearrangements within these complexes might be the switch between their inactive and active states, allowing appropriate and coordinated transcriptional reprogramming and defense activation.

1.6. NLR stability control

NLR accumulation needs to be tightly regulated, as overexpression of NLRs can lead to constitutive immune activation at the expense of plant fitness (Alcázar and Parker, 2011). Increasing evidence emphasizes the importance of NLR stability control for plant immunity (Trujillo and Shirasu, 2010; Furlan et al., 2012; Duplan and Rivas, 2014). SGT1 (suppressor of the G2 allele of *skp1*), together with its interactor RAR1 (required for *Mla12* resistance), is involved in *R* gene mediated defenses (Austin et al., 2002; Liu et al., 2002; Muskett et al., 2002; Peart et al., 2002; Schornack et al., 2004). Both proteins interacted

with HSP90 (heat shock protein 90) and worked as co-chaperones to influence R protein accumulation and signaling (Tornero et al., 2002; Hubert et al., 2003; Takahashi et al., 2003; Bieri et al., 2004; Liu et al., 2004; Zhang et al., 2004; Holt et al., 2005; Azevedo et al., 2006; Botër et al., 2007). Although HSP90, RAR1 and SGT1 were mainly implicated in stabilization of R proteins through their chaperone function, SGT1 was attributed an additional negative regulatory role (Holt et al., 2005). Indeed, SGT1 interacted with SKP1, a component of the SCF (SKP1-CULLIN-F-box)-type E3 ubiquitin ligase complex, and the COP9 signalosome, both involved in proteasome-mediated protein degradation (Austin et al., 2002; Azevedo et al., 2002; Liu et al., 2002), and with several R proteins (Bieri et al., 2004; Leister et al., 2005). This suggests that SGT1 negative regulatory function is exerted through stimulation of NLR degradation. Consistent with this idea, a loss-of-function mutation of *Arabidopsis* SGT1b caused increased SNC1 protein levels (Li *et al.*, 2010). Similarly, missense mutations of HSP90 rescued decreased NLR accumulation in *rar1* (Hubert et al., 2009), and a recent publication by Huang and co-workers reports that HSP90 allelic forms are involved in the turnover of NLRs, since specific missense mutations in two cytosolic HSP90s allow accumulation of NLRs SNC1, RPS4 and RPS2 (Huang et al., 2014a). Furthermore, mutations in these HSP90s both positively and negatively affected NLR-mediated resistance and suppressed the temperature-sensitive autoimmunity of an RPP4 gain-of-function mutant (Bao et al., 2014; Huang et al., 2014a), further supporting a negative regulatory role of HSP90s on NLR stability and function in addition to their traditional positive contributions to immunity. Establishing a potential link to SKP1-interacting SGT1, the F-box protein CPR1 (constitutive *PR* gene expression, 1) interacted with *Arabidopsis* SKP1-like (ASK) proteins (Gou et al., 2009). Like SGT1, CPR1 negatively regulated stability of autoactive snc1 and the CNL RPS2 as well as immunity mediated by these two and other R proteins in a plant 26S proteasome-dependent manner (Cheng et al., 2011; Gou et al., 2012). Recently, the E4 ubiquitin ligase MUSE3 (Mutant, *snc1*-enhancing 3) was implicated in CPR1-dependent NLR polyubiquitination, promoting NLR proteasome-dependent degradation (Huang et al., 2014b). Taken together, SGT1 and HSP90 might not only be involved in NLR folding, but also facilitate assembly and function of a SCF^{CPR1} E3 ligase complex to regulate NLR steady state accumulation by controlled NLR ubiquitination and proteasome degradation.

Moreover, mutation of the ubiquitin-activating E1 enzyme UBA1 (ubiquitin activating 1) partially suppressed *snc1* autoactivity and reduced basal as well as several R protein mediated defense responses (Goritschnig et al., 2007). Also, the 26S proteasome

subunits RPN1a, RPT2a and RPN8 were required for certain *Arabidopsis* immune responses (Yao et al., 2012), further supporting the importance of NLR stability control in immunity.

1.7. Temperature-dependency of plant defense

It is evident that plant physiology and fitness depends on the environmental conditions they are grown in. For optimal growth and efficient reproduction, plants have adapted to their environment, including temperature conditions. One major determinant of plant fitness is its health, but active pathogen defense imposes plant fitness costs, suggestedly due to its energy requirements (Tian et al., 2003; Penfield, 2008; McClung and Davis, 2010; Hua, 2013; Wigge, 2013). Thus, appropriate regulation of defense is essential for optimal plant performance. PTI and ETI responses are regulated antagonistically depending on temperature, with ETI being more effective at low and PTI at high growth temperatures (Cheng et al., 2013). This is plausible because bacterial secretion of effectors is suppressed, whereas bacterial proliferation is enhanced by high temperature (van Dijk et al., 1999; Smirnova et al., 2001). In line with this, several *R* gene mediated resistance responses are sensitive to high temperature (Alcázar and Parker, 2011). Resistance to tobacco mosaic virus (TMV) mediated by the TNL N was abolished above 28°C (Samuel, 1931; Whitham et al., 1996), and likewise high temperature suppressed resistance or cell death mediated by tomato *Mi-1*, *Cf4* and *Cf-9* and *Arabidopsis RPW1* (Resistance to powdery mildew 8; Hwang et al., 2000; de Jong et al., 2002; Xiao et al., 2003).

Furthermore, *snc1* dwarfism and constitutive defense activation in Col-0 at 22°C was suppressed at 28°C (Yang and Hua, 2004). Interestingly the temperature-sensitivity of snc1 was abolished by an E640K mutation in the LRR domain. Similarly, tobacco N heat-sensitivity was suppressed by analogous mutations of its LRR (Zhu et al., 2010a). SNC1 and N immune activity correlated to their nuclear accumulation (Cheng *et al.*, 2009; Padmanabhan *et al.*, 2013), which was reduced at high temperature (Zhu et al., 2010a; Mang et al., 2012). Unlike its temperature-sensitive alleles, the snc1^{E640K} heat-stable protein remained nuclear at high temperatures (Zhu et al., 2010a). Taken together, these data suggest that NLRs are temperature-sensing immune components and their activity is modulated through subcellular localization. Restriction of NLRs to or from certain

compartments might restrict downstream signaling through the presence or absence of NLR interactors in different cellular compartments.

Notably, *RPS4*-mediated resistance to *Pst* AvrRps4 was sensitive to high temperature, and *SNC1* contributed to this resistance in a temperature-dependent manner (Wang et al., 2009; Kim et al., 2010). Temperature sensitivity was also observed in transient assays, but interestingly high temperature suppression of SNC1 or RPS4 induced cell death was removed by enhancing their nuclear accumulation through the inhibition of abscisic acid (ABA) synthesis (Mang et al., 2012). Also, constitutive defense activation and stunted plant growth in stable transgenic *Arabidopsis* lines overexpressing *RPS4* was suppressed at 28°C (Wirthmueller et al., 2007; Heidrich et al., 2011; Heidrich et al., 2013). This inspired establishing a temperature-shift (T-shift) system in which *RPS4* overexpressing plants were grown at 28°C to suppress phenotype development and a shift to 19°C allowed synchronous and massive activation of *RPS4*-induced immunity (Heidrich et al., 2011; Heidrich et al., 2013). This provided a potentially powerful tool to analyze activated RPS4 pathways by circumventing the problem of low (active) RPS4 protein levels in a natural infection systems where only a subset of cells per leaf likely responds to pathogen attack. Notably, even in the context of RPS4 induced effector-independent autoimmunity, its signaling outputs after T-shift were partially dependent on *RRS1*, further pointing to a positive role of *RRS1* in *RPS4*-mediated resistance signaling (Heidrich et al., 2013).

1.8. Study aims

Recent research improved our understanding of the regulation and possible functions of NLR proteins in plant defense. However, more mechanistic knowledge is needed for a detailed dissection of NLR signaling which ultimately might enable well-conceived and safe application of this knowledge in agronomical plants in the field. This is especially true in the light of successful transfer of NLRs from *Arabidopsis* into crop plants or vice versa (Maekawa et al., 2012; Narusaka et al., 2013b; Narusaka et al., 2014), indicating the existence of conserved signaling pathways and thus illustrating the potential of *Arabidopsis* research to be transferred to other plant lineages.

My study focusses on the *Arabidopsis* NLR pair *RPS4* and *RRS1* as an example of an emerging new class of paired immune receptors working cooperatively in plant

immunity to repel multiple pathogens. More and more components participating in *RPS4/RRS1* signaling are uncovered, revealing an increasingly detailed view of a complex regulatory network summarized in Figure 2.

Nevertheless, many questions remain unanswered regarding *RPS4/RRS1* regulation, downstream signaling and especially the mechanisms by which paired NLRs operate to transduce effector sensing to defense activation. To this end, this study was conceived to (1) examine the genetic and molecular interplay of *RPS4* and *RRS1* and their interdependency, (2) develop a system to monitor RRS1 chromatin associations, (3) discern RRS1 domain functions through targeted mutations and (4) detect RPS4 interacting proteins in pre- and post-activation complexes.

(1) Given the interaction of RPS4 and RRS1 via their TIR domains and additional parts of the proteins (Williams et al., 2014), and the partial *RRS1*-dependency of *RPS4*-mediated transcriptional outputs after temperature shift (Heidrich et al., 2013), I propose a positive regulatory function of *RRS1* on *RPS4* signaling apart from a suggested sensor role. With the new data and material of the *RPS4b* and *RRS1b* NLR pair, transgenic *RPS4* overexpressing plants in an *rrs1a rrs1b* double mutant background were created to circumvent a potential complementation of *RRS1a* function by *RRS1b*. Characterization of these lines allowed further clarification of *RRS1* involvement in *RPS4*-mediated immunity.

(2) RRS1 WRKY domain and the finding that disrupted DNA binding leads to an activation of immune responses (Deslandes et al., 2002; Noutoshi et al., 2005) indicated negative regulatory functions of inactive RRS1 at the chromatin. To reexamine this hypothesis, transgenic lines expressing HA-/flag-tagged *RRS1* under its native promoter were characterized and subsequently used for chromatin-immunoprecipitation to obtain an overview of RRS1-targeted genes. Gained information would also be useful to dissect if RRS1 functions as a sensor by using its WRKY domain as a decoy to trap pathogen effector, or if its WRKY domain actively targets and regulates defense genes and can thus be seen as a guardee of RPS4 and RRS1 TNL protein parts.

(3) Analyses of single NLR domains, their activities and requirements for NLR protein functions have been a valuable tool for modeling the intramolecular processes connected to NLR activation (Qi and Innes, 2013). Similar to rice RGA5, a functional ATP-binding pocket is dispensable for RRS1 function (César et al., 2014; Williams et al., 2014). For a deeper insight into requirements of the distinct domains for functionality of this atypical NLR protein, targeted mutations were introduced in a full length protein context with the aim to monitor their effects on RRS1 functions in resistance to *Pst* AvrRps4.

(4) To gain further insight into RPS4 downstream signaling, RPS4 interactors were co-purified from both uninduced and temperature-shift activated *35S:RPS4-HS* plant tissue and samples subsequently analyzed by mass-spectrometry. Detection of RPS4 interacting proteins in pre- and/or post-activation complexes will help to understand the sophisticated regulation of NLR complexes, which is needed to achieve fast and efficient activation while preventing excessive activity at the expense of plant growth.

In conclusion, I suggest that RRS1 is more than an effector sensor and I will test the dependency of *RPS4* immune activation on *RRS1*. A major question to pin down *RRS1* immune functions remains its association with chromatin: Does RRS1 bind to defense-related genes? Is the RRS1 chromatin association dynamic, and where does is bind before and after defense activation? I claim that RPS4 and RRS1 assemble in distinct complexes depending on their activation state, and thus I will analyze autoactivated RPS4 complexes to identify biologically relevant components involved in *RPS4*/*RRS1* defense signaling.

Figure 2: Model of RPS4 and RRS1 regulation.

(A) In the absence of pathogen recognition, SRFR1 restrains RPS4 – possibly in a pre-activation complex with EDS1 and RRS1 – at endomembranes in the cytoplasm and facilitates NLR degradation via the proteasome. Constituting a possible link, SGT1 interacts with both SRFR1 and the E3 ligase complex component SKP1. Both the F-box protein CPR1 and an E4 ligase MUSE3 are involved in proteasomal NLR degradation. While HSP90 and SGT1 contribute to NLR degradation, they also positively regulate NLR stability through their chaperon function together with RAR1. Besides repressive effects on TCP transcription factors, nuclear SRFR1 might intercept nuclear NLRs to eliminate unintendedly active complexes to prevent autoimmunity. **(B)** Pathogen effectors can disrupt endomembrane associations of SRFR1 with NLRs and EDS1. Effector recognition might stimulate the release of NLR complexes into the cytosol and the de-repression of nuclear NLR complexes and transcription factors, allowing for example TCPs and – through repression of negative regulators DND1 and DND2 – TPR1 positive regulatory functions in plant defense. AvrRps4-activated EDS1-RPS4-RRS1 complexes might undergo different re-arrangements. While in the cytosol, RPS4 TIR domain homo-dimeric interactions could trigger cell death, hetero-dimeric TIR interactions of RPS4 and RRS1 in the nucleus might be needed for defense gene activation through interactions with transcription factors (TF) like WRKYs, RPS4-interacting bHLH84, or SPL6 which is required for *Pst* AvrRps4 resistance

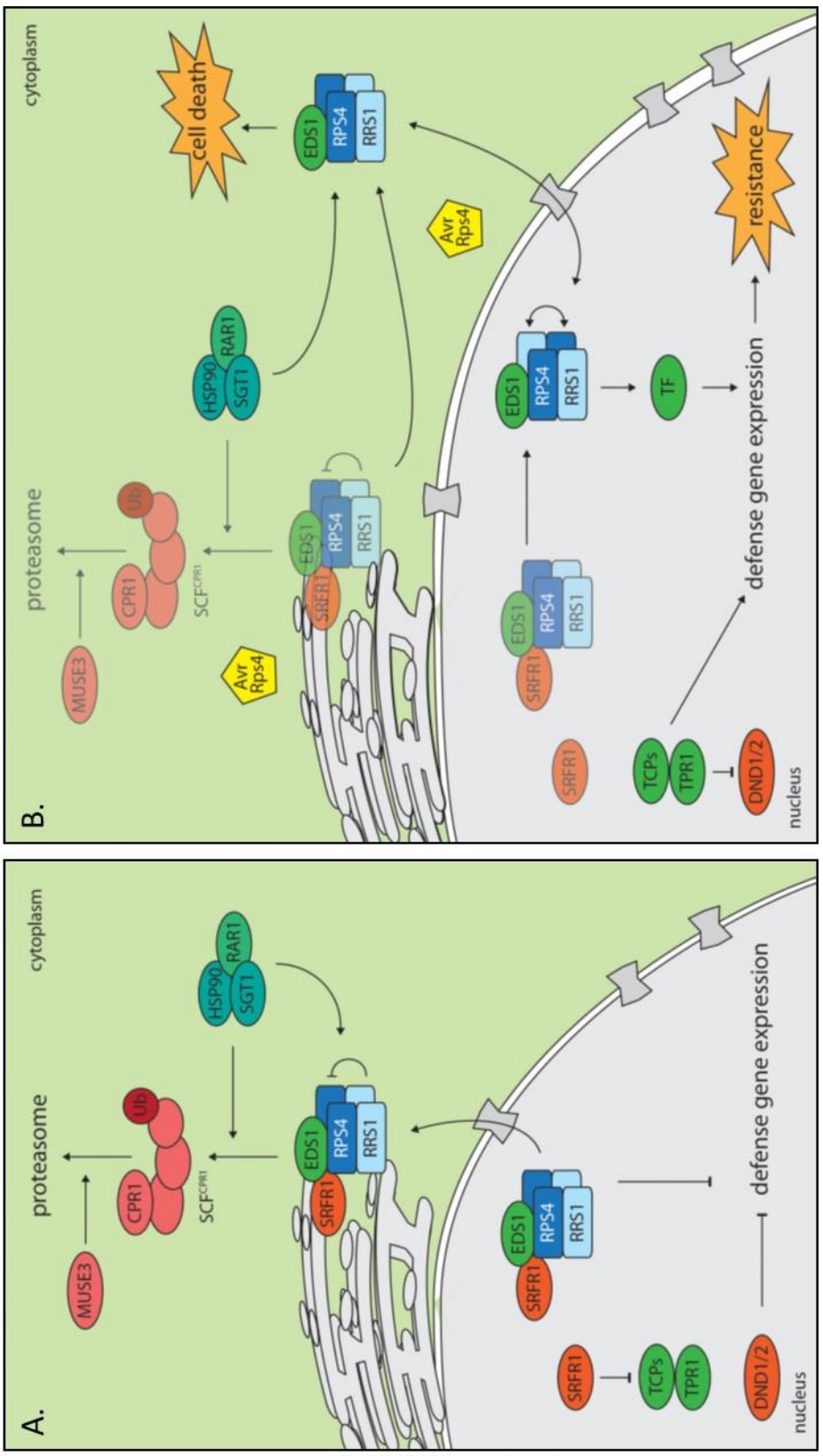

Figure 2: Model of RPS4 and RRS1 regulation.

2. Results

This study is divided into four parts. The aim of section 2.1 was to elucidate the contribution of *RRS1a* (*Resistance to Ralstonia solanacearum 1a*) and *RRS1b* to *RPS4* (*Resistance to Pseudomonas syringae 4*)-mediated immunity. For this, the effect of the *rrs1a/b* double mutation on autoimmunity induced by *RPS4* overexpression was examined by measuring immune outputs like plant stunting and transcriptional reprogramming and relating them to *RPS4* transcript and protein amounts. Section 2.2 describes the characterization of transgenic *Arabidopsis* plants expressing *RRS1-S*, which were subsequently used for chromatin-immunoprecipitation to identify RRS1-S target genes and dissect RRS1-S rearrangements at the chromatin before and after pathogen recognition. To clarify the requirement of RRS1-S domain integrity for its function and especially its chromatin-association, a targeted mutagenesis was performed to generate gain- and loss-of-function alleles of *RRS1-S* (section 2.3). In section 2.4, RPS4 pre- and post-activation protein complexes were purified and analyzed to acquire a concept of dynamic remodeling of RPS4-comtaining immune complexes during defense activation.

2.1. *RRS1* contributes to *RPS4*-induced autoimmunity

Overexpression of *RPS4* full length protein in stable transgenic *Arabidopsis* caused constitutive defense activation and stunted plant growth at low to normal growth temperatures but could be suppressed at high temperatures (Heidrich et al., 2013). *RPS4* like other TNLs (TIR-NB-LRR receptors) depends on the key immune regulator *EDS1 (Enhanced disease susceptibility 1)* for its function, as displayed by wildtype (wt)-like growth of *eds1-2* mutant plants overexpressing *HA-StrepII*-tagged *RPS4* (*35S:RPS4-HS*, referred to as *OE-RPS4-HS*) at low growth temperature (Wirthmueller et al., 2007; Heidrich et al., 2013).

Making use of the RPS4 temperature dependency (see section 1.7), a temperature shift (T-shift) system has been established for *RPS4* activation: *RPS4* overexpressing plants were grown at high temperature (28°C) to suppress autoimmunity and allow healthy and uniform plant growth. For a simultaneous activation of *RPS4*-dependent defense outputs, plants were shifted to low temperature (19°C). This released the inhibitory effects of high

growth temperature on RPS4 and triggered strong and homogenous defense signaling (Heidrich et al., 2013). Notably, OE-RPS4-HS autoimmune outputs partially depend on its signaling partner RRS1, as the growth phenotype of *OE-RPS4-HS* at 22° was partially suppressed in a *rrs1a* mutant background, and so was the transcriptional induction of a subset of genes induced after T-shift (Heidrich et al., 2013). The recent discovery of a second *RPS4-RRS1* related *NLR* gene pair, designated *RPS4b* and *RRS1b*, involved in *Arabidopsis* resistance to *Pseudomonas syringae* p.v. *tomato* DC3000 (*Pst*) expressing AvrRps4, and the generation of *rps4a/b* and *rrs1a/b* double mutant lines (Saucet, 2013) raised our interest to further elucidate the interplay of *RPS4* and *RRS1*. To clarify the role of *RRS1* for *RPS4*-triggered defense outputs, *Arabidopsis* lines overexpressing either *OE-RPS4-HS* or *YFP*-tagged *RPS4* (*35S:RPS4-YFP*, referred to as *OE-RPS4-YFP*) in the *rrs1a/b* double mutant background were generated and characterized.

2.1.1. *RPS4b* and *RRS1b* contribute to *Pst* AvrRps4 resistance

To test the role of *RPS4b* and *RRS1b* in AvrRps4 recognition (Saucet, 2013), plants were syringe-infiltrated with *Pst* AvrRps4 and pathogen growth in leaves was monitored 3 days later (3dpi). In agreement with the detection of *RPS4b* and *RRS1b* as additional *NLR* gene pair working in AvrRps4 recognition (Saucet, 2013), both *rps4a/b* and *rrs1a/b* showed increased susceptibility to *Pst* AvrRps4 compared with the intermediate pathogen growth on *rps4a* and resistant Col-0 (Figure 3 A). Notably, both *rps4a/b* and *rrs1a/b* did not display hypersusceptibilty to *Pst* AvrRps4, whereas the *eds1-2* mutant did (Figure 3 A). Therefore, the double mutant lines retain basal resistance.

Indeed, when infiltrated with virulent *Pst* DC3000, bacterial growth in *rps4a/b* and *rrs1a/b* is similar to Col-0 and *rps4a* at 3dpi (Figure 3 B), showing that loss of both alleles of *RPS4* or *RRS1* does not compromise basal immunity to this pathogen. Taken together, these results indicate that *RPS4* and *RRS1 a* and *b* alleles function additively in *Pst* AvrRps4 resistance. Still, residual *Pst* AvrRps4 resistance of *rps4a/b* and *rrs1a/b* compared to the hypersusceptible *eds1-2* raises the question if yet another NLR or NLR pair is involved in AvrRps4 recognition, or if this difference is merely due to *eds1-2*, but not *rrs1a/b* or *rps4a/b* defects in basal resistance.

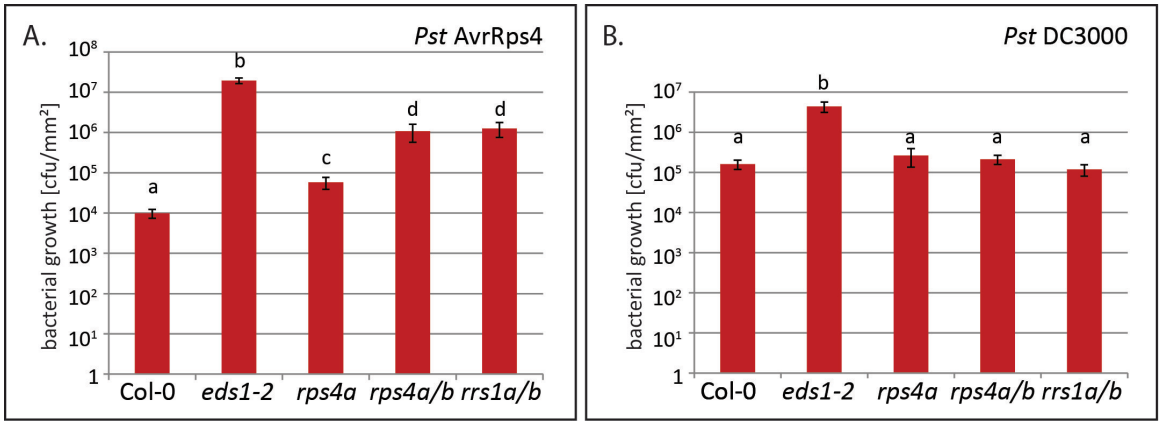

Figure 3: *RPS4b* and *RRS1b* contribute to resistance towards *Pst* AvrRps4.

Pathogen performance was monitored on Col-0, *eds1-2*, *rps4a*, *rps4a/b* and *rrs1a/b* double mutants. Bacterial growth quantification on 5-week-old plants at 3 days after bacterial infiltration (3dpi) of (**A**) avirulent *Pst* AvrRps4, OD_{600}=0.0001, or (**B**) virulent *Pst* DC3000, OD_{600}=0.0001. Values are means +/- standard errors ($n \geq 5$). ANOVA followed by a post-hoc Tukey's test was performed to group genotypes depending on significant differences as indicated by letters ($p<0.05$). Bacterial growth experiments were repeated independently at least three times with similar results. cfu = colony forming unit.

2.1.2. *OE-RPS4*-mediated dwarfism partially depends on *RRS1 a* and *b*

As both *RRS1* paralogs *a* and *b* mediated AvrRps4 recognition (see section 2.1.1) and autoimmunity caused by *RPS4* overexpression was partially suppressed by the mutation of *RRS1a* (Heidrich et al., 2013), the effect of a complete *RRS1* knock out (*rrs1a/b*) on *RPS4* induced autoimmunity was analyzed further. For that, either *35S:RPS4-HS* or *35S:RPS4-YFP* construct was crossed into the *rrs1a/b* double mutant background and homozygous T3 plants were selected for each transgene.

To quantify the *RPS4*-induced growth phenotype, *OE-RPS4-HS* or *OE-RPS4-YFP* overexpressing plants in different genetic backgrounds and Col-0 wt plants were germinated at 28°C, transferred to 19°C after one week and plant morphology and fresh weight were determined at different plant age for a qualitative and quantitative readout of plant growth at 19°C. Both *OE-RPS4-HS* (Col-0) and *OE-RPS4-YFP* (*rsp4a*) plants were severely stunted, while plant growth was restored to Col-0 wt-like growth in *OE-RPS4-HS eds1-2* or *OE-RPS4-YFP eds1-2* (Figure 4). In contrast to *eds1-2*, the *rrs1a/b* only partially rescued plant dwarfism caused by *OE-RPS4-HS* or *OE-RPS4-YFP* overexpression, allowing intermediate growth compared to Col-0 wt.

To validate that the measured growth phenotype of *OE-RPS4-YFP* plants is due to functional RPS4, the non-functional RPS4 P-loop mutant was included as additional

control (Zhang et al., 2004; Wirthmueller et al., 2007). The P-loop region is a highly conserved motif in NLR NB domains and includes a conserved lysine that binds the β-/γ-phosphate of ADP or ATP, respectively (Takken et al., 2006; van Ooijen et al., 2008; Bonardi et al., 2012). Mutations of this conserved lysine in RPS4 resulted in a loss-of-function allele (Zhang et al., 2004; Wirthmueller et al., 2007), probably due to reduced ATP binding. Indeed, the *OE-RPS4$^{P\text{-}loop}$-YFP rps4a* line grew Col-0 wt-like (Figure 4 A), suggesting that phenotypes observed with overexpressed native *RPS4* are resulting from its NLR function rather than being an artifact of protein over-accumulation.

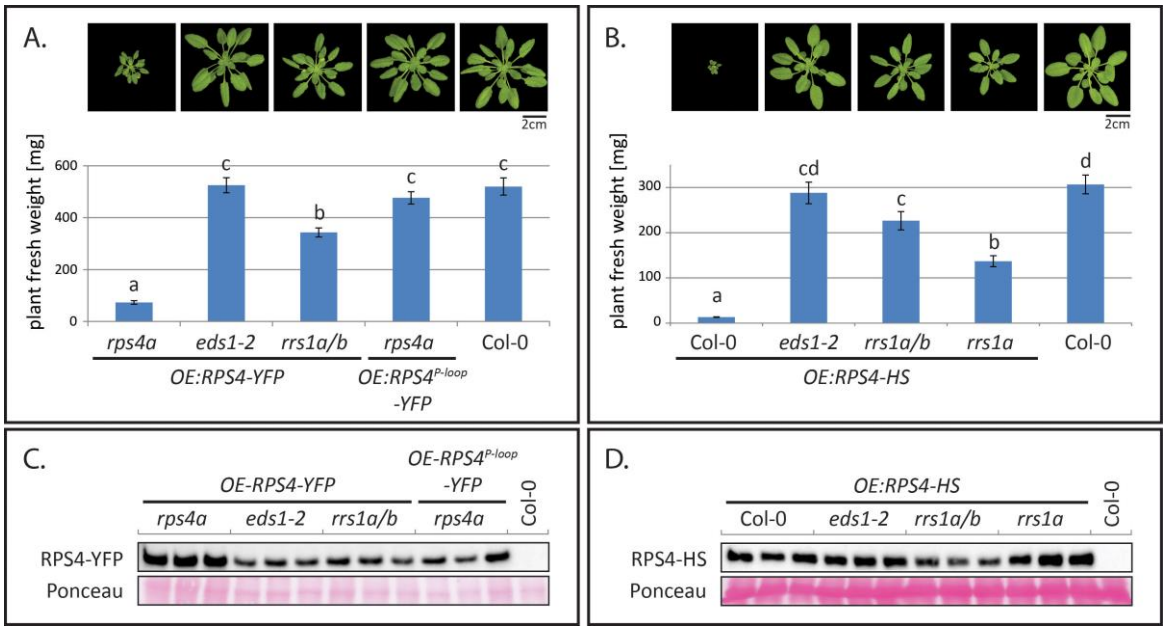

Figure 4: The *rrs1a/b* double mutation partially suppresses *RPS4* autoimmunity.
OE-RPS4-YFP or *OE-RPS4-HS* plants in different genetic backgrounds, as well as inactive *OE-RPS4$^{P\text{-}loop}$-YFP* and/or Col-0 were grown at 19°C to allow growth phenotype development. 5.5-week-old plants were harvested. **(A, B)** Growth phenotype was determined via plant fresh weight and morphology. ANOVA followed by a post-hoc Tukey's test was performed to group genotypes depending on significant differences as indicated by letters ($p<0.05$). **(C, D)** RPS4-YFP and RPS4-HS accumulation was monitored by western blot using αGFP and αHA antibody, respectively. Ponceau S staining indicated equal protein loading and transfer to the membrane.

Since *RPS4* overexpressing plants grown at moderate temperatures constitutively show effector-independent activation of immunity, the proposed RRS1 sensor function (see section 1.3.4) should be dispensable for the manifestation of plant dwarfism. The fact that both *rrs1a* and *rrs1a/b* suppress *RPS4*-induced growth reduction suggests RRS1 is an active part of *RPS4*-mediated defense initiation and signaling, rather than merely a sensor

for pathogen effectors. Interestingly, the suppressive effect of *rrs1a/b* double mutant on plant dwarfism was significantly higher than that of the *rrs1a* single (Figure 4 B), indicating a contribution of both *RRS1* alleles to *RPS4* autoimmune signaling and the ability of *RRS1b* to partially compensate for the loss of *RRS1a* in *RPS4*-overexpressing plants. However, in both *RPS4* overexpression lines tested the RPS4 protein levels at 19°C were reduced in *rrs1a/b* compared to *rps4* or *Col-0* backgrounds (Figure 4 C, D). The partial suppression of dwarfism might therefore be due to reduced RPS4 steady state accumulation, and RRS1 impact through the stabilization of RPS4 rather than RRS1 active participation in defense signaling.

2.1.3. RPS4 protein levels are reduced in *rrs1a/b* independent of growth conditions

As described above, RPS4-YFP and RPS4-HS protein amounts were lower in *rrs1a/b* compared to *rps4a* or Col-0 backgrounds, respectively, when plants are grown at 19°C and immunity is activated by autoactive RPS4. To elucidate if the *rrs1a/b* effect of reducing RPS4 protein accumulation is a general one or if it is connected to RPS4 protein activity at 19°C, RPS4 protein levels were monitored at 28°C where RPS4 autoactivity is suppressed. Furthermore, a time course experiment monitoring RPS4-YFP amounts after T-shift of plants grown at 28° was performed. Similar to RPS4 protein accumulation pattern at 19°C, RPS4 protein levels in plants grown constantly at 28°C were diminished in *rrs1a/b* compared to both *rps4a* and *eds1-2* (Figure 5 A). Moreover, RPS4 protein accumulation was slightly decreased in *rrs1a/b* and *eds1-2* when plants were exposed to moderate temperature of 19°C (Figure 5 B).

A possible reason for the decrease of RPS4 protein amounts after T-shift might be enhanced degradation of activated NLR receptors. Plants might sense a conformational change of NLRs upon activation and try to avoid excessive defense activation due to misregulation of these critical signaling components. Only *RPS4* over-expressing plants in the *rps4a* or Col-0 background were capable of triggering defense responses, thus initiating a positive feedback loop leading to increased RPS4 expression and defense outputs. This is feasible even though RPS4 is expressed not under its own promoter carrying its specific regulatory elements but under the cauliflower mosaic virus 35S-promoter, because this constitutive promoter is responsive to salicylic acid (Qin et al., 1994; Redman et al., 2002),

the plant hormone induced upon and involved in regulation of defense responses to biotrophic pathogens (An and Mou, 2011).

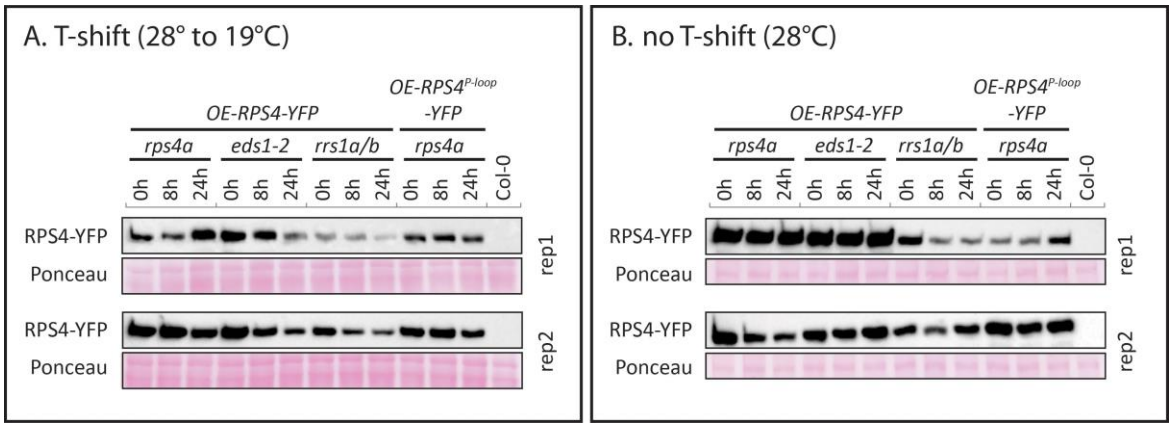

Figure 5: RPS4-YFP protein levels are reduced in *rrs1a/b* and further decrease after T-shift.
OE-RPS4-YFP lines in different genetic backgrounds were grown at 28°C to suppress autoimmune phenotype. Inactive *OE-RPS4$^{P\text{-}loop}$-YFP* and Col-0 wt plants were grown alongside as controls. RPS4-YFP accumulation in 3.5-week-old plants was monitored at 0, 8 and 24 hours (h) after T-shift or in plants grown continuously at 28°C by western blot using αGFP antibody. **(A)** RPS4-YFP accumulation in plants shifted to 19°C to activate *RPS4*-mediated autoimmunity. **(B)** RPS4-YFP accumulation in plants grown continuously at 28°C. Each sample contained leaf discs of 3 different plants, respectively. Ponceau S staining indicated equal protein loading and transfer to the membrane.

For several NLR receptors, including RPS4, defense activation requires their nuclear localization (see section 1.5.4; Shen et al., 2007; Wirthmueller et al., 2007; Cheng et al., 2009; Bai et al., 2012; Inoue et al., 2013; Padmanabhan et al., 2013), and temperature sensitivity of SNC1, RPS4 and tobacco N is related to their nuclear accumulation (see section 1.7; Cheng *et al.*, 2009; Padmanabhan *et al.*, 2013; Zhu et al., 2010a; Mang et al., 2012). To test whether the partial recovery of plant growth in *OE-RPS4-YFP rrs1a/b* is due to a changed localization of the RPS4-YFP protein, plants were examined by confocal microscopy to monitor protein localization at 28°C and after T-shift to 19°C (Figure 6). As described above (see section 2.1.2), RPS4-YFP signal was lower in *rrs1a/b* compared to *rps4a*. Still, for all lines tested, nuclear RPS4-YFP signal could be visualized both with and without T-shift (Figure 6).

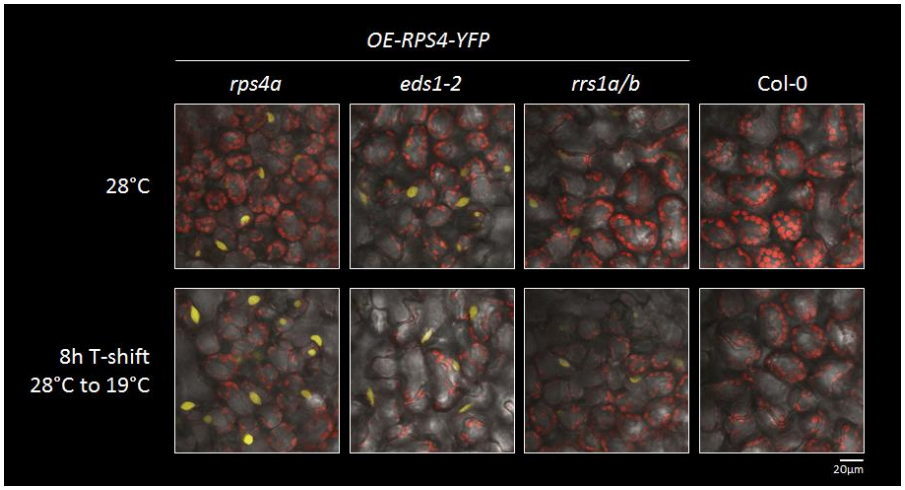

Figure 6: RPS4-YFP localization is not obviously altered in *rrs1a/b*.
Pictures were taken of 2.5-week-old plants grown continuously at 28°C or shifted to 19°C for 8h. RPS4-YFP localization was monitored under consistent microscopy conditions for all genotypes tested. Col-0 was included as an autofluorescence background control. Scale bar represents 20µm. Excited at 514nm, emission measured for YFP at 515-558nm and chlorophyll autofluorescence 650-720nm. Experiment was performed only once.

This result contrasts the published nucleo-cytoplasmic localization of RPS4 (Wirthmueller et al., 2007), but the lack of cytoplasmic RPS4 signal might be due to the overall low RPS4-YFP fluorescence in this experiment and the difficulty to detect RPS4 protein in the cytoplasm, potentially due to a dilution effect in the cytoplasm. However, since nuclear RPS4 is crucial for triggering immune responses (Wirthmueller et al., 2007) and nuclear RPS4-YFP could be detected in *rrs1a/b*, the suppression of dwarfism is likely not caused by aberrant subcellular localization.

To conclude, RRS1a and RRS1b contribute to RPS4 stability both in uninduced conditions at 28°C and after induction of RPS4 autoimmunity at 19°C without obviously affecting RPS4 localization.

2.1.4. *RPS4* transcripts are reduced in *rrs1a/b* only after T-shift

Besides the effect of RRS1 on RPS4 stability at the protein level discussed above, another potential reason for reduced RPS4 protein amounts in *rrs1a/b* could be silencing of the *RPS4* transgene, leading to lower mRNA expression and thus lower protein accumulation. Although the *RPS4* transgenes are stably expressed in other genetic backgrounds, the consequence of the *rrs1a/b* double mutant on *RPS4* transcripts was evaluated to exclude transgene silencing. For this, RNA samples were collected at 0, 8 and 24h after T-shift and

analyzed by qPCR. Because alternative splicing of *RPS4* mRNA is induced upon infection with *Pst* AvrRps4 (Zhang and Gassmann, 2007), and RPS4 alternative transcripts are essential for its resistance function against *Pst* AvrRps4 (Zhang and Gassmann, 2003), several RPS4 primer pairs were tested to monitor RPS4 expression throughout the gene (Figure 7 A).

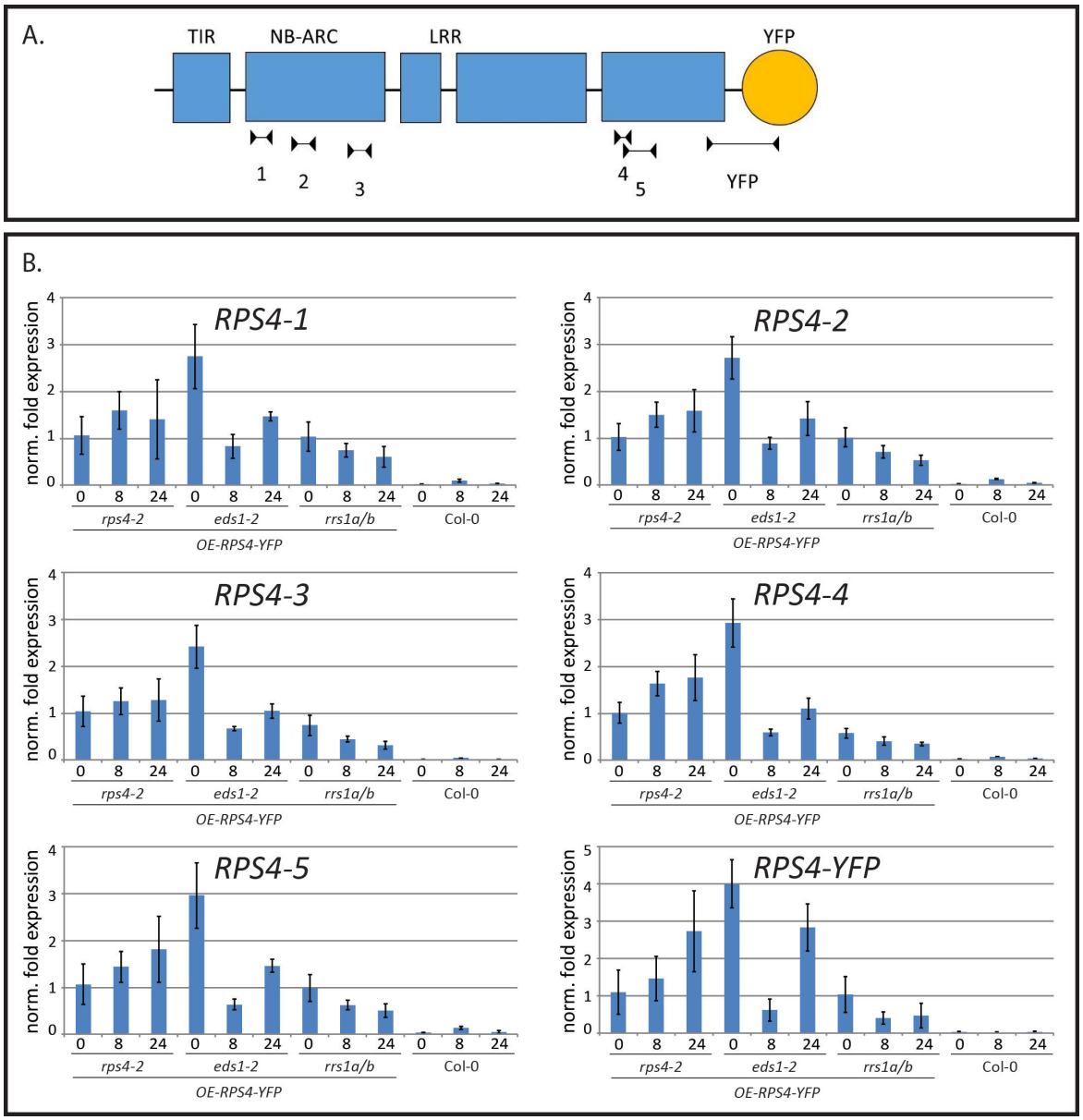

Figure 7: Abundance of *RPS4* mRNA in *OE-RPS4-YFP* transgenic lines upon T-shift.

OE-RPS4-YFP plants in different genetic backgrounds were grown at 28°C together with Col-0 wt controls. *RPS4* expression in 3.5-week-old plants before (0h) and at 8h and 24h after T-shift was analysed by qPCR. **(A)** Primer alignment to *RPS4* and nomenclature used in (B). **(B)** Normalized fold expression was calculated by relating sample values to the geometric mean of two reference genes (*GAPDH* and *expressed protein*) and normalizing to the *OE-RPS4-YFP rps4* uninduced (0h) sample. Replicates contained leaf discs of 3 different plants, respectively.

Starting amounts of *RPS4* transcript (0h, before T-shift) were higher in *eds1-2*, but similar in *OE-RPS4-YFP rps4a* and *rrs1a/b* for all primer pairs tested (Figure 7 B), suggesting an unvaried *RPS4* expression in *rrs1a/b* compared to *rps4* and thus arguing against a possible silencing of the transgene in *rrs1a/b*. At 8h and 24h after T-shift, *RPS4* mRNA levels were decreased in *rrs1a/b* compared to *rps4a* and *eds1-2*. Thus, reduced *RPS4* transcript accumulation due to lower transgene expression or transcript stability might be one of the mechanisms leading to reduced RPS4 protein amounts in the *rrs1a/b* double mutant after T-shift.

2.1.5. *RPS4*-induced defense gene activation is partially suppressed in *rrs1a/b*

Suppression of plant growth leading to dwarfism is an easy measurable trait and is generally connected to uncontrolled enhanced induction of plant immunity as reported in autoimmune mutants (Alcázar and Parker, 2011). To test whether the suppression of plant growth, which was used before as an output for *RPS4* immune signaling (see section 2.1.2), correlated with immune-related transcriptional reprogramming in *RPS4* over-expressing plants, the levels of defense gene expression in various lines after RPS4 activation by T-shift were analyzed. Several defense marker genes known to display *EDS1*-dependent regulation during *RPS4-RRS1* mediated resistance towards *Pst* AvrRps4 (García et al., 2010) were tested by qPCR: *PR1*, *ICS1* and *PBS3*, *FMO1* and *EDS1* itself were chosen as examples for *EDS1*-dependent gene induction, and *DND1* and *ERECTA* for *EDS1*-dependent repression (Figure 8).

Defense gene induction in *OE-RPS4-YFP rrs1a/b* was 10-100fold lower for the genes tested than in *OE-RPS4-YFP rps4a* and completely absent in *OE-RPS4-YFP eds1-2* (Figure 8 A). The defense-induced repression of genes was not detected in both *eds1-2* and *rrs1a/b* compared to *rps4a* mutant background (Figure 8 B). This demonstrated that the partial suppression of *RPS4*-mediated dwarfism in *rrs1a/b* is also reflected in reduced *RPS4*-induced immune activation in *rrs1a/b* measured by the transcriptional reprogramming of several defense marker genes. Together with the results on RPS4 protein and mRNA accumulation, it is likely that the suppression of effector-independent, T-shift induced *RPS4* signaling outputs in the absence of RRS1 is due to reduced RPS4 accumulation both at the mRNA and protein levels. This suggests that RRS1 has a stabilizing effect on RPS4.

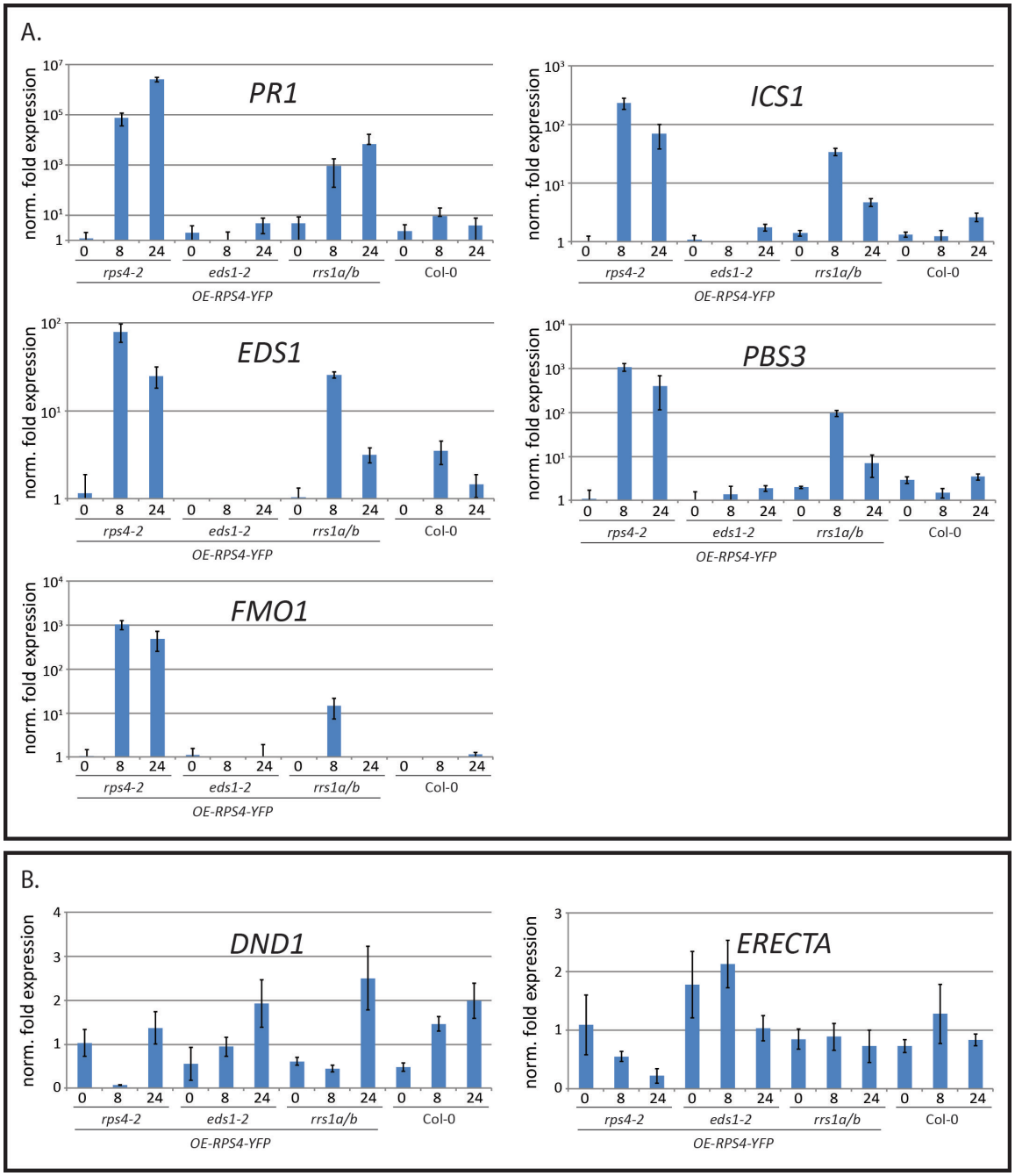

Figure 8: T-shift-induced regulation of defense-related genes in *OE-RPS4-YFP* is partially suppressed in *rrs1a/b*.

OE-RPS4-YFP plants in different genetic backgrounds were grown at 28°C to suppress autoimmune phenotype. Col-0 wt plants were grown alongside as controls. Transcriptional reprogramming of EDS1-dependent **(A)** induced and **(B)** repressed genes in 3.5-week-old plants before (0h) and at 8h and 24h after T-shift was analysed by qPCR. Normalized fold expression was calculated by relating sample values to the geometric mean of two reference genes (*GAPDH* and *expressed protein*) and normalizing to the *OE-RPS4-YFP rps4* uninduced (0h) sample. Replicates contained leaf discs of 3 different plants, respectively.

2.1.6. Growth suppression by *RPS4* overexpression depends both on RPS4 protein amounts and genetic background

To tackle the question whether suppression of *RPS4*-mediated autoimmunity in *rrs1a/b* is due to reduced RPS4 protein accumulation or due to impaired RPS4 signaling by removal of RRS1a and b, the *OE-RPS4-YFP* phenotyping experiments described above (see 2.1.2) were repeated including two additional lines with low levels of RPS4-YFP protein: (1) A *35S:RPS4-YFP rps4a* line designated *CP-OE-RPS4-YFP* which had reduced protein amounts and wt-like growth at 22°C and (2) a transgenic *rps4a* line expressing *RPS4-YFP* under its native promoter, designated *pRPS4:RPS4-YFP*, with very low protein expression levels (both lines kindly provided by Chunpeng Yao, Parker lab). The inactive *OE-RPS4*$^{P\text{-}loop}$*-YFP* and the low expression line *pRPS4:RPS4-YFP* showed normal growth which was not discriminable from Col-0 or signaling inactive *OE-RPS4-YFP eds1-2*. This indicates that a certain threshold of active RPS4 is required for the development of a dwarfed growth phenotype (Figure 9 A, B). Interestingly, when grown at 19°C, the *CP-OE-RPS4-YFP* also had reduced protein levels and a less severe, but not significantly reduced dwarfism compared to the original *OE-RPS4-YFP rps4a* line used before (Figure 9 A, B). This further emphasizes the correlation between protein amounts and growth impairment in *RPS4* overexpressing plants. Even though the protein amounts in *CP-OE-RPS4-YFP* were lower than in *OE-RPS4-YFP rrs1a/b* (Figure 9 B), the stunting was not: fresh weight of *CP-OE-RPS4-YFP rps4a* was not significantly different from the original *OE-RPS4-YFP rps4a* line, whereas there was a significant difference between *OE-RPS4-YFP* in *rps4a* and *rrs1a/b* (Figure 9 A). This suggests that not only reduced RPS4 protein amounts are responsible for the partial suppression of *RPS4*-dependent defense outputs in *rrs1a/b*, but also the genotypic background influences *RPS4* functions. Hence, *RRS1* might have an additional role in *RPS4* signaling beyond pathogen sensing and RPS4 stabilization.

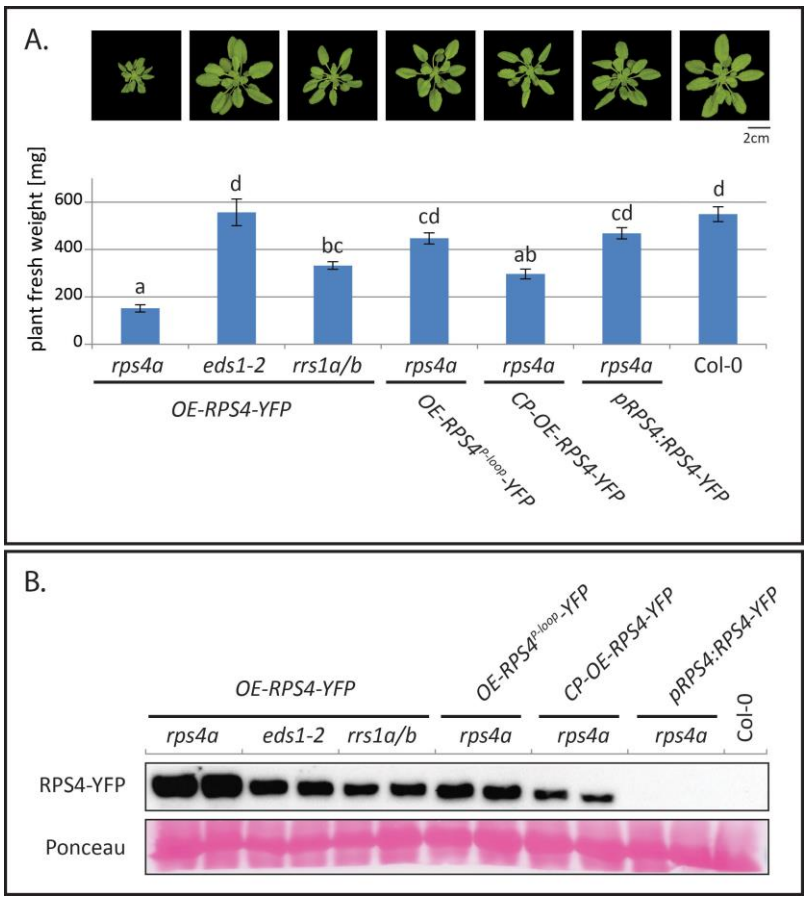

Figure 9: *OE-RPS4-YFP* plant growth phenotype depends on both RPS4 protein amounts and genetic background.

Different *RPS4-YFP* transgenic lines together with Col-0 wt were grown at 19°C to allow autoimmunity and harvested when 5.5 weeks old. **(A)** Growth phenotype was determined by measuring plant fresh weight and recording morphology of 15 individual plants per line. ANOVA followed by a post-hoc Tukey's test was performed to group genotypes depending on significant differences as indicated by letters ($p<0.05$). **(B)** RPS4-YFP accumulation was monitored by western blot using αGFP antibody. Ponceau S staining indicated equal protein loading and transfer to the membrane. Each sample contained leaf material of 3 different plants. This experiment was performed only once.

2.1.7. Inhibition of the 26S proteasome induces increased RPS4 protein accumulation

I have established that RRS1 is required for RPS4 protein accumulation, but the reason for lower RPS4 protein accumulation in *rrs1a/b* compared to the other genetic backgrounds remains elusive. There is increasing evidence for a role of 26S proteasome in the regulation of plant immunity by NLR degradation (see section 1.6). To test whether 26S proteasome-mediated protein degradation is responsible for the decreased RPS4 levels in *rrs1a/b*, the effect of the proteasome inhibitor MG132 on RPS4 stability was examined. Plants were

grown in MS liquid medium in sterile 24-well-plates at 19°C to allow constitutive activation of *RPS4*-triggered outputs. After 2.5 weeks, the medium was exchanged to MS with MG132 or DMSO as a mock control, and protein samples were harvested at different time points after treatment. Inhibition of the 26S proteasome led to an increase in RPS4-YFP protein amounts in *OE-RPS4-YFP rps4a* and *eds1-2*, and in inactive RPS4$^{P\text{-loop}}$ protein compared to the mock control at 8h post treatment (Figure 10 A). Similarly, an increase of RPS4-YFP protein was detected in the *rrs1a/b* genetic background when treated with MG132, even though total RPS4-YFP amounts remained lower compared to the other genotypes and the trend was not so clear among different replicates (Figure 10 A, data not shown). Thus, RPS4-YFP is degraded via the plant 26S proteasome in all genotypes tested, including *rrs1a/b*. Similarly, in *OE-RPS4-HS* transgenic lines, RPS4 accumulated in all genotypes tested. However, in *OE-RPS4-HS* plants the RPS4 accumulation was much more pronounced in *rrs1a* and *rrs1a/b* than in Col-0 or *eds1-2* (Figure 10 B). Thus, although RPS4 degradation depends on the plant proteasome, no conclusive effect of the *rrs1a/b* mutation could be established.

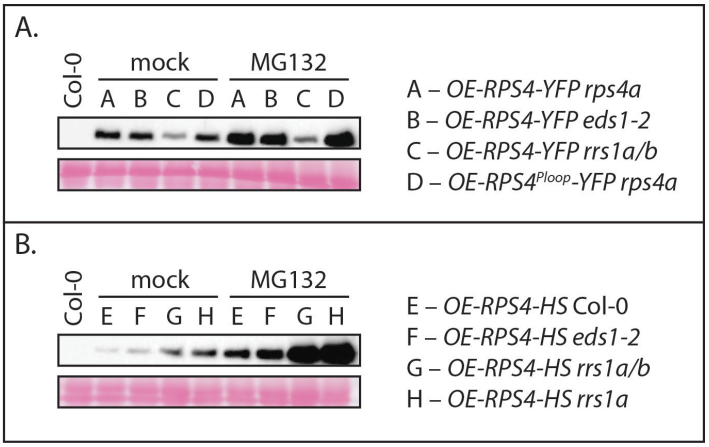

Figure 10: RPS4 is degraded via the plant 26S proteasome independent of the genetic background.
OE-RPS4-YFP or *OE-RPS4-HS* plants in different genetic backgrounds and Col-0 wt plants were grown in sterile liquid cultures in 24-well plates at 19°C. RPS4 protein accumulation in 2.5-week-old plants treated with 60µM MG132 proteasome inhibitor or DMSO (mock) was monitored at 8h post treatment. Each sample represented one well with several individual plants. Ponceau S staining indicated equal protein loading and transfer to the membrane. Experiment was performed twice independently with three technical replicates each.

2.2. Transgenic *RRS1-S* is functional in *Arabidopsis*

RRS1 is a unusual NLR protein not only because of its cooperative function with RPS4 against different pathogens (Birker et al., 2009; Narusaka et al., 2009a; Narusaka et al., 2009b), but also due to its C-terminal WRKY transcription factor DNA-binding domain (Deslandes et al., 2002). *RRS1a* is present in *Arabidopsis* ecotypes in different isoforms distinguishable by their ability to confer resistance to *Ralstonia solanacearum* expressing PopP2, named *RRS1-R* (for resistant) originally discovered in the ecotype Niederzenz Nd-1 and *RRS1-S* (for susceptible) found in Col-5 (Deslandes et al., 1998; Deslandes et al., 2002). Furthermore, *RRS1-R* but not *RRS1-S* induced cell death upon resistance signaling activation by PopP2 and AvrRps4, indicating not only possibly different ways of immune signaling, but also a greater signaling potency of *RRS1-R* compared to *RRS1-S* (Deslandes et al., 2002; Noutoshi et al., 2005), even though NLR triggered cell death could be uncoupled from disease resistance activation (Bendahmane et al., 1999; Gassmann, 2005; Heidrich et al., 2011; Bai et al., 2012). Because Col-0 remains the ecotype preferentially used in *Arabidopsis* research and Col-0 *RRS1-S* together with *RPS4* is fully functional in conferring resistance to *Pst* AvrRps4, I focused on the Col-0 allele of *RRS1*. Since Col-0 confers this resistance without inducing cell death, the Col-0/*Pst* AvrRps4 patho-system is of special interest since it allows the analysis RPS4 and RRS1-S cooperative resistance functions uncoupled from cell death response.

2.2.1. *3FTH-RRS1-S* confers resistance to *Pst* AvrRps4 without increasing basal resistance to *Pst* DC3000

Arabidopsis Col-0 *rrs1a* mutant lines expressing *RRS1-S*, the Col-0 allele of *RRS1a*, with an N-terminal triple-flag and triple-HA tag connected by a TEV cleavage site (3FTH) under its own promoter (hereafter named *3FTH-RRS1-S*, kindly provided by Laurent Deslandes) were characterized. After selection and propagation of homozygous lines, the ability of transgenic *3FTH-RRS1-S* to confer resistance to *Pst* AvrRps4 was tested in bacterial growth assays (Figure 11). Since both *rrs1a* and *rps4a* displayed the same intermediate susceptibility towards *Pst* AvrRps4 compared to wt (Heidrich et al., 2013), only *rps4a* single mutant was included as a control for pathogen growth. Compared to resistant Col-0 and hypersusceptible *eds1-2*, *rps4a* allowed intermediate pathogen growth (Figure 11 A). All three independent transgenic *3FTH-RRS1-S* lines were indistinguishable from Col-0,

showing no macroscopic disease symptoms at 4 days post infection (data not shown). *Pst* AvrRps4 proliferation was similar to Col-0 wt and statistically different from the intermediate susceptible *rps4a* mutant in all three *3FTH-RRS1-S* lines (Figure 11 A). Thus, *3FTH-RRS1-S* can complement the *rrs1a* mutant background and is functional in mediating AvrRps4-triggered resistance.

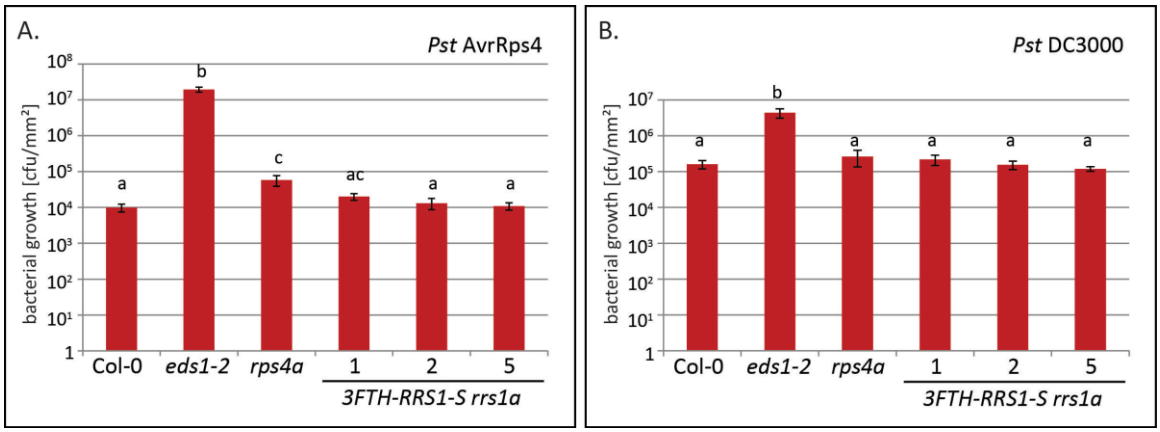

Figure 11: Transgenic *RRS1-S* confers resistance to *Pst* AvrRps4 without increasing basal immunity to *Pst* DC3000.

Pathogen performance was monitored on Col-0, *eds1-2*, *rps4a* and three independent *3FTH-RRS1-S* transgenic lines. Bacterial growth quantification 3 days post syringe infiltration with (**A**) avirulent *Pst* AvrRps4, OD_{600}=0.0001 of 4.5-week-old plants, or (**B**) with virulent *Pst* DC3000, OD_{600}=0.0001 of 5-week-old plants. ANOVA followed by a post-hoc Tukey's test was performed to group phenotypes depending on significant differences ($p<0.05$). Bacterial growth experiments were repeated at least three times with similar results.

Due to the close linkage of *RPS4* and *RRS1* on the chromosome and the short intergenic spacer of only 254bp in Col-0 (Gassmann et al., 1999), the own promoter fragment used for the generation of *RRS1* transgenic lines carried a substantial portion of the *RPS4a* gene: 1902bp of the *RPS4* coding region, covering exons 1 and 2 coding for the TIR-NB part of RPS4. Expression of *RPS4* induced effector-independent cell death in transient assays in tobacco (Zhang et al., 2004). This cell death inducing character of RPS4 was specifically mediated by the N-terminal part consisting of the TIR domain and parts of the NB domain (Swiderski et al., 2009). Also, overexpression of *RPS4* mediated enhanced resistance to *Pst* DC3000 and *Pst* AvrRps4 in *Arabidopsis* (Heidrich et al., 2013). To rule out that wt-like resistance to *Pst* AvrRps4 determined in *3FTH-RRS1-S* is due to autoimmunity of ectopically expressed *RPS4* from the cloned promoter element of *RRS1-S*, the transgenic lines were tested for basal resistance to *Pst* DC3000. Compared to hypersusceptible *eds1-2*

compromised in basal resistance, growth of *Pst* DC3000 was reduced in susceptible Col-0 and *rps4a* (Figure 11 B). Neither of the *3FTH-RRS1-S* lines showed increased basal resistance to *Pst* DC3000 compared to Col-0 (Figure 11 B), demonstrating that the resistance phenotype to *Pst* AvrRps4 described above is unlikely to be due to *RPS4* autoimmunity.

The accumulation of 3FTH-RRS1-S protein in the transgenic lines both in the absence and presence of *Pst* AvrRps4 was analyzed by western blot. While the different transgenic lines accumulated 3FTH-RRS1-S to various degrees, in all lines tested the 3FTH-RRS1-S protein levels were similar in untreated and *Pst* AvrRps4 spray inoculated leaf tissue (Figure 12). Hence, 3FTH-RRS1-S accumulates to detectable levels and is unaffected by AvrRps4 recognition.

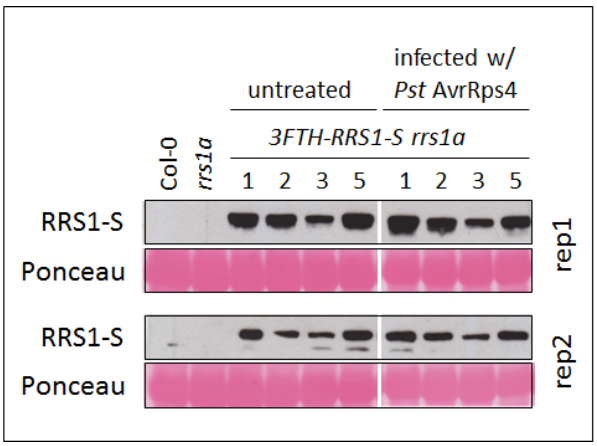

Figure 12: 3FTH-RRS1-S protein accumulation is unaltered upon *Pst* AvrRps4 infection.
Protein samples of healthy or *Pst* AvrRps4 spray-inoculated (OD_{600}=0.2, harvest at 8hpi) 4-week-old *3FTH-RRS1-S*, Col-0 and *rrs1a* were analyzed by western blot. Numbers denote independent transgenic lines. Ponceau S staining indicated equal protein loading and transfer to the membrane.

For future experiments, *3FTH-RRS1-S* line #5 was chosen as it consistently showed strong resistance to *Pst* AvrRps4 and had a high *3FTH-RRS1-S* protein level.

2.2.2. RRS1-S localizes predominantly to the nucleus

RRS1-R and RRS1-S interact with the *Ralstonia* effector PopP2, and upon transient co-expression in *Arabidopsis* protoplasts, both PopP2 and RRS1 proteins could be detected in the nucleus by confocal laser microscopy (Deslandes et al., 2003). However, when a nuclear localization signal of the effector was deleted and the effector localized to the cytoplasm, both RRS1-R and RRS1-S co-localized to the cytoplasm as well (Deslandes et

al., 2003). As the requirement of nuclear localization for functionality had been demonstrated for several NLR proteins including RRS1 (Deslandes et al., 2003; Burch-Smith et al., 2007; Shen et al., 2007; Wirthmueller et al., 2007; Cheng et al., 2009; Bai et al., 2012; Inoue et al., 2013; Padmanabhan et al., 2013), the nuclear localization of transgenic 3FTH-RRS1-S was tested in biochemical assays. For all three independent *3FTH-RRS1-S* transgenic lines, RRS1-S was detected predominantly in the nuclei-enriched fraction and partly in the cytoplasm, validating the expected localization of the transgenic fusion protein (Figure 13). RPS4 with reported nucleo-cytoplasmic distribution (Wirthmueller et al., 2007) was included as a control in fractionation experiments using T-shift activated *OE-RPS4-HS* leaf material. Purity of obtained fractions was determined by detecting the cytoplasmic marker PEPC or the nuclear histone H3 (Figure 13). It can therefore be concluded that in uninduced leaf tissue RRS1-S is localized mainly to the nucleus and partly to the cytoplasm.

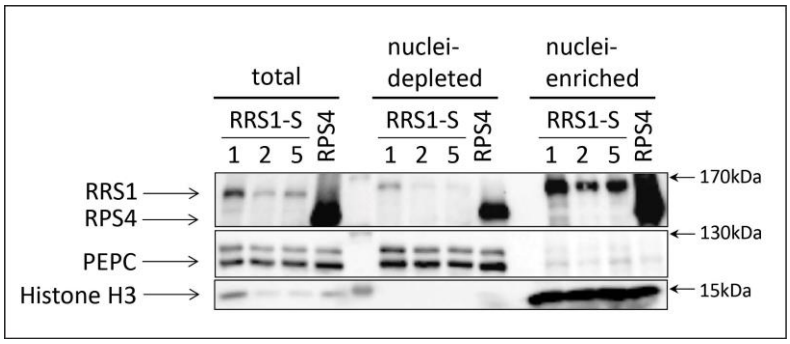

Figure 13: RRS1-S localizes partly to the cytoplasm and predominantly to the nucleus.

3.5-week-old healthy *3FTH-RRS1* plants was harvested and used for nuclear fractionation. Numbers denote independent transgenic lines. Temperature-shift activated *OE-RPS4-HS* (8h) was included as a control. 3FTH-RRS1 and RPS4-HS were detected with αHA antibody. Cytosolic PEPC and nuclear Histone H3 serve as localization markers and controls for efficient nuclei enrichment as well as loading controls.

To test if RRS1-S localization changes after triggering immune signaling by the AvrRps4 effector, nuclear fractionation was repeated using healthy and *Pst* AvrRps4 spray-infected leaf tissue. 3FTH-RRS1-S could be detected in the nucleus both before and after infection, whereas protein amounts were too low for detection in the input or nuclei-depleted fractions (Figure 14). Still, as both healthy and infected samples allowed 3FTH-RRS1-S detection in the nucleus, its localization is not obviously changed upon defense activation with *Pst* AvrRps4.

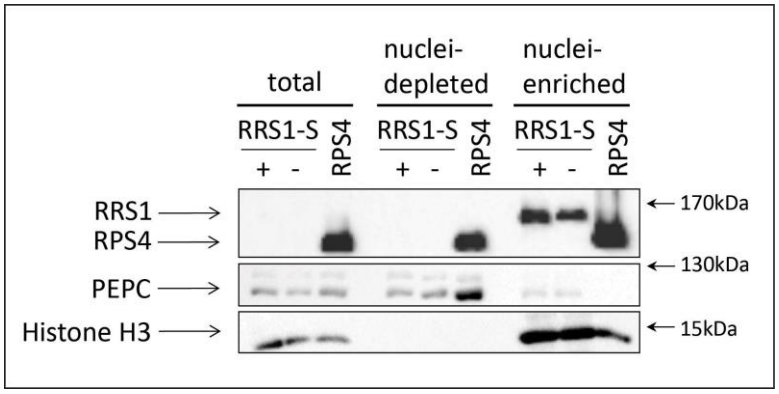

Figure 14: RRS1-S nuclear localization is independent of *Pst* AvrRps4 infection.
3.5-week-old *3FTH-RRS1* plants (line #5) were spray-inoculated with *Pst AvrRps4* OD_{600}=0.4 (+) or mock-treated with 10mM $MgCl_2$ (–). Leaf tissue was harvested at 6hpi and used for nuclear fractionation. T-shift activated *OE-RPS4-HS* (8h) was included as a control. 3FTH-RRS1 and RPS4-HS were detected with αHA antibody. Cytosolic PEPC and nuclear Histone H3 serve as localization markers and controls for efficient nuclei enrichment as well as loading controls.

2.2.3. Defense gene regulation comparable in Col-0 and *3FTH-RRS1-S*

To further elucidate whether transgenic RRS1 is able to trigger wt-like transcriptional reprogramming, regulation of defense-related genes was tested by qPCR at different time points after syringe infiltration with *Pst* AvrRps4. Besides Col-0 as a positive control, the *rrs1a/b* double mutant was included which was impaired in recognition of AvrRps4. Generally the difference between Col-0 as a positive control and *rrs1a/b* as a negative control for AvrRps4 recognition was difficult to define as *rrs1a/b* was still responding to the bacterial treatment due to active PTI signaling, leading to gene expression changes similar to the ones detected in AvrRps4-triggered ETI. However, subtle differences could be observed since in *rrs1a/b* (PTI) several genes were upregulated later than in Col-0 and *3FTH-RRS1-S* (ETI) due to bacterial suppression of PTI in the AvrRps4 non-recognizing background *rrs1a/b* (Figure S1), indicating (but not proving) a proper signaling function of *3FTH-RRS1-S* in terms of transcriptional defense outputs.

2.2.4. Approaches for RRS1 chromatin-immunoprecipitation (ChIP)

I could demonstrate that the *3FTH-RRS1-S* line (1) shows nuclear localization (Figure 14), (2) complements the *rrs1a* disease resistance phenotype towards *Pst* AvrRps4 (Figure 11) and (3) induces wt-like transcriptional reprogramming after *Pst* AvrRps4 infection (Figure S 1). Moreover, the biochemical nuclear fractionation method described above leads to

leakage of nucleoplasmic proteins (García et al., 2010; Parker group, unpublished), suggesting that 3FTH-RRS1-S showing a nuclear signal is closely linked to or even physically associated with chromatin. RRS1-R nuclear localization and *in-vitro* association with W-boxes-containing DNA has been published (Deslandes et al., 2002; Noutoshi et al., 2005). Disruption of the *in-vitro* DNA binding by an amino acid insertion in the WRKY domain immediately after the highly conserved WRKYGQK motif caused an *in-vivo* autoactive immune phenotype associated with stunting, activation of defense marker genes and cell death (Noutoshi et al., 2005). These observations suggest that RRS1 functions at the chromatin to repress defense gene activation, while disruption of DNA binding leads to de-repression of defense related genes and thus allows defense activation. Based on these data, the described *3FTH-RRS1-S* line was used in a ChIP-sequencing (ChIP-seq) approach with the aim to identify RRS1 DNA binding sites to gain fundamental insight into RRS1 location at the chromatin. For a trial ChIP-seq experiment healthy *3FTH-RRS1-S* leaf material was used, with the expectation that RRS1 is bound to the chromatin exerting a repressive effect on defense gene expression in unchallenged plants. As a negative control for unspecific background binding Col-0 plants were included, and as a positive control for the ChIP procedure the WRKY18 transcription factor stably expressed in *Arabidopsis* (*op:WRKY18-HA*, Rainer Birkenbihl) was processed. However, for a dynamic view of RRS1 location and function at the chromatin, proposedly in complexes together with RPS4 and other proteins such as EDS1 and transcription factors, further ChIP-seq experiments including different time points after *Pst* AvrRps4 challenge should reveal not only location of resting RRS1 at the chromatin, but also potential repositioning of RRS1-containing complexes after defense activation to induce or facilitate defense gene reprogramming.

For the trial ChIP-seq, chromatin was extracted after formaldehyde crosslinking of proteins with nearby other proteins and DNA. DNA was disrupted by ultrasonication and tagged RRS1-S and WRKY18 immunoprecipitated with αHA-antibody. The immuno-precipitated DNA was purified after reversing the crosslinking. WRKY18 samples were positively tested in qPCR for enrichment of target gene promoter fragments. For *3FTH-RRS1* and Col-0 input and αHA-ChIP samples, linear DNA amplification (LinDA) was performed before barcoding samples during library preparation for sequencing. Barcoded ChIP-seq libraries were PCR-amplified and fragments of ~200-400bp selected. Samples were sequenced by the Max Planck genome center using the Illumina HiSeq2500. Sequencing reads were processed and compared using the peak calling programs MACS

(Zhang et al., 2008), QuEST (Valouev et al., 2008) and peakzilla (Bardet et al., 2013). Around 200 genes could be identified as enriched in RRS1-S but not Col-0 αHA-ChIP samples (Barbara Kracher). Although the peaks in the RRS1-S αHA-ChIP samples were detected in the peak calling programs, closer inspection of individual peaks showed no strong enrichment of ChIP-seq reads in RRS1 compared to Col-0 (Figure 15).

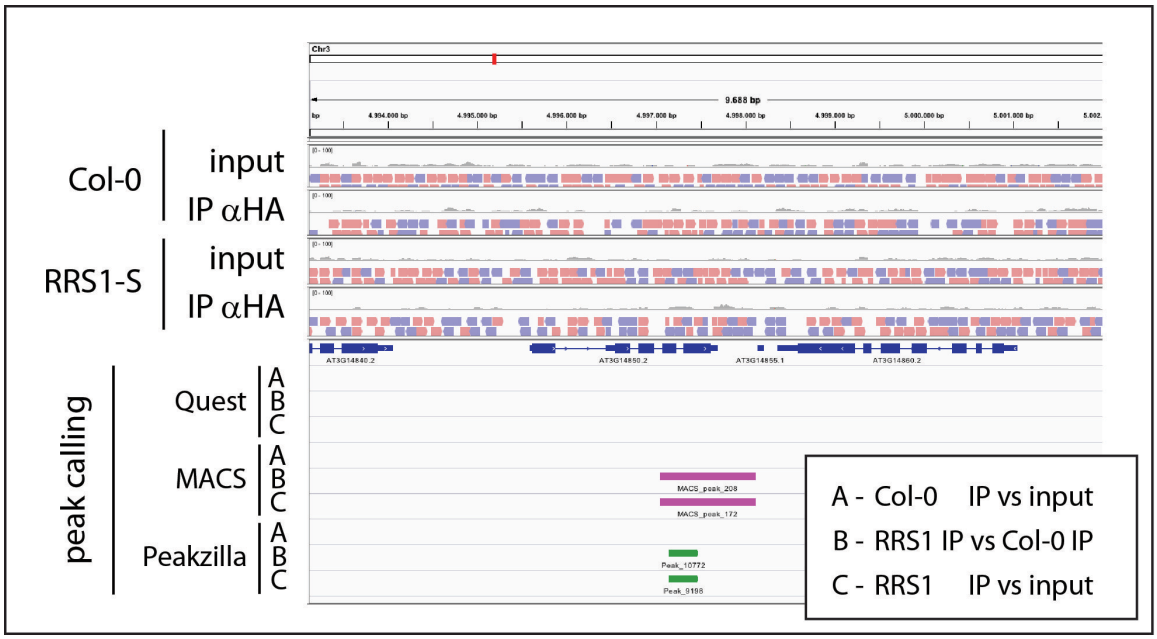

Figure 15: ChIP-seq alignment in integrative genome viewer (IGV) illustrates scarce/insufficient enrichment of DNA sequences in *RRS1* compared to Col-0 samples.

Healthy leaf tissue of 3-week-old *3FTH-RRS1* or Col-0 plants was used for ChIP-seq analysis. Sequencing reads were aligned and peak-calling performed with three different programs, formally resulting in ~200 RRS1-enriched genes detected by the MACS peak-calling program. Presentation in IGV revealed that peaks identified by peak-calling did not show strong enrichment in RRS1 αHA-ChIP samples.

Since the decision to use healthy plant material for the trial ChIP was based on the assumption rather than experimental proof that only inactive RRS1 is bound to the DNA, the ChIP was repeated including *Pst* AvrRps4 infected leaf tissue for a more dynamic view of RRS1-DNA associations during pathogen defense. For this, 3-week-old *3FTH-RRS1-S* as well as Col-0 were spray-inoculated with *Pst* AvrRps4 (OD_{600}=0.4) or mock-treated with 10mM $MgCl_2$ and leaf tissue was harvested at 8hpi. Mock-treated *WRKY18-HA* leaf tissue was included as positive ChIP control. *Pst* AvrRps4 induced defense gene activation was monitored by qPCR analysis of *ICS1* as an early induced defense marker gene, and protein levels of 3FTH-RRS1-S were monitored by western blot to ensure sufficient and comparable protein expression in both infected and mock-treated plants (Figure 16). All

samples were passed through the ChIP procedure described above. *3FTH-RRS1-S* and Col-0 input and αHA-ChIP samples are currently analyzed at the Max Planck genome center.

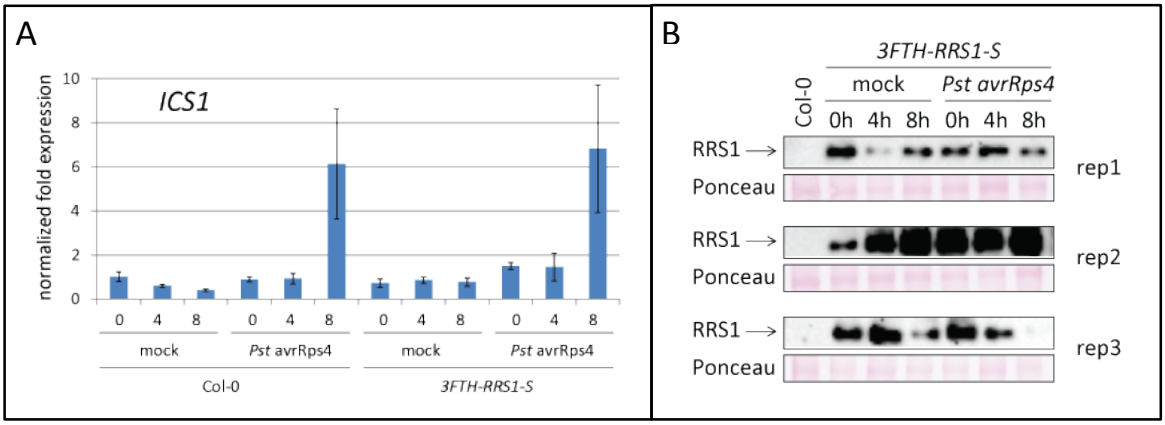

Figure 16: Defense gene induction and RRS1-S protein levels after *Pst* AvrRps4 infection in ChIP-seq material.

3-week-old *3FTH-RRS1* or Col-0 plants were spray-inoculated with *Pst* AvrRps4 (OD_{600}=0.4) or mock-treated with 10mM $MgCl_2$. Leaf tissue of several plants was harvested at 0, 4 and 8h post treatment in three replicates and used to monitor defense gene activation and protein accumulation. (**A**) qPCR analysis revealed induction of *ICS1* in *Pst* AvrRps4 infected, but not mock treated samples. (**B**) RRS1 protein levels were detected by western blot probing with aHA antibody. Equal loading and protein transfer to membrane was monitored by ponceau-S staining. Despite of low blot quality, no effect of time and treatment was detected for 3FTH-RRS1-S protein accumulation.

2.3. RRS1-S domain function and activity – a targeted mutational analysis

The canonical structure of TNL proteins has been introduced above (see section 1.2). In summary, they share a conserved domain structure consisting of an N-terminal TIR, a central NB-ARC and a C-terminal LRR domain (Takken et al., 2006; Eitas and Dangl, 2010; Bonardi et al., 2012). RRS1 additionally carries a WRKY transcription factor DNA-binding domain at its C-terminus (Deslandes et al., 2002). For a better insight into the domain functions of this unusual NLR protein, several targeted mutations were introduced into the genomic *RRS1-S* sequence to generate predicted gain-of-function (GOF) or loss-of-function (LOF) alleles of RRS1-S and test those mutated proteins for modified activity *in planta*.

2.3.1. Toll-/interleukin-1 receptor (TIR) domain

Because the TIR domain is proposed to be important for downstream signaling activation in plant TNLs (Frost et al., 2004; Michael Weaver et al., 2006; Swiderski et al., 2009; Chan et al., 2010; Krasileva et al., 2010) and the function of RPS4 and RRS1 depends on the integrity of the TIR domain dimerization interface (Williams et al., 2014), for the mutational study of RRS1 function several mutations in the TIR domain (R20A, H26A, Y101A) were chosen due to their ability to disrupt heterodimer formation with RPS4 while maintaining RRS1 TIR homodimerization in Y2H experiments (Williams et al., 2014). Since the αA-helix is part of the dimerization interface and contains the SH (serine-histidine)-motif (RRS1 S25H26) which is of critical importance for RPS4-RRS1 TIR association (Williams et al., 2014), later experiments were focused on the RRS1 H26A mutation.

2.3.2. Nucleotide-binding (NB-ARC) domain

For canonical NLRs, the NB-ARC domain is a major determinant of their activity, being responsible for the switch of the inactive ADP-bound to the active ATP-bound conformation (Qi and Innes, 2013). It consists of the three subdomains of (1) the NB catalytic core forming a classical NTPase fold, (2) the ARC1 establishing inhibitory intramolecular interactions with the LRR and (3) the ARC2 regulating the intramolecular interaction to transduce pathogen perception (van Ooijen et al., 2008; Lukasik and Takken, 2009). To study the importance of NB-ARC in RRS1 function, conserved motifs in these subdomains have been targeted for mutations. The P-loop ATPase motif with a conserved K (lysine) is of central relevance for ATP binding and hydrolysis, and P-loop mutations cause reduced ATP binding and frequently lead to loss-of-function (LOF) alleles in NLR proteins (Dinesh-Kumar et al., 2000; Tao et al., 2000; Howles et al., 2005; Ade et al., 2007; Wirthmueller et al., 2007; Williams et al., 2011; Bai et al., 2012). TO test RRS1-S functional dependency on ATP binding, the RRS1-S K185A P-loop mutation was included. Mutations of an invariant D (aspartate, in RRS1-S: D254) in the Walker B motif involved in indirect coordination of Mg^{2+}, a co-factor for ATP binding, might lead to reduced Mg^{2+} positioning and thus LOF (Dinesh-Kumar et al., 2000), whereas mutations in the second acidic residue D (in RRS1-S: D255) catalyzing ATP hydrolysis can lead to reduced ATP hydrolysis causing gain-of-function (GOF) alleles (Takken et al., 2006; Tameling et al., 2006; van Ooijen et al., 2008; Bonardi et al., 2012; Takken and Goverse, 2012). The

conserved R (arginine, in RRS1-S: R283) in the RNBS-B motif is thought to interact with the ARC2 MHD motif and to sense the ATP γ-phosphate, leading to protein activation. Mutations of this sensor amino acid can lead to LOF phenotypes (Dinesh-Kumar et al., 2000; Tao et al., 2000; Bendahmane et al., 2002; Yan et al., 2005; Takken et al., 2006; van Ooijen et al., 2008). The basic H in the highly conserved MHD motif binds and positions the β-phosphate of ADP, stabilizing the compact ADP-bound closed NLR conformation (Takken et al., 2006; van Ooijen et al., 2008; Bonardi et al., 2012). Mutations in the MHD motif often cause NLR autoactivity (Bendahmane et al., 2002; Howles et al., 2005; Tameling et al., 2006; van Ooijen et al., 2008; Kawano et al., 2010; Gao et al., 2011; Bai et al., 2012; Maekawa et al., 2012), probably due to the disruption of H ionic interaction which destabilizes the closed NB-ARC conformation, favoring ADP to ATP exchange and leading to NLR conformational change and activity. Although RRS1 deviates from the canonical MHD motif, comprising LHK instead (van Ooijen et al., 2008), the central H442 in RRS1-S is conserved and was mutated to achieve an RRS1-S GOF allele. However, the adjacent change from D (aspartate) to lysine (K443) inverts the negative charge which is thought to stabilize an α-helix in contact to RNBS-B (Sensor I) (Takken et al., 2006; van Ooijen et al., 2008). Thus, the function of RRS1-S LHK motif might be impaired in its wildtype allele already.

2.3.3. Leucin-rich repeat (LRR)

The variable LRR domain consisting of diverse numbers and lengths of leucine-rich repeats carries out a dual function of NLR autoinhibition and pathogen recognition. Although mutations in this part of RRS1 could be very interesting to test effector recognition specificities, due to the high variability of the LRR domain and the technical limitations for introducing and testing targeted amino acid exchanges, no mutations were included in this domain.

2.3.4. WRKY domain

Both RRS1-S and RRS1-R carry a conserved WRKY domain at their C-terminus, but the two proteins differ by a 90 amino acids extension in RRS1-R compared to RRS1-S (Deslandes et al., 2002). Disruption of RRS1-R *in vitro* DNA binding led to an *in vivo* autoactive phenotype in the *Arabidopsis* ecotype Nd-1 (Noutoshi et al., 2005). To study the

functional relevance of RRS1-S WRKY domain and its ability to bind to DNA, the same insertion mutation described for RRS1-R (Noutoshi et al., 2005) as well as a mutation of the highly conserved lysine K1215 in the WRKY motif, both predicted to disrupt DNA binding, were introduced into RRS1-S expecting GOF alleles.

2.3.5. Evaluating modified RRS1-S activities

According to the explanations given above, the own promoter construct of *RRS1-S* with an N-terminal triple flag and triple HA tag connected by a TEV-cleavage site (*3FTH-RRS1-S*) was modified by site-directed mutagenesis to implement a certain set of predicted loss- and gain-of-function mutations summarized in Table 1.

Table 1: Overview on planned mutations in *RRS1-S*

mutation	domain/motif affected	predicted effect
R20A	TIR	LOF – downstream signaling
H26A	TIR	LOF – interactions (w/ RPS4)
Y101A	TIR	LOF – interactions (w/ RPS4)
K185A	P-loop	LOF – ATP binding
D254A	Walker B	LOF – Mg^{2+}-coordination
D255E	Walker B	GOF – ATP hydrolysis
R283G	RNBS-B	LOF – ATP sensing
H442A	MHD-like	GOF – conformational change
K1215A	WRKY	GOF – loss of DNA binding
slh1	WRKY	GOF (Noutoshi *et al.*, 2005)

Red – predicted loss-of-function (LOF) mutations; green - predicted gain-of-function (GOF) mutations.

In order to rapidly screen for *RRS1-S* LOF or GOF alleles, transient assays were performed. *Agrobacterium*-mediated transient co-expression of *RPS4* and *RRS1* led to effector-dependent cell death in tobacco *Nicotiana* (*N.*) *benthamiana* or *N. tabacum*, respectively (Narusaka et al., 2013b; Williams et al., 2014). Expressing the mutated versions of *RRS1-S* in tobacco should then lead to loss of effector-dependent cell death response for LOF or gain of effector-independent cell death for GOF alleles. However, the positive control for *RPS4*- and *RRS1*-mediated effector-dependent cell death did not succeed. Unlike previously published (Williams et al., 2014), no clear cell death phenotype could be observed in any experimental setup despite of the use of different tobacco cultivars (*N. benthamiana* and *N. tabacum*) and various construct dilution combinations (data not shown).

Because of the unclear cell death phenotype in my hands, the transient expression system was not applicable to screen the functionality of the mutant *RRS1-S* constructs. Thus, several *RRS1-S* constructs were chosen to generate stable transgenic lines in *Arabidopsis* Col-0 (Table 2). After *Agrobacterium*-mediated transformation of Col-0 *rrs1a*, T1 plants were grown and selected based on their 3FTH-RRS1-S protein expression. Selected lines were propagated to obtain T2 generation. T2 with a 3:1 segregation ratio for the transgene, indicating a single insertion, were grown and again probed for protein levels. For all T2 plants evaluated, no obvious growth phenotype could be observed (data not shown) as would be expected for an autoimmune variant of an NLR as observed in the autoimmune mutant allele *snc1* or RPS4 over-expressing plants (Li et al., 2001; Zhang et al., 2003; Wirthmueller et al., 2007; Heidrich et al., 2013).

Table 2: *RRS1-S* constructs used for creating stable *Arabidopsis* transformants

mutation	domain/motif affected	predicted effect
H26A	TIR	LOF – interactions (w/ RPS4)
K185A	P-loop	LOF – ATP binding
D255E	Walker B	GOF – ATP hydrolysis
H442A	MHD-like	GOF – conformational change
K1215A	WRKY	GOF – loss of DNA binding

Red – predicted loss-of-function (LOF) mutations; green - predicted gain-of-function (GOF) mutations

In line with these findings was the observation that *3FTH-RRS1-S* over-expressed under the constitutive 35S-promoter did not show any obvious growth phenotype in various Col-0 genetic backgrounds (wt, *rrs1a/b*, *rps4a/b*, *eds1-2*) independent of the levels of transgenic protein (data not shown), which is in accordance with an hypothesized negative regulatory role of RRS1 in *Arabidopsis* before defense activation (Noutoshi et al., 2005; Williams et al., 2014).

For the mutated *3FTH-RRS1-S* alleles, T3 generations of single T2 plants were obtained and homozygous lines for the transgenes selected. Examination of protein levels, growth and defense phenotype of these homozygous lines is currently ongoing.

2.4. RPS4 pull-down reveals putative interactors

Although the immune outputs of NLR activation such as ROS burst, calcium signaling and MAP kinase cascade activation, SA production and transcriptional reprogramming of defense genes are well characterized, not much is known about direct NLR downstream signaling processes and their exact mode of action in defense. To improve the understanding of direct NLR downstream actions, the association of RPS4-HS in pre- and post-activation complexes was examined by StrepTactin-mediated pull-down analyses.

As both sufficient protein levels and efficient protein activation are critical for this analysis, *OE-RPS4-HS* plants in different genetic backgrounds were used in the T-shift system described above (see section 2.1), allowing a strong and simultaneous activation of RPS4-dependent immunity outputs. For this, plants were grown at 28°C to suppress autoimmune activity of RPS4-HS, while RPS4-dependent immunity was activated by shifting plants to 19°C. At 8h post T-shift, plants were harvested to examine post-activation RPS4-protein associations, whereas pre-activation complexes were determined using immune-suppressed control plants grown continuously at 28°C. For the post-activation analysis, *OE-RPS4-HS* in Col-0, *eds1-2* and *rrs1a* genetic backgrounds were used to evaluate the requirements of *EDS1* and *RRS1a* for RPS4 complex assembly. As *EDS1* expression and protein accumulation was suppressed by high growth temperature (Yang and Hua, 2004; Heidrich et al., 2013; Peine, 2013), and thus the *OE-RPS4-HS* Col-0 line already fails to accumulate considerable amounts of this key immune regulator at 28°C, the *OE-RPS4-HS eds1-2* mutant line was not included for pre-activation analysis, which was done in the *OE-RPS4-HS* Col-0 line only.

In signaling competent *OE-RPS4-HS* overexpression lines, a strong transcriptional reprogramming is induced after temperature shift (Heidrich et al., 2013) which probably leads to a re-composition of plant proteome, changing abundance of certain proteins and thus changing the probability to capture induced proteins due to their cellular abundance by unspecific background binding to the matrix. To enable discrimination of unspecific background and specific RPS4-HS-mediated binding, *OE-RPS4-YFP* plants were included as a control in which *RPS4*-mediated defense was induced after T-shift but RPS4-YFP could not bind to the matrix. StrepTactin-mediated RPS4-HS pull-down was done in four independent biological replicates using whole leaf extracts, thus including the sum of endomembrane-asscociated and nuclear RPS4 fractions (Wirthmueller et al., 2007). Biotin-eluted fractions were analyzed by LC/MS using Easy nLC1000/QExactive MS by

the Protein Mass Spectrometry Service at the Max Planck Institute for Plant Breeding Research.

The total number of proteins identified varied between samples, with some replicates showing a much lower number of identified proteins, but for a common set of identified proteins good consistency was found (Figure S 2). Pull-down efficiency of RPS4 was evaluated by western blot and showed variable RPS4 protein amounts in the eluate fractions of the various *OE-RPS4-HS*, but not *OE-RPS4-YFP* samples after biotin elution (Figure 17).

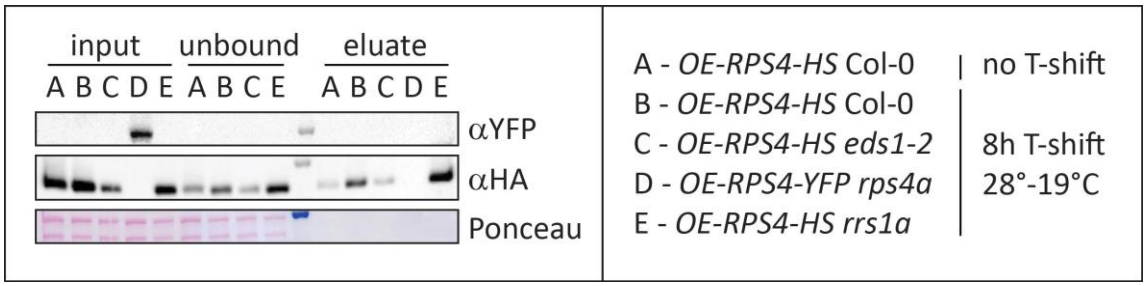

Figure 17: RPS4-HS, but not RPS4-YFP can be pulled down with and specifically eluted from StrepTactin beads.

OE-RPS4-HS and *OE-RPS4-YFP* plants in different genetic backgrounds were grown at 28°C to suppress autoimmunity. 3-week-old plants were shifted to 19°C to induce RPS4-dependent signaling and tissue was harvested 8h after T-shift. For pre-activation complexes, *OE-RPS4-HS* plants continuously grown at 28°C were harvested at the same time. Whole leaf extracts were used for StrepTactin-mediated protein pull-down. RPS4-YFP or RPS4-HS was monitored by western blot using αGFP or αHA antibody, respectively. Ponceau S staining indicated equal protein loading and transfer to the membrane. In eluate fractions, background protein bands were missing due to previous purification steps.

However, detected label-free quantification (LFQ) values for RPS4 by the sensitive mass-spectrometry approach ranged from 25.5 to 27, describing differences in RPS4-HS amounts ranging from not significantly different (*OE-RPS4-HS* Col-0 and *rrs1*a, T-shift) to a 2.5 to 2.7 fold higher detection in *OE-RPS4-HS* Col-0 after T-shift compared to uninduced samples or *OE-RPS4-HS eds1-2*, respectively. Although these differences were classified as statistically significant by student's t-test (Iris Finkemeier), RPS4-HS was detected in all samples in considerable amounts allowing a between-sample comparison of the identified proteins. Most of the proteins identified during pull-down were detected in one condition, but not in another, thus rendering the comparison of protein hits qualitative and not quantitative.

Between different samples, the total number of detected proteins varied between 425 and 474. For further analysis, proteins identified in at least two replicates of the respective *OE-RPS4-HS* samples, but completely absent in the *OE-RPS4-YFP* sample were taken into account.

2.4.1. 70% of identified proteins are shared among RPS4 pre- and post-activation complexes

Comparison of proteins associated with RPS4 before (pre-activation) and after (post-activation) T-shift revealed a core set of 40 proteins shared between inactive and active RPS4, while 8 and 10 proteins were identified only in the pre- or post-activated states of RPS4, respectively (Figure 18, Table S 3).

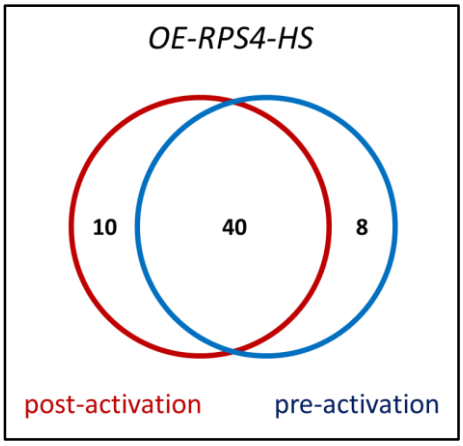

Figure 18: Pre- and post-activation complexes share ~70% of RPS4 interactors.
Venn diagram summarizing total number of specific RPS4 co-purified protein hits detected in pre-activation (plants permanently grown at 28°C) versus post-activation (plants shifted to 19°C for 8h) complexes. Protein hits designated as RPS4-HS specific were detected in at least 2 independent biological replicates and with at least 2 unique peptides in pre- and/or post-activation samples, but were absent in *OE-RPS4-YFP*.

Most of the proteins identified in RPS4 pre- and post-activation complexes were shared between both samples, and the number of hits unique for each sample was in a range not suitable for bioinformatical enrichment analysis. Thus, gene-ontology (GO-) term enrichments were determined for the complete dataset of RPS4 co-purified proteins using agriGO (http://bioinfo.cau.edu.cn/agriGO/analysis.php) to gain insight into the functional relevance and cellular distribution of identified proteins. As summarized in Table 3A, significant GO term enrichment was found for stress response, more specifically response

to temperature, abiotic stimulus and defense response, which is in agreement with the applied treatment of the T-shift and concomitant RPS4 defense activation. Moreover, proteins involved in amino acid and protein metabolism/translation, as well as protein folding were enriched in the RPS4 pull-down samples, hinting at an implication of RPS4 in these processes.

Table 3: Chosen GO-terms enriched in RPS4-HS co-purified proteins based on agriGO

A.

GO-term	# input	# reference	p-value	FDR-corrected
response to stress	16	2320	$2.2 \cdot 10^{-7}$	$1.2 \cdot 10^{-5}$
metabolic process	32	10614	$8.5 \cdot 10^{-6}$	$1.7 \cdot 10^{-4}$
response to temperature stimulus	7	485	$9.1 \cdot 10^{-6}$	$1.7 \cdot 10^{-4}$
response to abiotic stimulus	11	1471	$1.1 \cdot 10^{-5}$	$1.8 \cdot 10^{-4}$
protein folding	5	275	$6.6 \cdot 10^{-5}$	0.0009
cellular protein metabolism	15	3487	$1.6 \cdot 10^{-4}$	0.0017
cellular nitrogen compound metabolism	5	506	0.001	0.0076
cellular amino acid and derivative metabolism	5	682	0.0037	0.022
defense response	5	766	0.0061	0.032
translation	7	1445	0.006	0.032

B.

GO-term	# input	# reference	p-value	FDR-corrected
cytoplasm	37	6822	$8.6 \cdot 10^{-15}$	$1.4 \cdot 10^{-12}$
chloroplast stroma	10	249	$6.2 \cdot 10^{-12}$	$1.5 \cdot 10^{-10}$
organelle	35	8155	$1.0 \cdot 10^{-10}$	$1.7 \cdot 10^{-9}$
intracellular organelle part	20	2561	$4.6 \cdot 10^{-10}$	$6.4 \cdot 10^{-9}$
chloroplast	20	2740	$1.5 \cdot 10^{-9}$	$1.9 \cdot 10^{-8}$
cytosol	10	912	$1.1 \cdot 10^{-6}$	$9.4 \cdot 10^{-6}$
thylakoid	7	376	$1.8 \cdot 10^{-6}$	$1.5 \cdot 10^{-5}$
macromolecular complex	13	2180	$1.8 \cdot 10^{-5}$	$1.2 \cdot 10^{-4}$
ribosome	5	524	0.0012	0.0063
protein complex	8	1443	0.0014	0.0072

p-value – probability value; FDR – false discovery rate

The enrichment of GO terms in protein metabolism and stability might be due to the temperature stress plants have been exposed for the activation of RPS4, inducing a heat stress response accompanied by the reorganization of protein synthesis and production of HSPs. Enrichment in protein folding components can be caused by the overexpression of RPS4 which requires as effective regulation as possible to contain autoactivity. Also, as

mentioned above, highly abundant proteins might be detected independent of RPS4 interaction. However, the absence of these proteins in the *OE-RPS4-YFP* T-shifted control sample suggests their specific identification in the pull-downs of RPS4-HS.

Notably, regarding their localization proteins were enriched mostly for chloroplast stroma and thylakoids as well as cytosol, but also enrichment for ribosome and protein complexes was displayed (Table 3 B), former supporting the finding of functions in protein metabolism.

Apart from GO term analysis, manual scrutiny of the protein list revealed a couple of interesting candidates involved in processes such as transcription (RNA binding protein 47A (RBP47A), Decapping 5 (DCP5)), translation (ribosomal proteins At1G59359, At3G09500, At5G24490, At5G27700, At5G60670, an Elongation factor P (EF-P) family protein and the Ribosome recycling factor RRF), redox processes (Thioredoxin 3 (TRX3)), proteasome (proteasome regulatory particle Hapless 15 (HAP15), 26S proteasome regulatory complex subunit Rpn2), secretion (ARF-GAP domain 9 (AGD9)) and immunity (Binding partner of ACD11 1 (BPA1)) which will be discussed below (see section 3.4).

2.4.2. RPS4 post-activation complex partners depend on EDS1 and partly on RRS1a

Apart from the comparison of RPS4 pre- and post-activation complexes, the analysis was intended to establish the dependency of RPS4 co-purified proteins on its signaling partners EDS1 and RRS1a. For this purpose, T-shifted samples of *OE-RPS4-HS* in Col-0, *eds1-2* and *rrs1a* backgrounds were compared, revealing an almost complete dependency of RPS4-HS co-pulled down proteins on *EDS1* and a partial dependency on *RRS1a* (Figure 19 A, Table S 1). While the RPS4 quantification values were similar in *OE-RPS4-HS* Col-0 and *rrs1a*, they were lower in the *eds1-2* mutant background. However, RPS4 quantities were similarly lower in the *OE-RPS4-HS* pre-activation compared to the post-activation sample, but still majority of the identified proteins were shared among both samples. Thus, absence of EDS1 probably led to the loss of interactions independent of the lower RPS4 quantity in *eds1-2*.

As illustrated in Figure 19 B, all proteins identified in *OE-RPS4-HS* Col-0 were absent in *eds1-2*, except RPS4 which was detected in all genotypes and two other protein hits, namely RBP47A and CP12 (Figure 19 B, cluster 1, 2). Only a small subset of 12 out of 44 proteins identified in *OE-RPS4-HS* Col-0, including RPS4 itself, were present in the *rrs1a* mutant background, suggesting that the other 32 are *RRS1*-dependent (19 B,

cluster 3). Interestingly, some proteins could be detected in *OE-RPS4-HS rrs1a* only, creating a cluster (4) of proteins enriched in the *rrs1a* mutant background (Figure 19 B) containing another ribosomal protein (AT3G47370), the 26S proteasome regulatory subunit Rpn7, a cysteine synthase (CYCS1) and the eukaryotic translation initiation factor 4g (EIF4G).

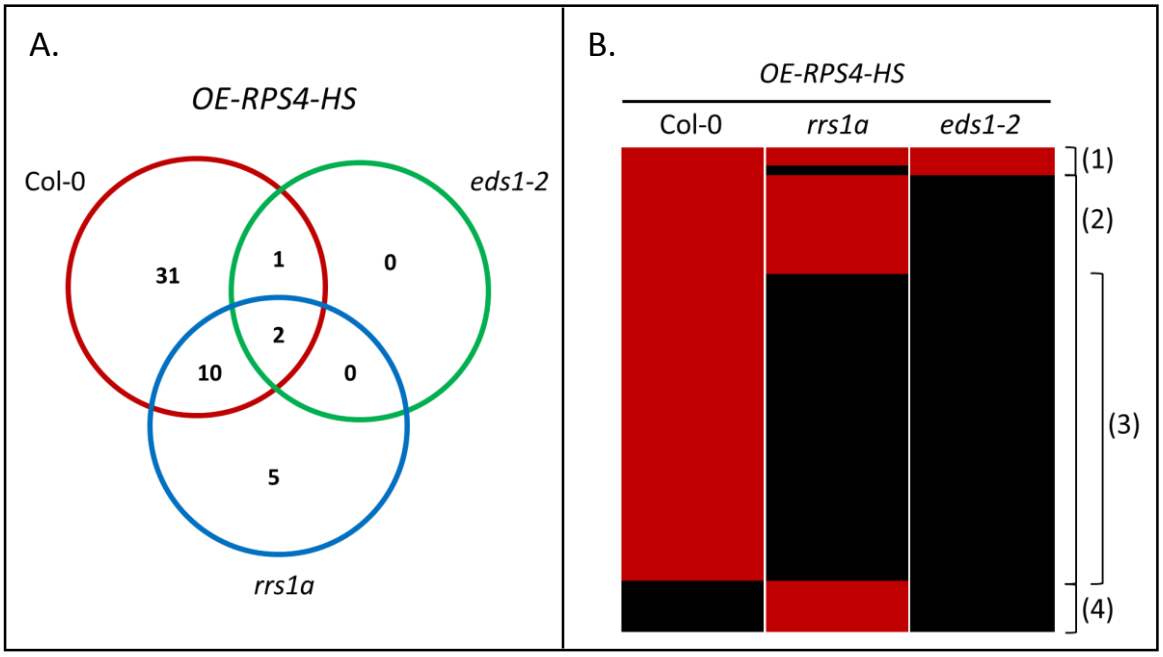

Figure 19: Genotype comparison shows detected proteins almost completely depend on *eds1-2* and partially on *rrs1a*.

Proteins detected in at least 2 independent biological replicates with at least 2 unique peptides in T-shifted *OE-RPS4-HS* Col-0, *eds1-2* or *rrs1a*, but absent in *OE-RPS4-YFP rps4* were compared. (**A**) Venn diagram summarizing total number of specific protein hits detected in different genetic backgrounds. (**B**) Alignment of RPS4-HS co-purified proteins among Col-0, *eds1-2* and *rrs1a* background revealed four main clusters of (1) *EDS1*-independent, (2) *EDS1*-dependent, (3) *RRS1a*-dependent RPS4-HS interactors and (4) RPS4-HS interactors enriched in *rrs1a*. Red – detected in RPS4-HS pull-downs at least two replicates. Black – not detected or detected only in one replicate.

In summary, proteins identified with the RPS4-HS pull-down approach are almost completely dependent on EDS1 and partially depend on the presence of RRS1a. Since the proteins identified mostly overlap with shared and post-activation hits in section 2.4.1 above, they will be discussed together.

3. Discussion

The presented study aimed at extending current knowledge on plant NLR-mediated immunity by examining the paired TNL receptors RPS4 and RRS1. NLR regulation is sophisticated and multi-layered: from (1) the modulation of gene expression, to (2) RNA processing and transport, through to (3) positive and negative regulation of NLR degradation via the plant proteasome and (4) control of NLR localization, manifold surveillance mechanisms play a role in NLR-mediated immune responses (Kadota et al., 2010; Johnson et al., 2012; Copeland et al., 2013; Xia et al., 2013; Duplan and Rivas, 2014).

Nonetheless, little is known about the signaling leading to resistance conditioned by NLR receptors, including *Arabidopsis* RPS4 and RRS1. Recent publications linking RPS4 and other nuclear NLRs to transcription factors suggest a short downstream pathway for some NLRs, leading to transcriptional reprogramming of host cells for defense (Zhu et al., 2010b; Chang et al., 2013; Inoue et al., 2013; Padmanabhan et al., 2013; Kim et al., 2014; Xu et al., 2014b). Uncoupling of cell death initiation from transcriptional reprogramming and defense (Heidrich et al., 2011; Bai et al., 2012) indicates differential NLR signaling mechanisms in the nucleus and in the cytoplasm. However, the precise nature of these defense pathways remains elusive. In this study, the interplay of RPS4 and RRS1 as well as their protein or chromatin associations were examined to identify novel NLR downstream components.

A fascinating feature of *RPS4*/*RRS1* and *RPS4b*/*RRS1b* is their head-to-head linkage in the genome, which is correlated with functional cooperativity. A main open question is how these two or even four TNLs are interconnected on a molecular basis. Although a sensor-executor interaction was suggested for RPS4 and RRS1, this model fails to explain the entirety of available information on RRS1 contribution to RPS4-induced autoimmunity. Investigation of paired NLR functions as a plant mechanism to broaden effector recognition capacities will help to understand how plants stand up to a plethora of rapidly evolving pathogens.

3.1. *RRS1* contributes to *RPS4*-induced autoimmunity

To explore the interdependency of *RPS4/RRS1* and *RPS4b/RRS1b*, *rrs1a/b* double mutants overexpressing *RPS4* were characterized. I showed that *Arabidopsis* immune outputs induced by *RPS4* overexpression, such as dwarfism and transcriptional reprogramming of defense genes, partially depend on *RRS1 a* and *b* (Figures 4, 8). RPS4 protein accumulation and post-activation *RPS4* mRNA levels were reduced in *rrs1a/b* (Figures 5, 7), but the underlying mechanism remain elusive. Although I showed that RPS4 is degraded by the 26S proteasome, the effect of *rrs1a/b* on RPS4 degradation remains unclear, since different quantitative results were obtained using different tagged versions of RPS4 (Figure 10). This might be due to differing RPS4 activity or steric hindrances due to different tag sizes.

Supporting the role of the 26S proteasome in RPS4 stability control and immunity, the *HSP90* mutant allele *hsp90.3-1* allowed increased RPS4 accumulation, but showed increased susceptibility to *Pst* AvrRps4 (Huang et al., 2014a). Notably, this uncouples NLR accumulation and resistance activity. *hsp90.3-1* might be impaired in its chaperone function, thus preventing proper folding of RPS4 and causing enhanced *Pst* AvrRps4 susceptibility due to conformational hindrances in the NLR. The increased RPS4 accumulation could be a side-effect of the conformational hindrance, which might prevent interactions needed to target RPS4 for proteasomal degradation, for example with SRFR1 (Li et al., 2010). However, misfolding of proteins usually stimulates rather than prevents their degradation (Liu and Li, 2014). Thus the increased RPS4 accumulation observed in *hsp90.3-1* implies an active contribution of HSP90s to RPS4 folding and stability control. Which other translational or posttranslational mechanisms influence RPS4 accumulation and stability, particularly in the *rrs1a/b* double mutant background, remains unclear.

Besides decreased RPS4 protein amounts, lower *RPS4-YFP* mRNA levels were observed in *rrs1a/b* compared to Col-0 and *eds1-2* after T-shift activation of immunity (Figure 7), suggesting a transcriptional or posttranscriptional regulation of *RPS4* in dependence of *RRS1*. One obvious idea is that disruption of *RRS1a* (and *RRS1b*) in a native genomic context negatively influences *RPS4* transcription due to the close linkage and shared bidirectional promoter of the genes. In animals and humans, head-to-head arrangement of genes is commonly associated with their co-expression and regulation by a common set of transcription factors, and further co-regulation has been observed between pairs of head-to-head genes (Li et al., 2006; Chen et al., 2010; Chen et al., 2014). However,

the rice cooperative CNL gene pairs *Pikh-1*/*Pikh-2* and *Pi5-1*/*Pi5-2* are differentially expressed upon pathogen recognition (Zhai et al., 2014; Lee et al., 2009).

An effect of the *rrs1a/b* mutation on native *RPS4* transcription cannot be ruled out, but in my study the effect of *rrs1a/b* on transcripts of *RPS4* expressed under the constitutive 35S promoter was determined. T-DNA insertions can exert a silencing effect on 35S-promoter driven constructs (Daxinger et al., 2008), but since *RPS4-YFP* mRNA resting levels were equal in *rrs1a/b* and Col-0 and changed only after T-shift activation of immunity, post-transcriptional processes might be involved in reducing *RPS4* mRNA stability in *rrs1a/b*.

There is increasing evidence for the importance of RNA-based regulation in plant immunity (Staiger et al., 2013). One process involved specifically in *TNL*-mediated defense is nonsense-mediated RNA decay (NMD), a surveillance mechanism to degrade aberrant mRNAs resulting from mutations, transcription errors or alternative splicing (Gloggnitzer et al., 2014). Upon bacterial infection, plant cells inhibit NMD to allow increased *TNL* transcript accumulation, and impairing NMD caused autoimmunity through *TNL* gene deregulation (Riehs-Kearnan et al., 2012; Gloggnitzer et al., 2014). These data raised the question if decreased *RPS4* mRNA accumulation in *rrs1a/b* might depend on its degradation via the NMD pathway. However, in an RNA sequencing dataset generated by Gloggnitzer and coworkers, no significant change in transcript accumulation could be detected for *RPS4a*, *RPS4b*, *RRS1a* or *RRS1b* in NMD deficient plants compared to the control (Gloggnitzer et al., 2014). Despite the facts that *RPS4* alternative splicing is induced upon pathogen challenge and its alternative transcripts are necessary for defense (Zhang and Gassmann, 2003, 2007), *RPS4* is unlikely to be targeted by NMD. However, it would be interesting to examine the levels of alternative *RPS4* transcripts in *rrs1a/b* as one measure of the effects of *rrs1a/b* on *RPS4* mRNA processing.

What other RNA-related regulatory mechanisms could be involved in the control of *RPS4* transcripts in the presence or absence of RRS1? Plant endogenous microRNAs (miRNA) and small interfering RNA (siRNA) cause transcript degradation or silencing (Staiger et al., 2013). Both miRNA and siRNAs were shown to impact plant immunity by post-transcriptional regulation of *CNL* genes (Shivaprasad et al., 2012; Boccara et al., 2014). Although to date no role of miRNAs or siRNAs in *RPS4/RRS1*-mediated resistance has been reported, certain *TNL* transcripts might be regulated by these endogenous regulatory RNAs. Indeed, cosuppression of *TNL* transcripts from the Col-0 *RPP5* locus was reported upon *SNC1* overexpression (Yi and Richards, 2007). To test if RNA silencing induced by

aberrant *RRS1* mRNA in *rrs1a/b* could potentially affect *RPS4* mRNA stability, *RPS4* and *RRS1* genomic or cDNA sequences were aligned by ClustalW2 (*www.ebi.ac.uk/Tools/msa/clustalw2/*) or Blast (*www.ncbi.nlm.nih.gov/blast/Blast.cgi*). However, no nucleotide overlap between both genes in a range needed for co-silencing of *RPS4* with *RRS1* was detected.

Another unsolved issue is whether decreased RPS4 protein accumulation in *rrs1a/b* is the cause for the weakened growth phenotype of overexpressed *RPS4* (Figure 4), or if disruption of RPS4 functionality by the absence of RRS1 causes a reduction of both RPS4 protein levels and phenotype severity. RRS1 protein might be necessary for the assembly of a functional RPS4 pre-activation complex, thus stabilizing RPS4 and supporting its function even in the context of overexpression. While in an *rrs1a* single mutant background the highly similar RRS1b might be able to complement for the loss of RRS1a, the complete absence of RRS1 a and b in *rrs1a/b* would impede proper complex formation and leave RPS4 vulnerable for degradation.

This would also explain the suppressive effect of *rrs1a/b* on *RPS4*-induced transcriptional outputs after T-shift (Figure 8). A specific effect of *RRS1a* on *RPS4*-mediated T-shift-induced transcriptional outputs was reported previously, with only a subset of all *RPS4*-regulated, *EDS1*-dependent genes being quantitatively affected by the absence of *RRS1a* (Heidrich et al., 2013). Moreover, promoters of those genes were enriched for W-boxes, constituting a putative link to the RRS1 WRKY domain (Heidrich et al., 2013). By contrast, the *rrs1a/b* double mutant constitutes a strong – though not complete – suppressive effect on all *RPS4*-induced genes tested, including selected *rrs1a*-dependent genes from the microarray analysis by Heidrich and coworkers (data not shown). This suggests a general rather than specific influence of *rrs1a/b* on *RPS4*-induced gene expression changes upon T-shift, probably due to decreased RPS4 protein accumulation in *rrs1a/b*.

3.2. Towards the detection of RRS1-S chromatin association sites in *Arabidopsis*

Both NLR receptors and WRKY transcription factors are well-known components of plant immunity, but a combination of NLR and WRKY domains in a single protein is rare. Only three genes (*RRS1a*, *RRS1b* and *At4G12020*) encoding for these of chimeric proteins have been predicted in *Arabidopsis* (Saucet, 2013). Immune activation by disruption of RRS1-R WRKY DNA binding suggested negative regulatory functions at the chromatin (Noutoshi et al., 2005). Thus, I performed ChIP to test RRS1-S chromatin binding and to identify its target genes.

I showed that transgenic N-terminally 3FTH-tagged *RRS1-S* is fully functional in *Pst* AvrRps4 defense without affecting basal defense to *Pst* DC3000 (Figure 11). Predominantly nuclear localization was detected for 3FTH-RRS1-S (Figure 14), supporting a nuclear function. Several ChIP-qPCR approaches testing for RRS1-S enrichment at selected promoter regions (data not shown) as well as ChIP-seq aimed to obtain a genome-wide view of RRS1-S DNA associations did not identify convincing RRS1-S binding sites at the chromatin. Since the ChIP protocol was optimized for WRKY transcription factors, and enrichment of WRKY18 promoter regions could be detected in the positive ChIP control pWRKY18:WRKY18-HA (Rainer Birkenbihl, unpublished), RRS1 ChIP was repeated with both *Pst* AvrRps4 and mock treated samples to improve sample replication and provide a broadened view on RRS1 chromatin association dynamics in *Arabidopsis* defense signaling.

Before approaching further ChIP-seq experiments, RRS1-S chromatin-binding capacities in general should be evaluated, since to date DNA binding was reported for RRS1-R only (Noutoshi et al., 2005). The C-terminal extension of RRS1-R compared to RRS1-S might not only differentiate PopP2 recognition (Deslandes et al., 2002; Deslandes et al., 2003), but also their DNA binding capacities. Although transgenic 3FTH-RRS1-S is functional in *Pst* AvrRps4 resistance (Figure 11), the N-terminal 3FTH-tag could disturb DNA binding without affecting AvrRps4-triggered resistance. To test for general DNA binding ability of 3FTH-RRS1-S, an *in-vitro* W-box binding assay should be performed, as was done for RRS1-R (Noutoshi et al., 2005). Also, a DNA adenine methyltransferase identification (DamID) approach (Germann et al., 2006; Orian, 2006) might prove useful to generally demonstrate RRS1-S DNA binding, and furthermore could be used to identify RRS1-S DNA binding sites by sequencing of obtained DNA fragments.

A ChIP-seq repeat experiment is currently under analysis, and general RRS1-S DNA-binding capacities can be further tested. However, the relatively small protein levels in the 3FTH-RRS1-S lines might be too low for efficient immunoprecipitation, and thus not allow enrichment of chromatin above background. Markedly higher RRS1-S protein amounts in generated 35S-promoter driven overexpression lines could tip the balance to enable sufficient chromatin enrichment in *35S:3FTH-RRS1-S* versus control samples, but also entail the risk of unspecific DNA binding artefacts due to excessive protein accumulation in the nucleus.

The identification of RRS1 chromatin binding sites to provide a dynamic view of RRS1 DNA association before and after effector activation would advance current knowledge on the mode of *RPS4/RRS1* action in plant immunity, which is particularly meaningful in the light of conserved NLR signaling pathways among different plant families (Maekawa et al., 2012; Narusaka et al., 2013b, a; Narusaka et al., 2014).

3.3. Requirement of domain integrity for RRS1-S function and activity

To dissect the requirement of distinct RRS1-S domains for its function in *RPS4/RRS1* defense activation and signaling, several targeted point mutations were introduced into the *RRS1-S* genomic construct. A transient screening for gain- or loss-of-function alleles of *RRS1-S* was not useful as the reported read-out of cell death induction in *N. tabacum* upon co-expression of *RPS4, RRS1* and *AvrRps4* (Williams et al., 2014) could not be reproduced under our conditions. While the published cell death phenotype was obtained with *RPS4/RRS1* overexpression, I was working with own promoter constructs and could hardly detect RPS4 and RRS1 protein accumulation in tobacco (data not shown). The use of different vector backbones and *Agrobacterium* strains for infiltration might further influence construct expression. Most crucially, I used the Col-0 *RRS1-S* allele, while the cell death assays described by Williams and coworkers were using *RRS1-R* (Williams et al., 2014). In *Arabidopsis*, *RRS1-R* in Ws-0 triggered a strong HR after AvrRps4 recognition, while Col-0 *RRS1-S* restricted *Pst* AvrRps4 growth without cell death (Heidrich et al., 2011). Thus, *RRS1-S* might lack cell death inducing capacities which are present in *RRS1-R*, and thus fail to induce cell death in *Arabidopsis* and tobacco. Stable transgenic expression of *RRS1-R* in *Arabidopsis* Col-0 conferred the capacity to induce cell

death upon PopP2 recognition (Williams et al., 2014), substantiating the idea that not genetic background, but intrinsic characteristics of *RRS1-S* and *RRS1-R* are responsible for the difference in *RRS1* cell death induction. The Col-0 *RRS1-R* transgenic lines could be used to compare *RRS1-R* and *RRS1-S* characteristics independent of plant genetic background. For example, testing the dynamics of RRS1-R and RRS1-S chromatin associations with or without cell death induction after effector recognition might help to unravel the molecular framework for RRS1-R and RRS1-S distinct recognition specificities and outputs.

The number of *RRS-S* variants was narrowed down to test their functionality in stable transgenic *Arabidopsis* Col-0 *rrs1a*. No obvious growth phenotype could be detected in T1 and T2 generations. Testing of homozygous T3 generations for plant growth at low temperatures and for *Pst* AvrRps4 resistance should reveal the functionality of RRS1-S alleles and improve our understanding of RRS1-S domain functions. Potential gain- or loss-of-function alleles would constitute excellent tools to further explore RRS1-S functions, for example by extending analyses such as ChIP or CoIP/pulldowns to differentiate between DNA or protein associations of active, native or inactive RRS1-S.

For example, a mutation in the conserved RRS1 P-loop motif (K185A) did not impair effector-triggered *RPS4-RRS1*-induced cell death in transient tobacco expression (Williams et al., 2014). Also, the usually highly conserved MHD motif in the ARC2 subdomains deviates in RRS1 compared to other NLRs (van Ooijen et al., 2008). These data support an ATP-independent non-canonical function of *RRS1*.

In contrast to this, *RPS4* function depends on the integrity of its nucleotide binding pocket, as mutation of its P-loop motif suppressed *RPS4* defense inducing capacities (Zhang et al., 2004; Wirthmueller et al., 2007). Interestingly, the same was shown for the rice CNL pair *RGA4* and *RGA5*, where the executor *RGA4*, but not the sensor *RGA5* relied on an intact ATP binding pocket and a functional MHD motif for its function (Césari et al., 2014).

RRS1-S P-loop (K185A), MHD (H442A) and Walker B motif (D255E) variants created in this study are expected to impact RRS1-S ATP binding and hydrolysis and will be functionally characterized in stable transgenic *Arabidopsis*. Despite conservation of defense signaling pathways across plant lineages (Maekawa et al., 2012; Narusaka et al., 2013b; Narusaka et al., 2014), studies in the native *RPS4* and *RRS1* plant background *Arabidopsis*, rather than transient assays in tobacco will help to draw a conclusive model

of the molecular functions and the complex interplay of the two *RPS4/RRS1* TNL pairs during effector recognition and pathogen resistance.

RRS1 WRKY domain was proposed to be an effector virulence target guarded by the canonical NLR part of the protein, because an amino acid insertion in the WRKY domain constitutively activated resistance (Noutoshi et al., 2005). Besides RRS1 direct interaction with the effectors AvrRps4 and PopP2 (Deslandes et al., 2003; Williams et al., 2014), it was shown recently that PopP2 acetylation targets RRS1 WRKY domain and several WRKY transcription factors, many of them implicated in *Arabidopsis* defense responses (Laurent Deslandes, personal communication). PopP2 acetylation activity is required for its avirulence function (Tasset et al., 2010), and actetylation disrupted RRS1 DNA binding (Laurent Deslandes, personal communication). Taken together, these data suggest that RRS1 is a sensor for PopP2 virulence function. Surrogating a variety of WRKY transcription factors, RRS1 might be guarded by the executor RPS4 to intercept effector functions on these essential transcriptional regulators. RRS1 might thus constitute either a guardee or a decoy (see section 1.3). The *rrs1a/b* double mutation retains basal resistance to virulent *Pst* DC3000 (Figure 3), negating a role of *RRS1* in basal resistance and substantiating its role as a decoy. Pathogen perturbance of RRS1 WRKY domain could be conveyed to its guard and signaling partner RPS4 independent of RRS1 canonical NLR functions. Subsequent release of RRS1 inhibitory constraints on RPS4 would then allow downstream signaling activation (compare Figure 1).

The *Arabidopsis* RRS1-S^{K1215A} allele is predicted to lose DNA binding (Marco Llorca et al., 2014) and cause autoimmunity in accordance to the *slh1* phenotype (Noutoshi et al., 2005). Analysis of *Pst* AvrRps4 resistance in this plant line might help to unravel the importance of the RRS1-S DNA binding during AvrRps4 recognition. The mutated conserved K is not only crucial for WRKY function, but also a potential PopP2 acetylation site. Thus, RRS1-S^{K1215A} together with native RRS1-S could potentially be used to test if PopP2 acetylation of K1215 alters RRS1-S capabilities to confer *Pst* AvrRps4 resistance.

Notably, *RRS1* sensor function alone does not explain the impact of *rrs1a* or *rrs1a/b* on effector-independent autoimmunity by overexpressed *RPS4* (Heidrich et al., 2013; Figures 4, 8). An additional positive contribution of *RRS1* in defense responses might be illuminated by the RRS1-S^{H26A} allele that is predicted to disrupt RPS4 and RRS1 TIR heterodimerization (Williams et al., 2014). RRS1 TIR domain suppressed RPS4 TIR-induced cell death in tobacco, whereas RRS1 TIR^{H26A} did not (Williams et al., 2014). Full length RRS1-R^{H26A} misses TIR domain heterodimerization capacity, but still interacts with

RPS4 (Williams et al., 2014). Thus, RRS1-R^{H26A} should be able to form intact signaling complexes with RPS4, and even facilitate RPS4 TIR domain homodimerization through the loss of TIR heterodimerization. Nonetheless, PopP2 recognition is impaired in the RRS1-R^{H26A} mutant (Williams et al., 2014), indicating the requirement of RRS1-RPS4 TIR heterodimers rather than RPS4 homodimer for defense activation. This should be further tested for *Pst* AvrRps4 defense in Col-0 expressing RRS1-S^{H26A}.

Integrating currently available information on *RRS1* and *RPS4*, I propose that full length RPS4 and RRS1 assemble in a pre-activation complex where TIR domain dimerization is prevented by NLR autoinhibitory effects or auxiliary proteins, or preformed TIR dimers are buried in the complex to prevent downstream signaling (Figure 20 C).

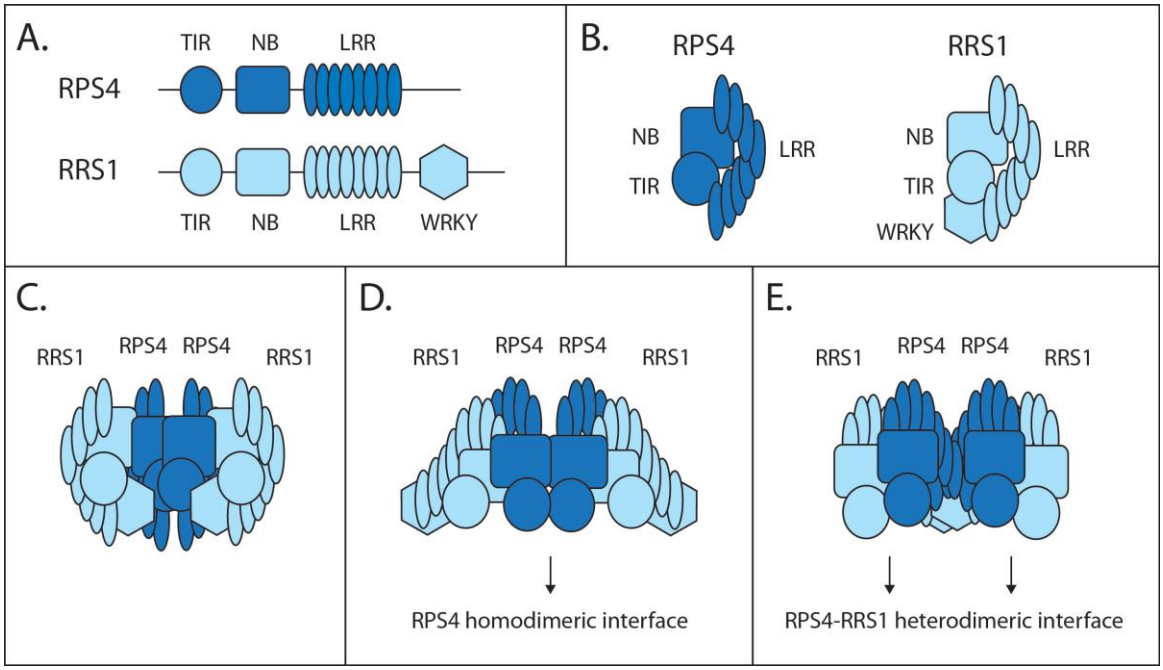

Figure 20: RPS4 and RRS1 domain structure and their rearrangements upon activation.
(A) Domain structure of RPS4 and RRS1. TIR, Toll-/interleukin-1 receptor; NB, nucleotide-binding; LRR, leucine-rich repeat; WRKY, transcription factor DNA binding domain. **(B)** Model for RPS4 and RRS1 three-dimensional (3D) conformation in their inactive state. LRR domain is covering and thus inhibiting TIR and NB for downstream signaling. **(C)** Proposed arrangement of a pre-activation RPS4-RRS1 hetero-tetramer. TIR interactions might be pre-formed but buried in the 3D structure of the complex. **(D, E)** Activation through effector recognition causes rearrangements to allow either TIR homodimeric **(D)** or heterodimeric **(E)** interactions depending on distinct recruitment of downstream components, thereby triggering compartment-specific defense responses.

RRS1 sensing of effector perturbations induces conformational changes, allowing either formation of new TIR dimers or release of preformed TIR dimers to form new interaction

interfaces (Figure 20 D, E). Homodimerization of RPS4 TIR domains might be necessary to trigger cell death in the cytoplasm, whereas nuclear RPS4/RRS1 TIR heterodimers might allow induction of transcriptional reprogramming and trigger pathogen resistance. I suggest that differentiation between RPS4 TIR homomeric and RPS4/RRS1 TIR heteromeric interactions might be assisted by distinct interaction partners in different cellular compartments.

3.4. RPS4 pulldown reveals interactors in defense-related pathways

Plant immune outputs after PTI and ETI induction are well characterized and include ROS burst, calcium signaling and MAP kinase cascade activation, SA production and transcriptional reprogramming of defense genes (Buscaill and Rivas, 2014). Still, direct NLR downstream signaling components remain elusive, suggesting a short signaling pathway or high levels of redundancy. To illuminate the elaborate regulation network of NLR downstream signaling, I analyzed RPS4 protein associations in pre- and post-activation complexes.

RPS4-associated immune complexes were purified from uninduced and T-shift activated *OE-RPS4-HS* leaf tissue and analyzed by mass-spectrometry. A large overlap of detected proteins in *OE-RPS4-HS* samples and the *OE-RPS4-YFP* background control hints at a high proportion of unspecifically bound proteins. To apply stringency for further analysis, only RPS4-HS co-purified proteins detected in at least two replicates with at least two unique peptides, but absent in the *OE-RPS4-YFP* control are discussed.

Meta-analysis of the identified proteins revealed enrichment for chloroplast-localized and cytosolic proteins (Table 3). The strong enrichment of chloroplast proteins was surprising given a nucleo-cytoplasmic localization of RPS4 (Wirthmueller et al., 2007). T-shift activated RPS4-HS was detected weakly in soluble and strongly in microsomal fractions (Heidrich et al., 2011), while transiently expressed RPS4 was detected in microsomal, but not soluble cell fractions in tobacco (Bhattacharjee et al., 2011). A chloroplastic localization of RPS4 – though not specifically tested – is very unlikely, as no chloroplastic signal could be detected in confocal analysis performed to date.

Although annotated protein localization might not always represent the true or exclusive localization of a protein, the enrichment of chloroplastic proteins in the RPS4 pull-down might reflect contaminations rather than actual RPS4 interactors. However, for a couple of defense-related proteins a change of localization has been reported upon certain stimuli. Most interestingly, the nucleo-cytoplasmic tobacco TNL N resistance function to tobacco mosaic virus (TMV) depends on the N receptor interacting protein 1 (NRIP1), which is normally localized to the chloroplast stroma (Caplan et al., 2008). Interaction with the TMV effector p50 redirects NRIP1 to the nucleo-cytoplasmic compartments, where it can associate with N only in complex with p50 to induce cell death (Caplan et al., 2008). Also, the relocalization of potato CNL R3a from cytoplasm to the endosomal compartment upon recognition of its cognate effector AVR3a^{KI}, as well as AVR3a^{KI} recruitment to the endosomes is necessary for HR induction (Engelhardt et al., 2012). The rice pattern recognition receptor XA21 confers broad-spectrum resistance to *Xanthomonas* by detecting the MAMP Ax21. Upon activation, XA21 is cleaved and releases its intracellular kinase domain for translocation to the nucleus, a step crucial for its immune function (Park and Ronald, 2012). *Arabidopsis* Accelerated Cell Death 2 (ACD2), a chloroplastic protein involved in cell death regulation upon infection with virulent and avirulent *Pseudomonas*, shifts localization to chloroplasts, mitochondria and cytosol after pathogen challenge (Yao and Greenberg, 2006).

Even though no chloroplast-localized NLR receptor was reported so far, the chloroplast as a site of SA and ROS production plays important roles in plant defense signaling (Padmanabhan and Dinesh-Kumar, 2010). Notably, chloroplasts are targeted by several *Pseudomonas* effectors, further substantiating an important role of chloroplastic proteins in plant immunity (Jelenska et al., 2007; Jelenska et al., 2010; Rodríguez-Herva et al., 2012). Strikingly, one of those effectors is AvrRps4, which targets chloroplasts through an N-terminal chloroplast transit peptide to allow its virulence function, while its avirulence function was retained in an AvrRps4 form disabled for chloroplast import (Li et al., 2014a). This suggests that AvrRps4 virulence targets are located in the chloroplast, and hints at a role of chloroplastic proteins in *RPS4/RRS1*-mediated resistance to *Pst* AvrRps4.

Besides chloroplast localization, RPS4 co-purified proteins were enriched for the cytosol. This is not surprising, as activated RPS4 was detected in the soluble fraction (Heidrich et al., 2011). The analysis of cytoplasmic interactors can be very interesting as distinct functions of nucleo-cytoplasmic RPS4 have been reported, with nuclear RPS4 mediating translational reprogramming and resistance to *Pst* AvrRps4, and cytoplasmic

RPS4 triggering cell death upon effector recognition (Heidrich et al., 2011). Analysis of cytoplasmic RPS4 interactors could reveal mechanisms involved in the onset of cell death upon RPS4 activation. Although *Arabidopsis* ecotype Col-0 does not induce HR upon *Pst* AvrRps4 recognition, the downstream signaling components in Col-0 and cell death-inducing Ws-0 ecotype are likely conserved. I suggest that immune complexes and signaling cascades are similar among different *Arabidopsis* ecotypes, but more efficient in some (i.e. Ws-0) compared to others (i.e. Col-0) due to minor protein changes like the ones described for *RRS1-R* and *RRS1-S*. Indeed, expression of *RRS1-R* in Col-0 mediates resistance to *Pst* expressing PopP2 and triggers HR upon PopP2 delivery via *Pseudomonas fluorescence* (Williams et al., 2014), suggesting that *RRS1-R* signaling pathways for HR initiation are conserved in Col-0.

Since transcriptional reprogramming of defense gene and *Pst* AvrRps4 resistance is determined by nuclear RPS4, its interactions in the nucleus would be of greatest interest. However, meta-analysis of the achieved data revealed neither enrichment of RPS4 co-purified proteins in the nucleus, nor involvement in transcriptional processes. Also, neither of the described RPS4 interactors EDS1, RRS1 or bHLH84 (Heidrich et al., 2011; Williams et al., 2014; Xu et al., 2014b) was detected. Potentially, subpools of RPS4 are assembled into complexes with different proteins. The interactions with EDS1, RRS1 and bHLH84 might be too weak or transient to allow efficient co-purification with RPS4. This is plausible especially in the context of overexpression, which floods the cells with RPS4 protein and disturbs protein stoichiometry. Also, incomplete leaf tissue homogenization insufficient to disrupt nuclei and release nuclear proteins at the beginning of the pull-down could explain the absence of nuclear interactors. The use of isolated nuclei rather than whole leaf tissue samples for pull-down experiments should allow the identification of nuclear RPS4 interacting proteins to facilitate an insight into RPS4 nuclear functions.

Nevertheless, close examination of identified RPS4-HS interactors gave rise to a number of interesting candidates. The interaction with RPS4 should be verified by alternative methods such as Y2H, *in planta* bimolecular fluorescence complementation (BiFC) or coIPs, particularly since overexpressed RPS4 might unspecifically aggregate with proteins due to its high abundance. If interaction with RPS4 can be confirmed, further studies of protein functions and impact on resistance responses to *Pst* AvrRps4 should be conducted. In the following sections, chosen candidate hits will be discussed regarding their biological functions and relevance in plant immunity.

3.4.1. Transcription and translation

Nuclear RNA binding protein 47A (RBP47A) was detected in the pull-down of all *OE-RPS4-HS* samples. Though missing genotype dependency might be a concern of unspecific binding, RBP47 was not detected at all in the *OE-RPS4-YFP* samples, ruling out its detection was due to stickiness to the beads. RBP47 consists of three RNA-recognition motifs (RRMs) and a glutamine-rich, prion-related N-terminus (Lorković et al., 2000). It binds poly(A)$^+$-mRNA and has a binding specificity for oligouridylates usually highly enriched in intronic sequences and 3'UTRs found in pre-mRNAs (Lorković et al., 2000). RBP47 is structurally related to RBP45 and UBP1 (Oligouridylate binding protein 1), latter functioning in nuclear pre-mRNA maturation (Lorković et al., 2000). Although so far no discrete RNA-modulating function could be detected for RBP45 or RBP47, they are still presumed to play a role in RNA maturation processes due to their structural and biochemical properties (Lorković et al., 2000; Lorković and Barta, 2002). This is further supported by the involvement of nuclear RBP47 in the formation of cytoplasmic stress granules (SG) upon heat stress (Weber et al., 2008). SGs are large aggregates of untranslated mRNPs (messenger-ribonucleoprotein particles) that form under stress conditions, when translation is stalled to re-evaluate which mRNAs are targeted for translation, storage or degradation (Weber et al., 2008). This further supports a role for RBP47 in the regulation of post-trancriptional mRNA processing.

An *EDS1*- and *RRS1*-dependent RPS4-interacting protein found in pre- and post-activation samples is DCP5 (Decapping 5). Decapping of mRNAs irreversibly triggers their degradation. DCP5 interacts with DCP1 and DCP2, components of the *Arabidopsis* decapping complex, and was required for the formation of processing bodies (P bodies), the sites of mRNA storage and decapping (Xu and Chua, 2009). Disruption of P bodies in a *dcp5* mutant led to stabilization and overaccumulation of certain mRNAs (Xu and Chua, 2009), and adaptation to dehydration stress by stress-induced decapping depended on DCP5 (Xu and Chua, 2012). Interestingly, the decapping complex also plays a role in the accumulation of miRNAs (Motomura et al., 2012; Boccara et al., 2014).

Since post-transcriptional RNA regulation generally impacts plant immunity (section 0; Staiger et al., 2013), and SNC1, which contributes to *Pst* AvrRps4 resistance (Kwon et al., 2004; Kim et al., 2010), is targeted for post-transcriptional gene silencing (Yi and Richards, 2007), both RBP47A and DCP5 are worth further examination.

Besides proteins involved in post-transcriptional regulation, the RPS4 pull-down identified a couple of ribosomal proteins (At1G59359, At3G09500, At5G24490,

At5G27700, At5G60670), as well as the chloroplast ribosome recycling factor (RRF) and an elongation factor P (EF-P) family protein, all involved in mRNA translation. Not much is known about the role of translation in plant defense. However, it constitutes an additional layer of regulation to fine-tune the synthesis and accumulation of defense-induced proteins. The specificity of these protein hits has to be scrutinized, though, because the T-shift treatment might induce a plant heat stress response. This might lead to changed transcriptional and translational emphases and increased recruitment or synthesis of ribosomes.

3.4.2. Redox processes

Thioredoxin 3 (TRX3) was found in both pre- and postactivation complexes of RPS4, but was absent in *eds1-2* or *rrs1a*. TRX3 belongs to the cytoplasmic group of thioloxido-reductases involved in cellular redox processes. TRX proteins can buffer cellular redox changes and store redox power to catalyze reduction of disulfide bridges in their target proteins (Meyer et al., 2012). Reduction of intermolecular disulfide bridges disrupts covalent protein-protein linkage, releasing the reduced interaction partners. TRX3 and its closest homolog TRX5 interacted with NPR1 (non-expressor of PR genes 1) (Tada et al., 2008), a crucial component of SA-mediated defense responses and systemic acquired resistance (SAR). In the absence of pathogen infection, NPR1 resides mainly in the cytoplasm in homo-oligomers formed by intermolecular disulfide bridges (Mou et al., 2003). SA accumulation during plant defense responses led to a change in cellular redox conditions, releasing NPR1 monomers for translocation to the nucleus through its reduction by TRX5 and TRX3 (Mou et al., 2003; Tada et al., 2008). Nuclear localization of NPR1 was needed for defense gene activation (Kinkema et al., 2000; Zhang et al., 2010b), likely through NPR1 direct interaction with plant TGA transcription factors (Zhang et al., 1999; Després et al., 2000; Zhang et al., 2003; Rochon et al., 2006; Boyle et al., 2009). Thus, TRX3 together with its homolog TRX5 plays an important role in NPR1-mediated defense gene activation.

Apart from its reductase activity, TRX3 enhanced *Arabidopsis* heat-shock tolerance by functioning as a molecular chaperone at high temperatures (Park et al., 2009). Whether its identification in the RPS4 pull-down can be assigned to its thioloxidoreductase function in plant resistance, or to heat stress induced chaperone function caused by the T-shift treatment needs to be evaluated.

3.4.3. Protein stability and degradation

Stability control and the regulation of degradation are important switches to fine-tune NLR mediated immunity. Besides the role of chaperones for NLR stability and degradation control, involvement of ubiquitinating complexes and components of the plant 26S proteasome in plant immunity has been shown (section 1.6; Kadota et al., 2010; Furlan et al., 2012; Duplan and Rivas, 2014). Interestingly, 26S proteasome-mediated degradation of TRX3-regulated NPR1 (see above) was facilitated by SA-induced nuclear translocation and phosphorylation of NPR1, and its turnover promoted transcriptional activity of NPR1 target genes (Spoel et al., 2009), suggesting that degradation of immune components can also positively contribute to their defense outputs.

A couple of proteasome components were identified in the RPS4 pull-down: (1) HAP15, a proteasome regulatory particle in the lid subcomplex, associates with RPS4 in pre-activation complexes, (2) the 26S proteasome regulatory complex subunit Rpn2 is found in both pre- and post-activation complexes and (3) 26S proteasome regulatory subunit Rpn7 was co-purified with RPS4 in the *rrs1a* mutant background only. Together with the published data of the *rpn1a* proteasome mutant displaying increased susceptibility to *Pst* AvrRps4 (Yao et al., 2012), these RPS4 interactors constitute an interesting link to the plant 26S proteasome. It is possible that in analogy to the positive effect of the proteasome on NPR1 transcriptional outputs discussed above, timely and spatially coordinated and tightly regulated degradation of RPS4 via the plant proteasome might be required for a full immune response. To test this, *Pst* AvrRps4 resistance after inhibition of the plant proteasome or in several proteasome mutants should be tested, if possible alongside other effector-triggered defense responses to rule out general effects of the proteasome on disease resistance.

Notably, two HSP70 family chaperone proteins as well as a HSP40 co-chaperone were identified in pre- and/or post-activation *OE-RPS4-HS* samples, but not in *eds1-2* or *rrs1a* background. HSP40 is a co-chaperone of HSP70, and an isoform in soybean was induced upon soybean rust infection and involved in virus resistance (Liu and Whitham, 2013). Overexpression of the soybean HSP40 in tobacco induced cell death, further supporting its function in disease resistance (Liu and Whitham, 2013). HSP70 interacts with SGT1 (Noël et al., 2007), an HSP90 co-chaperone involved in the regulation of multiple resistance responses (see section 1.6). Overexpression of an HSP70 isoform in *Arabidopsis* impaired both basal resistance and ETI, including resistance to *Pst* AvrRps4 (Noël et al., 2007). BIP, one of the identified HSP70 family proteins, formed complexes

with the positive cell death regulator ACD6 (accelerated cell death 6), suggestedly targeting it for proteasomal degradation (Zhang et al., 2014). As ACD6 associated with and facilitated plasmamembrane-accumulation of the PTI receptors FLS2 (flagellin sensing 2) and BAK1 (BRI1-asscociated receptor kinase 1), HSP70 proteins might be involved in the regulation of resistance receptor folding, accumulation and localization (Zhang et al., 2014). Also, the *Pseudomonas* effector HopI1 has a typical plant co-chaperone domain and it interacted with different HSP70 isoforms to induce their ATP-hydrolysis activity (Jelenska et al., 2007; Jelenska et al., 2010). Interestingly, HSP70 was recruited to the chloroplast by HopI1 and was essential for HopI1 virulence function in a temperature-dependent manner (Jelenska et al., 2007; Jelenska et al., 2010). Which role the interaction of RPS4 with HSP70 has in the context of *Pst* AvrRps4 resistance remains to be solved. However, HSP70 importance in resistance responses as well as the targeting of HSP70 by HopI1, which is chloroplast-localized just like AvrRps4, suggests its possible involvement in plant responses to *Pst* AvrRps4.

It is worth mentioning that AvrRps4 is not only targeted to the chloroplast by its N-terminal signal peptide, but also its processed form could be detected exclusively inside chloroplasts, suggesting it is cleaved by a chloroplast peptidase (Li et al., 2014a). One *EDS1*- and *RRS1a*-dependent RPS4 co-purified protein detected in both pre- and post-activation complexes is CLPP4 (Chloroplast protease P4), a nuclear-encoded chloroplast protease which might be interesting to explore further.

3.4.4. Secretion and vesicle trafficking

Plant secretory pathways are important for plant resistance. Not only the secretion of antimicrobial compounds to the extracellular space, but also the correct localization of membrane-bound pathogen receptors rely on a functional plant secretory network (Wang and Dong, 2011; Kwon and Yun, 2014).

The ARF-GAP domain 9 (AGD9) protein was detected as an *EDS1*- and *RRS1*-dependent post-activation hit in the RPS4 pull-down. AGD9 is a GTPase-activating protein involved in recruitment of ADP-ribosylation factor 1 (ARF1) to the Golgi apparatus (Min et al., 2013). ARF small GTP-binding proteins help forming coat protein complex 1 (COPI) vesicles at the Golgi, which is essential for Golgi-to-ER retrograde membrane trafficking (Brandizzi and Barlowe, 2013). ARFs are regulated by activating ARF guanine nucleotide exchange factors (GEFs) stimulating GDP to GTP exchange, and inactivating ARF

GTPase-activating proteins (GAPs) stimulating ARF GTPase activity to hydrolyse ARF-bound GTP to GDP (Brandizzi and Barlowe, 2013). Notably, ARFs are involved in *Pseudomonas* resistance. The ARF-GEF AtMIN7 (*Arabidopsis thaliana* HopM interactor 7) was targeted for proteasome-mediated degradation by the *Pst* DC3000 effector HopM1, which was blocked during ETI to allow AtMIN7 accumulation (Nomura et al., 2006; Nomura et al., 2011). A knock-out of AtMIN7 increased plant susceptibility to virulent and avirulent *Pst* (Nomura et al., 2006; Nomura et al., 2011). This emphasizes an important role of vesicle trafficking and secretory pathways in plant immunity, which has been discussed previously (Wang and Dong, 2011; Kwon and Yun, 2014).

AGD9 targeted ARF1 is involved in virus resistance in *Arabidopsis*. Viral auxiliary replication protein p27 from Red clover necrotic mosaic virus (RCNMV) interfered with the cellular secretion pathway (Hyodo et al., 2014). Also, p27 targeted ARF1 and mislocalized it to the site of viral replicase complex formation (Hyodo et al., 2013), and *ARF1* silencing resulted in decreased accumulation of viral RNA, suggesting a positive function of *ARF1* in RCNMV replication (Hyodo et al., 2013). Besides, a positive role in plant immunity was described for *ARF1*. Overexpression of *ARF1*, but not an inactive *ARF1* GDP-locked form induced cell death in tobacco, whereas silencing of *ARF1* increased tobacco susceptibility to the non-host pathogen *P. cichorii* and impaired *N*-mediated ETI to tobacco mosaic virus (TMV) (Coemans et al., 2008).

Taking together *ARF1* involvement in pathogen resistance, the important role of secretory pathways and RPS4 endomembrane association as a potential site of interaction, *AGD9* together with its targeted *ARF1* are interesting candidates for further exploration of their roles in *RPS4*-mediated resistance.

3.4.5. Plant metabolism

The most prominent purpose of plant primary metabolism is the allocation of compounds needed for plant growth and development. However, primary metabolism is important for plant defense responses as well, suggestedly both through provision of energy and substrates needed for defense activation and through direct involvement of primary metabolism components in defense responses to pathogens (Rojas et al., 2014).

OASA1 (O-acetylserine (thiol) lyase isoform A1) is an *EDS1*-dependent RPS4 interactor detected in pre-and post-activation samples independently of *RRS1a*. O-acetylserine (thiol) lyases (OASTLs) are cysteine synthesizing enzymes, and a mutation

in OASA1 reduced its OASTL activity *in vitro* and caused auto-necrosis in specific *Arabidopsis* accessions depending on the *RPP1*-like NLR cluster (Tahir et al., 2013). Lack of functional OASA1 impaired resistance to virulent and avirulent pathogens, and HR induction upon avrRpm1 recognition depended on cytosolic cysteine, emphasizing the importance of OASA1 in immunity and cell death (Álvarez et al., 2012; Tahir et al., 2013).

PAL2 (phenylalanine ammonia-lyase) is another *EDS1*-dependent, *RRS1a*-independent RPS4 interactor in pre-and post-activation samples. PALs catalyzes the deamination of phenylalanine, working as a switch between plant primary and secondary metabolism. It produces cinnamic acid as a substrate for the phenylpropanoid pathway (Rohde et al., 2004; Huang et al., 2010) as a first step of flavonoid synthesis. Flavonoids exert diverse functions, and some are involved in pathogen defense (Rohde et al., 2004; Ferrer et al., 2008). Moreover, PAL-produced cinnamic acid is a precursor for SA synthesis. Although the majority of pathogen-induced SA is produced by ICS1 (isochorismate synthase 1), inhibition of PAL activity reduced pathogen-induced SA accumulation and rendered *Arabidopsis* susceptible to powdery mildew *Hyaloperonospora arabidopsidis* (*Hpa*) (Mauch-Mani and Slusarenko, 1996; Chen et al., 2009).

Ribose-5-phosphat isomerase is an *EDS1*- and *RRS1a*-dependent RPS4 interactor in pre-and post-activation complexes. It is one of several proteins involved in sugar metabolism whose transcripts accumulate upon infection with *Pst* AvrRpt2, presumably increasing the accumulation of soluble sugars and thus providing accessible energy to mount an adequate defense response (Bolton, 2009; Rojas et al., 2014).

3.4.6. Cell death and NLR association

One highly interesting *EDS1*- and *RRS1a*-dependent, activation-independent RPS4 interacting candidate is BPA1 (Binding partner of ACD11), which associates with ACD11 (accelerated cell death 11) (Petersen et al., 2009). Stunningly, the auto-necrotic phenotype of *acd11* depends on the RPS4-like NLR receptor LAZ5 (Lazarus 5) and is suppressed by *laz5* mutations in the P-loop and LRR regions (Palma et al., 2010). Interestingly, the *LAZ5* locus is targeted by the histone lysine methyltransferase SDG8 (SET domain group 8), and decreased trimethylation of histone 3 lysine 36 (H3K36me3) in *sdg8* correlates with decreased *LAZ5* expression and suppression of *acd11* autoimmunity (Palma et al., 2010). Despite of the high homology of *RPS4* and *LAZ5*, *sgt8* mutation had neither an effect on *RPS4* expression, nor did it impair resistance to *Pst* AvrRps4 (Palma et al., 2010). However,

due to its co-purification with RPS4 and its interactions with ACD11, the functions of BPA1 and possibly ACD11 in *Pst* AvrRps4 resistance should be examined closer.

3.5. Summary and conclusions

Immense progress has been made in the understanding of paired NLR receptors in the last years and allowed further reshaping and refining of the classical models for NLR actions in plant immunity. The latest theory for paired NLRs suggests their action as an executor which is regulated by the sensor (compare Figure 1). Direct interaction with the resting sensor represses executor activity. Effector recognition by direct binding of the sensor leads to either complex rearrangements or release of the executor from sensor interaction, which then allows homodimerization of executor N-terminal domains and downstream signaling activation (Césari et al., 2014; Nishimura and Dangl, 2014).

Advancing this model for RPS4 and RRS1, I suggest that upon NLR activation, distinct interfaces formed by homo- and heteromeric TIR interactions are exposed (compare Figure 20). While RPS4 TIR homodimers might participate in cytoplasmic events triggering cell death upon effector recognition, RPS4-RRS1 TIR heterodimeric interactions could be needed in the nucleus for transcriptional reprogramming and defense induction (Figure 21).

Unraveling the functions of compartment-specific NLR-containing immune complexes will be a major challenge for future research: What are the differences between cytoplasmic and nuclear immune complexes? How does their composition change upon pathogen recognition? Are proteins released from or recruited to immune complexes to fulfil their function, or are dynamic rearrangements within a preformed complex determining its functionality? How are NLRs connected to effector-induced transcriptional reprogramming? Do they stimulate defense gene expression indirectly through transcription factor activation, or are they directly associated with chromatin, potentially through interactions with transcription factors? If so, does activation change immune complex localization at the chromatin and/or enhance transcription factor activity?

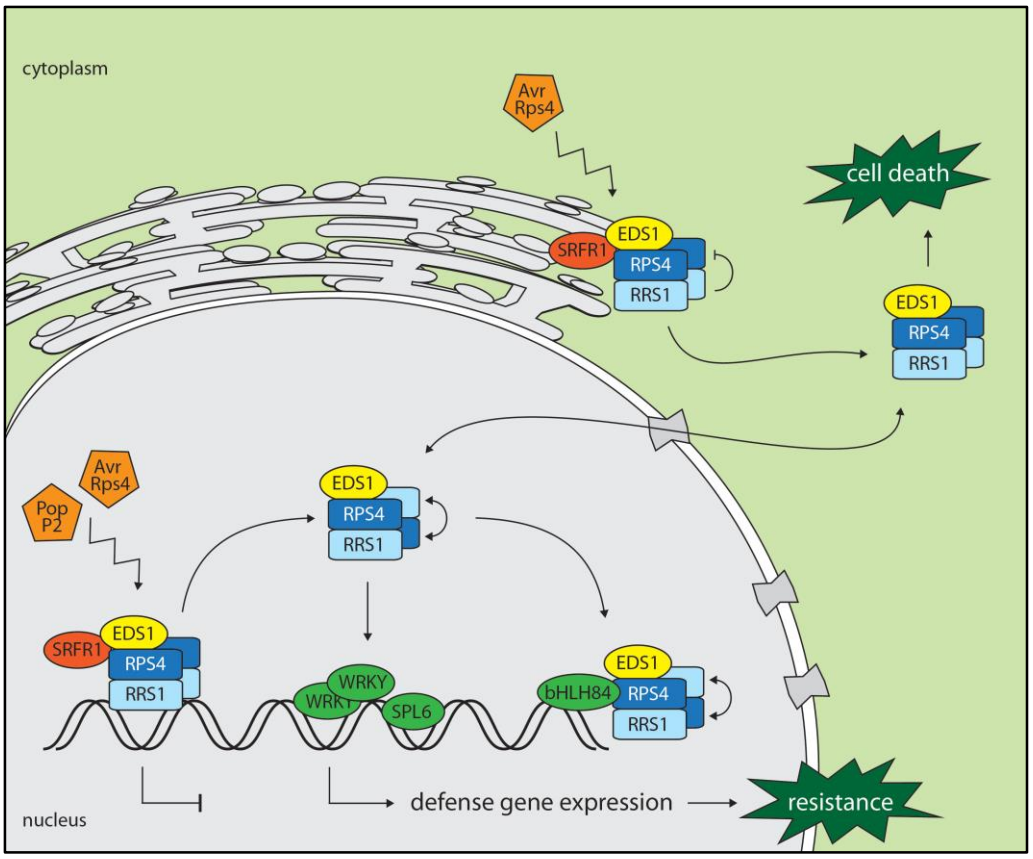

Figure 21: Extended model of *RPS4* and *RRS1* cooperative function.

Inactive RPS4 and RRS1 are assembled in pre-activation complexes together with positive and negative defense regulators such as EDS1 and SRFR1. Effector recognition releases active complexes for the induction of cell death in the cytoplasm, possibly through interactions via the RPS4 TIR homodimeric interface. Activation of nuclear complexes involves disruption of RRS1 DNA binding and conformational changes, allowing the formation of an RRS1-RPS4 TIR heterodimeric interface. Recruitment and activation of transcription factors either indirectly or through direct interaction then induces transcriptional reprogramming and leads to pathogen resistance.

Furthermore, the recent characterization of *RPS4b* and *RRS1b* as additional contributors to *Pst* AvrRps4 resistance (Saucet, 2013) suggests a more complicated interplay between these four TNL receptors. The TIR domains of all four TNL can interact with each other, and RRS1b interacts with PopP2 and AvrRps4 as RRS1a does (Saucet, 2013). Elaborate research is needed to unravel their synergistic or antagonistic interactions in hetero-complexes, potentially assembled of different portions of a and b pair TNLs. Deslandes' observations about *RRS1-R* segregating as a recessive locus in a cross between Nd-1 and Col-5, but behaving as a dominant trait upon transgenic expression (Deslandes et al., 1998; Deslandes et al., 2002) could be explained by the incompatibility of the *RPS4b-RRS1b* pairs in a cross of Nd-1 and Col-5, while upon transgenic expression only one native b pair is

present. It would be interesting to test *RRS1-R* resistance phenotype segregation in crosses of other resistant and susceptible *Arabidopsis* accessions while comparing their genetic features regarding both *RPS4* and *RRS1* a and b pairs. Also, examination of chimeric RPS4a/RPS4b and RRS1a/RRS1b proteins currently performed in the group of Jonathan Jones will illuminate the domain functions and interdependencies of these four TNL receptors.

In line with Ralph W. Sockman's observation "The larger the island of knowledge, the longer the shoreline of wonder", the accumulating knowledge on *RPS4* and *RRS1* probably raises more questions than it solves.

The differences in AvrRps4 and PopP2 recognition are striking: While *RRS1-R* is capable of recognizing both effectors and inducing a strong HR, *RRS1-S* confers cell-death independent resistance to *Pst* AvrRps4 only (Deslandes et al., 1998; Birker et al., 2009; Narusaka et al., 2009a; Narusaka et al., 2009b). Adding another layer of complexity, *RPS4b* and *RRS1b* contribute to *Pst* AvrRps4, but not *R.s.* PopP2 defense (Saucet, 2013). Furthermore, all of these TNL proteins differ to various degrees in different *Arabidopsis* accessions, as do the pathogen recognition capacities.

However, these differences not only pose a big challenge for future research, but also a big chance to uncover detailed structural requirements and interdependencies of these TNL receptors for their distinct immune functions towards *Pst* AvrRps4 and *R.s.* PopP2. Connecting structural properties of *RPS4a/b* and *RRS1a/b* in different *Arabidopsis* accessions with their functionalities in immunity will allow the dissection of their modes of action. Together with the proven functional transferability of *RPS4* and *RRS1* into other plant families, detailed understanding of NLR pairwise immune regulation could facilitate the application of basic research in crop plants to establish new ways of disease control.

4. Materials and Methods

4.1. Materials

4.1.1. Plant material

All *Arabidopsis thaliana* plants used in this study were in the Columbia (Col-0) accession. Mutant and wt plants are listed in Table 4, transgenic plants in Table 5.

Table 4: *Arabidopsis* wt and mutant lines

name	description	reference/source
Col-0	wildtype	J. Dangl
eds1-2	mutant/FN	Bartsch et al., 2006
rps4-2 (rps4a)	mutant/T-DNA	Wirthmueller et al., 2007
rrs1-11 (rrs1a)	mutant/T-DNA	Birker et al., 2009
rrs1a/b (rrs1-3/rrs1b)	mutant/T-DNA	Simon Saucet, unpublished
rps4a/b	mutant/T-DNA	Simon Saucet, unpublished

FN – fast neutron mutagenesis; T-DNA – transfer-DNA mutagenesis

Table 5: *Arabidopsis* transgenic lines

name	background	construct	reference/source
3FTH-RRS1	Col-0 *rrs1a*	*pRRS1:3FLAG-TEV-3HA-RRS1-S (RRS1a)*	Laurent Deslandes, unpublished
WRKY18-HA	Col-0 *wrky18*	*pWRKY18:WRKY18-HA*	Rainer Birkenbihl, unpublished
OE-RPS4-HS	Col-0	*35S:RPS4a-HA-Strep*	Wirthmueller et al., 2007
OE-RPS4-HS eds1-2	Col-0 *eds1-2*	*35S:RPS4a-HA-Strep*	Wirthmueller et al., 2007
OE-RPS4-HS rrs1a	Col-0 *rrs1a*	*35S:RPS4a-HA-Strep*	Heidrich et al., 2013
OE-RPS4-HS rrs1a/b	Col-0 *rrs1a/b*	*35S:RPS4a-HA-Strep*	crossed from *OE-RPS4-HS eds1-2*
OE-RPS4-YFP	Col-0 *rps4a*	*35S:RPS4a-YFP*	Baufumé et al., submitted

Table 5: *Arabidopsis* transgenic lines (continued)

OE-RPS4-YFP eds1-2	Col-0 *eds1-2*	*35S:RPS4a-YFP*	Baufumé et al., submitted
OE-RPS4-YFP rrs1a/b	Col-0 *rrs1a/b*	*35S:RPS4a-YFP*	crossed from *OE-RPS4-YFP eds1-2*
RPS4$^{P\text{-}loop}$-YFP	Col-0 *rps4a*	*35S:RPS4a$^{P\text{-}loop}$-YFP*	Baufumé et al., submitted
CP-OE-RPS4-YFP rps4a	Col-0 *rps4a*	*35S:RPS4a-YFP*	Chunpeng Yao, unpublished
pRPS4:RPS4-YFP rps4a	Col-0 *rps4a*	*pRPS4:RPS4a-YFP*	Chunpeng Yao, unpublished

4.1.2. Pathogens

Pseudomonas syringae pv *tomato* strain DC3000 (*Pst*) carrying an empty vector control (pVSP61) and *Pst* expressing the *P. syringae* pv. *pisi* effector AvrRps4 (*Pst* AvrRps4) were used for *Arabidopsis* infections in this study. They were obtained from R. Innes (Indiana University, Bloomington USA) and grown as described (Hinsch and Staskawicz, 1996). For stable transformation of *Arabidopsis* or transient protein expression in tobacco, *Agrobacterium tumefaciens* strain GV3101 was used (Koncz and Schell, 1986).

4.1.3. Oligonucleotides

Primers used in this study were purchased from Sigma-Aldrich and resuspended in H_2O to a concentration of 100µM. Working solutions were further diluted to 10µM. Primers are summarized in Table 6.

Table 6: Primers

purpose	gene	direction/name	primer sequence (5' to 3')
qPCR	*actin*	fw	ATGGAAGCTGCTGGAATCCAC
	(At3G18780)	rev	TTGCTCATACGGTCAGCGATA
	GAPDH	fw	TTGGTGACAACAGGTCAAGCA
	(At1G13440)	rev	AAACTTGTCGCTCAATGCAATC
	expressed protein	fw	GAGCTGAAGTGGCTTCCATGAC
	(At4g26410)	rev	GGTCCGACATACCCATGATCC
	EDS1	fw	TTTATGGGCTTGACACTTTGG
	(At2G48090)	rev	AGATTATTCAGGTGATCGAGCA
	ICS1	fw	TTCTGGGCTCAAACACTAAAAC
	(At1G74710)	rev	GGCGTCTTGAAATCTCCATC
	PR1	fw	TTCTTCCCTCGAAAGCTCAA
	(At2G14610)	rev	AAGGCCCACCAGAGTGTATG
	PBS3	fw	ACACCAGCCCTGATGAAGTC
	(At5G13320)	rev	CCCAAGTCTGTGACCCAGTT
	FMO1	fw	GTTCGTGGTTGTGTGTACCG
	(At1G19250)	rev	TGTGCAAGCTTTTCCTCCTT
	DND1	fw	CTCCCATGGTGGTTCCTCTA
	(At5G15410)	rev	ATCGATCCCAGTCGTTTGTC
	ERECTA	fw	CATGGCCCTACGAAGAAAAA
	(At2G26330)	rev	TGGACGACTTCACGTCTCTG
	RRS1_NB	fw	AGCTGCTGGAGATTGAAAACA
	(At5G45260)	rev	CAAGAAGCATCAAAGGCGCT
	RPS4_1	LW4_fw	AATACCACCGGAGGGAAGTC
	(At5G45250)	LW14_rev	TCACGATCCAACTTCTCTTCCA
	RPS4_2	SB94_fw	TGGAGTTGGATCGCTTGCCTCA
	(At5G45250)	SB93_rev	CCCTGCTTCCCTCCTTACCCTCC
	RPS4_3	LW6_fw	AGCCCCAGCCCTAATATTGT
	(At5G45250)	PM110_rev	GAGAGATTTGACTGCACTCATT
	RPS4_4	LW11_fw	CCACATTGGCATGACAAGAA
	(At5G45250)	LW21_rev	ACAAGCGGCTGACTTGATCT
	RPS4_5	A007_fw	GGGCAACTGGTGTATCCAAT
	(At5G45250)	A006_rev	TTGACCCCCAAGATCAAGTC
	RPS4-YFP	A015_fw	GACGGCCAAAGAAGAAGCAG
	(At5G45250)	AG8_rev	GAACTTCAGGGTCAGCTTGC

Table 6: Primers (continued)

purpose	gene	name/direction	primer sequence (5' to 3')
genotyping	*rrs1-3*	C90_LP	AAGTGGTGCCACAAAATCAAC
	mutant	C91_RP	ACTCGGAGAAGCTTCCTATGC
	wt	CV10	ATTTTGCCGATTTCGGAAC
	rrs1b	C79_LP	TATTTCAGAAAACCGAGTGCG
	mutant	C80_RP	ACCCTGGATAGTCTCGAGCTC
	wt	CV10	ATTTTGCCGATTTCGGAAC
	rps4-2	PM109_LP	TTGTCCAAGTTAAACCATCCT
	mutant	PM110_RP	GAGAGATTTGACTGCACTCATT
	wt	CV10	ATTTTGCCGATTTCGGAAC
	rps4b	C83_LP	GCTGAGTTGATCTTGGCTGTC
	mutant	C84_RP	CACCAGTCTTAAAATGGGTCG
	wt	CV10	ATTTTGCCGATTTCGGAAC
	eds1-2	105/E2	ACACAAGGGTGATGCGAGACA
	mutant	EDS4	GGCTTGTATTCATCTTCTATCC
	and wt	EDS6	GTGGAAACCAAATTTGACATTAG
	rrs1-11	KH71	TGTAGAAGAGATTGTGAGAGATGT
	mutant	KH72	CTGGGAATGGCGAAATCAAGGCATC
	rrs1-11	KH125	GTTTGACTGGCTAGGACCCGGAAG
	wt	KH126	CTGCAGATCAAATCTTAAGTTTGATGTGTCTAGA
purpose	**mutation**	**name/direction**	**primer sequence (5' to 3')**
RRS1 mutagenesis	R20A	C40_fw	GCGTAGAAGAGGTA**GC**GTACTCTTTCGTGAG
	R20A	C41_rev	CTCACGAAAGAGTAC**GC**TACCTCTTCTACGC
	Y101A	C42_fw	TGGTTTCAGTGTTG**GC**CGGTGACAGTCTATT
	Y101A	C43_rev	AATAGACTGTCACCG**GC**CAACACTGAAACCA
	K185A	C44_fw	TGCCTGGCATAGGA**GC**GACAACACTTGCTAA
	K185A	C45_rev	TTAGCAAGTGTTGTC**GC**TCCTATGCCAGGCA
	D254A	C46_fw	TTCTTGTTGTTCTCG**C**TGACGTGCGCAATGC
	D254A	C47_rev	GCATTGCGCACGTCA**G**CGAGAACAACAAGAA
	D255E	C48_fw	TTGTTGTTCTCGAT**GA**GGTGCGCAATGCTCT
	D255E	C49_rev	AGAGCATTGCGCACC**TC**ATCGAGAACAACAA
	R283G	C50_fw	TCATCATAACCTCT**G**GAGATAAACAAGTGTTTTGC
	R283G	C51_rev	GCAAAACACTTGTTTATCTC**C**AGAGGTTATGATGA
	H442A	C52_fw	ACCGAGTTTGGTTG**GC**TAAGCTGACCCAGGA
	H442A	C53_rev	TCCTGGGTCAGCTTA**GC**CAACCAAACTCGGT
	K1215A	C54_fw	TATGGACTTGGCGA**GC**GTACGGTCAAAAAGA
	K1215A	C55_rev	TCTTTTTGACCGTAC**GC**TCGCCAAGTCCATA

Table 6: Primers (continued)

purpose	mutation	name/direction	primer sequence (5' to 3')
RRS1 mutagenesis	L1222_G1223insL	C56_fw	CGGTCAAAAAGACATCTTA**CTG**GGTTCTCGTTTTCC
	L1222_G1223insL	C57_rev	GGAAAACGAGAACC**CAG**TAAGATGTCTTTTTGACCG
	H26A	C71_fw	ACTCTTTCGTGAGC**GC**CCTCTCTGAAGCTCT
	H26A	C72_rev	AGAGCTTCAGAGAG**GC**GCTCACGAAAGAGT

4.1.4. Enzymes

Restriction enzymes were purchased from New England Biolabs (NEB; Frankfurt, Germany) unless otherwise stated. NEB Enzymes were supplied with 10x reaction buffer which was used for restriction digests.

Standard PCR reactions were performed using home-made Taq DNA polymerase. For genotyping using the DNA extraction method II, PCR reactions were performed using commercially available *Phire II* polymerase. To achieve high accuracy when PCR products were generated for cloning, *Phusion* or *Pfu* polymerases were used.

Nucleic acid modifying enzymes and their suppliers are listed below:

Taq DNA polymerase	home-made
Phire Hot Start II DNA Polymerase	Thermo Scientific (Schwerte, Germany)
Phusion DNA Polymerase	NEB (Frankfurt, Germany)
PfuTurbo DNA Polymerase	Stratagene (Heidelberg, Germany)
PrimeStar DNA Polymerase	Takara Clontech (Saint-Germain-en-Laye, France)
Kappa HiFi DNA Polymerase	PEQLAB (Erlangen, Germany)
SuperScript II Reverse Transcriptase	Invitrogen (Karlsruhe, Germany)
Gateway LR Clonase Enzyme mix	Invitrogen (Karlsruhe, Germany)

4.1.5. Chemicals

Laboratory grade chemicals and reagents were purchased from Sigma-Aldrich (Deisenhofen, Germany), Roth (Karlsruhe, Germany), Merck (Darmstadt, Germany), Invitrogen™ (Karlsruhe, Germany), Serva (Heidelberg, Germany), and Gibco™ BRL® (Neu Isenburg, Germany) unless otherwise stated.

4.1.6. Antibiotics stock solutions

Ampicillin (Amp) 100 mg/ml in ddH2O

Carbenicillin (Carb) 50 mg/ml in ddH2O

Gentamycin (Gent) 15 mg/ml in ddH2O

Kanamycin (Kan) 50 mg/ml in ddH2O

Rifampicin (Rif) 100 mg/ml in DMSO

Spectinomycin 10 mg/ml in ddH2O

Tetracycline (Tet) 10 mg/ml in 70 % ethanol

Stock solutions (1000x; 100x for Spectinomycin) stored at -20° C. Aqueous solutions were sterile filtrated.

4.1.7. Media

Media were sterilised by autoclaving at 121° C for 20 min. For the addition of antibiotics and other heat labile compounds the solution or media were cooled to 55° C. Heat labile compounds were filter-sterilised prior to use.

Escherichia coli medium: Luria-Bertani (LB) broth or agar plates

Pseudomonas syringae medium: Nutrient-Yeast-Glycerol (NYG) broth or agar plates

Agrobacterium tumefaciens media: Yeast Extract broth (YEB) or LB broth or agar plates

Arabidopsis thaliana medium: liquid Murashige and Skoog (MS) or MS agar plates

4.1.8. Antibodies

Listed below are primary and secondary antibodies used for immunoblot detection.

Table 7: Primary antibodies

Antibody	Source	Dilution	Reference
α-HA 3F10	rat monoclonal	1:5000	Roche (Mannheim, Germany)
α-GFP	mouse monoclonal	1:5000	Roche (Mannheim, Germany)
α-EDS1	rabbit polyclonal	1:500	S. Rietz, J. Parker[a]
α-Histone H3	rabbit polyclonal	1:5000	ab1791, Abcam (Cambridge, UK)
α-PEPC	rabbit polyclonal	1:5000	Rocklands, Gilbertsville, PA, USA

[a]Max-Planck-Institute for Plant Breeding Research, Carl-von-Linné-Weg 10, 50829 Cologne, Germany

Table 8: Secondary antibodies

Antibody	Feature	Dilution	Reference
goat anti-rabbit	IgG-HRP conjugated	1:5000	Santa Cruz (Santa Cruz, USA)
goat anti-mouse	IgG-HRP conjugated	1:5000	Santa Cruz (Santa Cruz, USA)
goat anti-rat	IgG-HRP conjugated	1:5000	Santa Cruz (Santa Cruz, USA)

4.1.9. Buffers and solutions

General buffers and solutions are displayed in the following listing. Buffers and solutions not displayed here are described in the corresponding methods. All buffers and solutions were prepared using Milli-Q water. Buffers and solutions for molecular biological experiments were autoclaved or filter-sterilised.

Molecular biology work:

DNA extraction buffer I	Tris-HCl, pH 7.5	200 mM
	NaCl	250 mM
	EDTA	25mM
	SDS	0.5%
DNA extraction buffer II	Tris-HCl, pH 7.5	50mM
	NaCl	300mM
	Sucrose	300mM
DNA gel loading dye (6x)	Sucrose	4g
	EDTA (0.5 M)	2ml
	Bromphenol blue	25mg
	H_2O to 10 ml	
PCR reaction buffer (10x)	Tris-HCl, pH 9.0	100mM
	KCl	500mM
	$MgCl_2$	15mM
	Triton X-100	1%

TE buffer	Tris-HCl pH 8.0	10mM
	EDTA	1mM

SDS-PAGE:

Laemmli buffer (2x)	Tris-HCl pH 6.8	0.125M
	SDS	4%
	Glycerol	20% (v/v)
	Bromphenol blue	0.02%
	Dithiothreitol (DTT)	0.2M
SDS running buffer (10x)	Tris	30.28g
	Glycine	144.13g
	SDS	10g
	H_2O to 1000 ml	

Western blotting:

Transfer buffer (10x)	Tris	58.2g
	Glycine	29.3g
	SDS (10 %)	12.5mL
	adjust pH tp 9.2; H_2O to 1000 mL	
	Before use dilute 100mL 10x buffer with 700ml H_2O and add 200mL methanol.	
Ponceau S staining	Ponceau S working solution was prepared by dilution of ATX Ponceau S concentrate (Sigma-Aldrich) 1:5 in H_2O.	
TBST buffer	Tris-HCl pH 7.5	10mM
	NaCl	150mM
	Tween 20	0.05%

4.2. Methods

4.2.1. Plant growth

Arabidopsis seeds were germinated on moist soil after 2 days of vernalisation at 4°C. Plants were grown in controlled growth chambers under a 10/14h day/night cycle (150–200 $\mu E/m^2s$) and ~65% relative humidity at 22°C. For temperature-shift experiments, plants were grown in chambers under a 12/12h day/night cycle (150–200 $\mu E/m^2s$) and ~65% relative humidity at 28°C and shifted in the morning to 19°C for 8h. To obtain progeny plants were transferred to long day conditions (16h photoperiod) and flowering tissue was enclosed in a paper bag until seeds ripened.

4.2.2. Crossing *Arabidopsis* plants

Individual flowers with immature stamina were emasculated with fine tweezers. Stigmas were pollinated by tapping three to four donor stamens from different flowers onto them. Mature siliques containing F1 seeds were harvested and allowed to dry. F1 seeds were grown and allowed to self-pollinate. Produced F2 seeds were sown and used for genotyping.

4.2.3. Bacterial growth assays

For *Pseudomonas* spray infections, *Pst* and *Pst* AvrRps4 strains were grown for 24h at 28°C on NYGA solid medium supplemented with the corresponding antibiotics. 4- to 5-week-old plants were spray-inoculated with bacterial suspensions at $1x10^8$cfu/ml in 10mM $MgCl_2$ containing 0.04% (v/v) Silwet L-77 (Lehle seeds, USA) or syringe infiltrated with bacterial suspensions at $5x10^4$cfu/ml in 10mM $MgCl_2$. *In planta* bacterial titers were determined shortly after inoculation (day 0) and 2-4 days post infection (dpi) by shaking leaf discs in 10mM $MgCl_2$ with 0.01% Silwet L-77 at 28°C for 1h, as described (Tornero and Dangl, 2001; García et al., 2010). Infected plants were kept in a growth cabinet with a 10/14 h day/night cycle at 23°C. Means and standard errors were calculated from at least three (day 0) or five (day 3) biological replicates per experiment. Bacterial numbers were compared between lines using ANOVA (analysis of variance) followed by a post-hoc Tukey test. Genotypes with significant differences ($p<0.05$) were assigned to different groups indicated by letters (a,b,c) whereas genotypes showing no significant differences belong to the same group.

4.2.4. *Arabidopsis* total protein extraction

For comparable starting amounts, leaf tissue was harvested using a cork borer, then frozen in liquid nitrogen and homogenized 2x30sec using a Mini-Bead-Beater-8 (Biospec Products) and 1.2 mm stainless steel beads (Roth). Equal amounts of 2xLaemmli sample buffer was added to each tube, samples were boiled for 5-10min in a heating block and used directly for western blot analysis or frozen at -20°C.

4.2.5. Denaturing SDS-polyacrylamide gel electrophoresis (SDS-PAGE)

Polyacrylamide gels for SDS-PAGE were prepared by pouring first the resolving gel followed by the stacking gel containing a comb to produce slots for sample loading. Composition of gels is listed in Table 9.

Table 9: Composition of polyacrylamide gels

	6% resolving	**8% resolving**	**5% stacking**
H_2O	53 mL	46.4 mL	20.4 mL
30% Acrylamide/Bis solution 29:1 (BioRad)	20 mL	26.6 mL	5.1 mL
Tris-HCl pH 8.8	25 mL	25 mL	-
Tris-HCl pH 6.8	-	-	3.9 mL
10% SDS	1 mL	1 mL	300 µL
10% ammonium persulfate (APS)	1 mL	1 mL	300 µL
TEMED (BioRad)	80 µL	60 µL	30 µL

Total protein extracts from *Arabidopsis* leaves were prepared as described above (4.2.4) or 2xLaemmli sample loading buffer was added to protein samples followed by sample boiling to denature proteins. Gels were placed into electrophoresis tanks submerged in 1x SDS running buffer. A prestained protein ladder (PageRuler Prestained Protein Ladder, Thermo Scientific) was loaded alongside with the denatured protein samples and samples were separated at 80-120V.

4.2.6. Western blot and immunodetection of proteins

Proteins separated by SDS-PAGE were electro-blotted onto Hybond-ECL-nitrocellulose membranes (Amersham Biosciences) for 75min at 100V. Equal protein transfer was monitored by staining membranes with Ponceau S (Sigma-Aldrich). Destained membranes

were blocked for 1h in 5% milk in TBST (Tris buffered saline with Tween20) before incubation in 2% milk in TBST containing primary antibody overnight. The appropriate horseradish peroxidase (HRP)-conjugated secondary antibody was applied and proteins were detected using Enhanced Chemiluminiscence Reagent (ECL; Pierce Thermo Scientific) either by exposure on a photographic film (BioMax light film, Kodak) or by using the ChemiDoc MP imaging system (BioRad).

4.2.7. Nuclear fractionation

Nuclear fractionation of *Arabidopsis* leaf tissue was performed as previously described (Kinkema et al., 2000). Briefly, 2g leaf tissue of 3-week-old plants was ground in liquid nitrogen for homogenization, resuspended in Honda buffer (2.5% Ficoll400, 5% Dextran T40, 0.4M Sucrose, 25mM Tris-HCl pH7.4, 10mM $MgCl_2$, 5mM DTT, proteinase inhibitors) and then filtered through nylon mesh. After addition of Triton X-100 to a final concentration of 0.5% and incubation on ice, the solution was centrifuged at 1500*g* for 5 min, and the pellet washed with Honda buffer containing 0.1% Triton X-100. The pellet was resuspended gently in Honda buffer and centrifuged at 100*g* for 5 min to pellet starch and cell debris. The supernatant was centrifuged subsequently at 1800*g* for 5 min to pellet the nuclei. Nuclei-enriched fractions were 30× more concentrated than nuclei-depleted fractions based on the final volume of each fraction. For immunoblot analysis, cytoplasmic marker PEPC (phosphoenolpyruvate carboxylase) and nuclear marker Histone H3 were included. Following antibodies were used: α-HA (3F10; Roche), α-PEPC (Rockland), α-Histone H3 (Abcam).

4.2.8. Strep-tag mediated protein pulldown

2g leaf tissue of 3,5-week-old plants was homogenized in liquid nitrogen before adding 3mL of lysis buffer (50mM Tris-HCl pH 8; 1mM EDTA; 150mM NaCl; 10% glycerol, 5mM DTT; 0,05% Triton X-100; proteinase inhibitors), centrifuged to remove cell debris and incubated with StrepTactin superflow sepharose beads (IBA) rotating at 4°C for 1h. Samples were loaded on a spin column, washed four times with wash buffer (50mM Tris-HCl pH 8; 1mM EDTA; 150mM NaCl; 10% glycerol, 5mM DTT) and eluted with biotin elution buffer (20mM Tris-HCl pH 8, 150mM NaCl, 2mM DTT). Samples were analysed by western blot. Subsequent proteomic analysis was performed at the Protein Mass Spectrometry Service of the Max Planck Institute for Plant Breeding Research. After in

solution digest and label-free quantification, RPS4 co-eluted proteins were identified on an Easy nLC1000 liquid chromatograph coupled to a QExactive mass spectrometer (ThermoFisher Scientific). Data was evaluated using MaxQuant.

4.2.9. *Arabidopsis* genomic DNA extraction I and PCR

Leaf material was harvested into Corning® 96well PP 1.2 mL cluster tubes (8-tube strip) and homogenized in liquid nitrogen using a Mini-Bead-Beater-8 (Biospec Products) and stainless steel beads. After addition of 400µL DNA extraction buffer I samples were centrifuged and 300 µL supernatant transferred to new tubes containing 300µL icecold isopropanol. After pelleting precipitated DNA by centrifugation, supernatant was discarded and pellet washed 1-2x with 70% EtOH. Dried pellet was resolved in 100µL H_2O and 2µL used for PCR in the following PCR conditions:

PCR reaction composition:

Component	**volume per 20µL reaction (µL)**
home-made Taq Polymerase	0.5
10x PCR buffer	2
2.5mM dNTPs	2
10µM primer (forward)	1
10µM primer (reverse)	1
H_2O	11.50
DNA solution	2

PCR thermal conditions:

Stage	**Temperature (°C)**	**Duration (sec)**	**N° of cycles**
Initial denaturation	94	120	1
Denaturation	94	20	
Annealing	55	20	35
Elongation	72	60 per kb	
Final extension	72	300	1

Amplified PCR products were loaded onto an agarose gel containing ethidiumbromide for DNA staining. After electrophoretic separation of DNA fragments, resulting bands were monitored under UV light to evaluate PCR results.

4.2.10. *Arabidopsis* genomic DNA extraction II and PCR

Leaf material was harvested into Corning® 96well PP 1.2 mL cluster tubes (8-tube strip) and homogenized in 200µL DNA extraction buffer II using a Mini-Bead-Beater-8 (Biospec Products) and stainless steel beads. Immediately boil samples in a water bath at 95°C for 10min, followed by incubation on ice for 30min. Use 1 µL of DNA sample in the following PCR conditions:

PCR reaction composition:

Component	**volume per 20µL reaction (µL)**
Phire Hot Start II DNA Polymerase	0.2
Phire or *Phusion* 5x buffer	4
2.5mM dNTPs	0.4
10µM primer (forward)	1
10µM primer (reverse)	1
H_2O	12.4
DNA solution	1

PCR thermal conditions:

Stage	**Temperature (°C)**	**Duration (sec)**	**N° of cycles**
Initial denaturation	98	30	1
Denaturation	98	10	
Annealing	60	15	35
Elongation	72	10-15 per kb	
Final extension	72	300	1

Amplified PCR products were loaded onto an agarose gel containing ethidiumbromide for DNA staining. After electrophoretic separation of DNA fragments, resulting bands were monitored under UV light to evaluate PCR results.

4.2.11. Site-directed mutagenesis

Plasmid *pDONR207* containing *pRRS1:3FTH-RRS1-S* genomic sequence was used for PCR with proof-reading polymerases *Phusion*, *Pfu*, *PrimeStar* or *Kappa HiFi* using primers designed to insert basepair changes at required positions (see Table 6).

Phusion PCR reaction composition:

Component	**volume per 20µL reaction (µL)**
Phusion DNA Polymerase	0.2
Phusion 5x HF buffer	4
2.5mM dNTPs	2
5µM primer (forward)	0.5
5µM primer (reverse)	0.5
H_2O	10.8
Plasmid (~20ng/µL)	2

Phusion PCR thermal conditions:

Stage	**Temperature (°C)**	**Duration**	**N° of cycles**
Initial denaturation	98	1 min	1
Denaturation	98	10 sec	
Annealing	60	20 sec	18
Elongation	72	6 min	
Final extension	72	15 min	1

Pfu PCR reaction composition:

Component	**volume per 20µL reaction (µL)**
Pfu DNA Polymerase	0.4
Pfu 10x buffer	2
2.5mM dNTPs	2
5µM primer (forward)	0.5
5µM primer (reverse)	0.5
H_2O	12.6
Plasmid (~20ng/µL)	3

Pfu PCR thermal conditions:

Stage	**Temperature (°C)**	**Duration**	**N° of cycles**
Initial denaturation	98	1 min	1
Denaturation	98	10 sec	
Annealing	60	20 sec	18
Elongation	72	14 min	
Final extension	72	15 min	1

PrimeStar PCR reaction composition:

Component	**volume per 20µL reaction (µL)**
PrimeStar DNA Polymerase	0.5
PrimeStar 5x buffer	4
2.5mM dNTPs	4
10µM primer (forward)	0.5
10µM primer (reverse)	0.5
H_2O	12.9
Plasmid (~2ng/µL)	2

PrimeStar PCR thermal conditions:

Stage	**Temperature (°C)**	**Duration**	**N° of cycles**
Initial denaturation	98	2 min	1
Denaturation	98	30 sec	
Annealing	60	15 sec	18
Elongation	72	13 min	
Final extension	72	20 min	1

Kappa HiFi PCR reaction composition:

Component	**volume per 20µL reaction (µL)**
Kappa HiFi DNA Polymerase	0.5
Kappa HiFi 5x buffer	5
10mM dNTPs	0.75
10µM primer (forward)	0.75
10µM primer (reverse)	0.75
H_2O	14.75
Plasmid (~2ng/µL)	2.5

Kappa HiFi PCR thermal conditions:

Stage	**Temperature (°C)**	**Duration**	**N° of cycles**
Initial denaturation	95	4 min	1
Denaturation	98	30 sec	
Annealing	60	15 sec	18
Elongation	72	7 min	
Final extension	72	10 min	1

PCR reactions were digested by incubation with 0.5µL DpnI restriction enzyme for 1h at 37°C to remove methylated original plasmid DNA and subsequently heat-shock transformed into *E. coli* DH10b for amplification. Plasmids were purified from overnight cultures and sequenced at the Max Planck genome center to verify mutations.

Mutated *pRRS1:3FTH-RRS1-S* fragments were cloned into the plant expression vector pAM-PAT using the Gateway LR Clonase II enzyme mix in the following conditions:

Component	**volume per 20µL reaction (µL)**
Entry clone (*pDONR207-RRS1-S*, 75ng/µL)	0.5
Destination vector (*pAM-PAT*, 75ng/µL)	0.5
TE buffer, pH 8.0	1
LR clonase II enzyme mix	0.5

Incubate overnight at 25°C.

To terminate the reaction, incubate with 0.5µL Proteinase K at 37°C for 10min. Plasmids were heat-shock transformed into *E. coli* DH10b for amplification. Correct insertions were verified by sequencing at the Max Planck genome center. *pAM-PAT* vectors including mutated *pRRS1:3FTH-RRS1-S* sequences were transformed into *Agrobacterium tumefaciens* GV3101 PMP90 RK (hereafter *Agrobacteria*) by electroporation for delivery into plants.

4.2.12. Transient protein expression in tobacco

Agrobacteria carrying pAM-PAT *pRRS1:3FTH-RRS1-S*, as well as *pRPS4:RPS4-HS* and *35S:AvrRps4-YFP* were grown for 2 days on selective YEB or LB plates at 28°C and incubated for 3-5h in infiltration medium (10mM MES pH 5.6, 10mM $MgCl_2$, 0.15mM acetosyringone) at OD_{600}=1. 3-week-old to 4-week-old tobacco *Nicotiana benthamiana* or *N. tabacum* plants were syringe-infiltrated with different v/v mixes of the prepared *Agrobacteria* strains. Leaf samples to monitor protein expression were taken 2 days after infiltration. Macroscopic HR symptoms (necrosis) were monitored at several consecutive days after infiltration.

4.2.13. Agrobacterium-mediated Arabidopsis transformation:

Arabidopsis flowers were dipped into transformation solution containing *Agrobacteria* grown for 2 days on YEB plates (30mL liquid YEB medium with *Agrobacteria*, 120mL 5% sucrose, 0.03% Silwet L-77) for 10-30 sec under gentle agitation. Plants were kept under high humidity for 48h, then grown under long day conditions until seed maturity to obtain T1 generation.

4.2.14. qPCR analysis of *Arabidopsis* gene expression

Leaf material of Arabidopsis plants was harvested (i.e. 4.5-week-old plants syringe infiltrated with *Pst* AvrRps4 or 10mM $MgCl_2$ (mock) as described above (4.2.3), or 3-week-old *RPS4*-overexpressing plants after temperature-shift at different time points after treatment). Plant tissue was homogenized using a Mini-Bead-Beater-8 (Biospec Products) and stainless steel beads. Total RNA was extracted using the RNeasy Plant Minikit (Qiagen) according to the manufacturer's protocol. 1ug of total RNA was used for reverse transcription with SuperScript II enzyme (Invitrogen) using the following protocol:

cDNA synthesis reaction setup:

Component	volume per 20µL reaction (µL)
0.5µg/µL Oligo dT	1
2.5mM dNTPs	4
1µg RNA	2µL of 0.5µg/µL
RNase-free H_2O	5

Incubate for 5min at 65°C.

Prepare following master mix and add 8µL to each sample:

Component	volume per 20µL reaction (µL)
5x First Strand Buffer	4
0,1M DTT	2
RNase Out (40 units/µL)	1
SuperScript II (Reverse transcriptase)	1

Incubate for 60min at 42°C, then heat-inactivate enzyme for 15min at 70°C.

cDNA was diluted 1:20 and 4µL each were used for quantitative RT-PCR (qPCR).

qPCR reaction composition:

Component	volume per 25µL reaction (µL)
H_2O	14.5
10x PCR buffer	2.5
EVAgreen	1.25
2.5mM dNTPs	1
10µM primer (forward)	0.5
10µM primer (reverse)	0.5
home-made Taq polymerase	0.75
cDNA dilution	4

qPCR thermal conditions:

Stage	Temperature (°C)	Duration (sec)	N° of cycles
Initial denaturation	95	180	
Denaturation	95	10	
Annealing	58	10	55
Elongation	72	15-30	
Denaturation	95	60	
Renaturation	55	60	
Melting Curve	55	10	81

Results were analysed using the BioRad iQ5 software and Microsoft Office Excel.

4.2.15. Chromatin-immunoprecipitation (ChIP)

3-week-old plants were harvested either untreated or 6h after spray inoculation with *Pst* AvrRps4 (OD_{600}=0.4) or 10mM $MgCl_2$ mock treatment, respectively. ChIP samples were processed according to Gendrel et al. (2005) and Birkenbihl et al. (2012) with modifications. In short, leaf material was cross-linked by three subsequent 5min vacuum infiltrations of 1% formaldehyde solution. Tissue was frozen and ground in liquid nitrogen. Nuclei were extracted from 2g of leaf material. Nuclei were disrupted by sonication on an UP50H sonicator (Hielscher) ten times for 30sec each with 30sec break. Sheared chromatin was diluted to reduce SDS concentration. Input samples were set aside. After chromatin solutions were pre-clearing with protein A agarose beads (Sigma), they were incubated with rabbit polyclonal αHA antibody (Sigma, H6908) overnight at 4°C on a rotator. Immune complexes were collected with protein A agarose beads. After washing, eluted immune complexes and input samples were incubated at 65°C overnight to reverse the cross-linking. Proteins were digested and DNA extracted with phenol/chloroform and resolved in 50µL nuclease-free H_2O. 2µL of pWRKY18:WRKY18-HA samples was used to test enrichment of targeted gene promoters by qPCR.

For *3FTH-RRS1* and Col-0 input and αHA-ChIP samples, linear DNA amplification (LinDA) was performed according to Shankaranarayanan et al. (2012), but with an additional repeat of the *in vitro* transcription for enhanced DNA amplification. Eluted DNA was barcoded using the NuGene "Ovation Ultralow Library Systems" kit and amplified by 15-16 cycles of PCR during library preparation. DNA of approximately 200-400bp length

was extracted from an agarose gel. Samples were sequenced on the Illumina HiSeq2500 by the Max Planck genome center. Sequencing reads were processed and mapped to the *Arabidopsis* genome (Barbara Kracher): Remaining LinDA adapters were removed from the sequencing data using cutadapt (Martin, 2011), then poly-A and poly-T tails and low quality ends were trimmed. Reads with low quality or with less than 36 bases remaining after trimming were removed using PRINSEQ lite (Schmieder and Edwards, 2011). Remaining high quality reads were mapped to the *Arabidopsis thaliana* reference genome TAIR10 (*http://www.arabidopsis.org*) using Bowtie (Langmead et al., 2009). To identify genomic DNA regions enriched in sequencing reads in the RRS1-S ChIP sample, sequencing reads of all samples were compared using the peak calling programs MACS (Zhang et al., 2008), QuEST (Valouev et al., 2008) and peakzilla (Bardet et al., 2013).

5. Literature cited

Ade, J., DeYoung, B.J., Golstein, C., and Innes, R.W. (2007). Indirect activation of a plant nucleotide binding site–leucine-rich repeat protein by a bacterial protease. Proceedings of the National Academy of Sciences **104,** 2531-2536.

Alcázar, R., and Parker, J.E. (2011). The impact of temperature on balancing immune responsiveness and growth in *Arabidopsis*. Trends in Plant Science **16,** 666-675.

Alfano, J.R., and Collmer, A. (2004). TYPE III SECRETION SYSTEM EFFECTOR PROTEINS: Double Agents in Bacterial Disease and Plant Defense. Annual Review of Phytopathology **42,** 385-414.

Álvarez, C., Ángeles Bermúdez, M., Romero, L.C., Gotor, C., and García, I. (2012). Cysteine homeostasis plays an essential role in plant immunity. New Phytologist **193,** 165-177.

An, C., and Mou, Z. (2011). Salicylic Acid and its Function in Plant Immunity. Journal of Integrative Plant Biology **53,** 412-428.

Ashikawa, I., Hayashi, N., Yamane, H., Kanamori, H., Wu, J., Matsumoto, T., Ono, K., and Yano, M. (2008). Two Adjacent Nucleotide-Binding Site–Leucine-Rich Repeat Class Genes Are Required to Confer Pikm-Specific Rice Blast Resistance. Genetics **180,** 2267-2276.

Austin, M.J., Muskett, P., Kahn, K., Feys, B.J., Jones, J.D.G., and Parker, J.E. (2002). Regulatory Role of SGT1 in Early *R* Gene-Mediated Plant Defenses. Science **295,** 2077-2080.

Axtell, M.J., and Staskawicz, B.J. (2003). Initiation of RPS2-Specified Disease Resistance in *Arabidopsis* Is Coupled to the AvrRpt2-Directed Elimination of RIN4. Cell **112,** 369-377.

Azevedo, C., Sadanandom, A., Kitagawa, K., Freialdenhoven, A., Shirasu, K., and Schulze-Lefert, P. (2002). The RAR1 Interactor SGT1, an Essential Component of *R* Gene-Triggered Disease Resistance. Science **295,** 2073-2076.

Azevedo, C., Betsuyaku, S., Peart, J., Takahashi, A., Noël, L., Sadanandom, A., Casais, C., Parker, J., and Shirasu, K. (2006). Role of SGT1 in resistance protein accumulation in plant immunity. The EMBO Journal **25,** 2007-2016.

Bai, S., Liu, J., Chang, C., Zhang, L., Maekawa, T., Wang, Q., Xiao, W., Liu, Y., Chai, J., Takken, F.L.W., Schulze-Lefert, P., and Shen, Q.-H. (2012). Structure-Function Analysis of Barley NLR Immune Receptor MLA10 Reveals Its Cell Compartment Specific Activity in Cell Death and Disease Resistance. PLoS Pathog **8,** e1002752.

Bao, F., Huang, X., Zhu, C., Zhang, X., Li, X., and Yang, S. (2014). *Arabidopsis* HSP90 protein modulates RPP4-mediated temperature-dependent cell death and defense responses. New Phytologist **202,** 1320-1334.

Bardet, A.F., Steinmann, J., Bafna, S., Knoblich, J.A., Zeitlinger, J., and Stark, A. (2013). Identification of transcription factor binding sites from ChIP-seq data at high resolution. Bioinformatics **29,** 2705-2713.

Bendahmane, A., Kanyuka, K., and Baulcombe, D.C. (1999). The *Rx* Gene from Potato Controls Separate Virus Resistance and Cell Death Responses. The Plant Cell Online **11,** 781-791.

Bendahmane, A., Farnham, G., Moffett, P., and Baulcombe, D.C. (2002). Constitutive gain-of-function mutants in a nucleotide binding site–leucine rich repeat protein encoded at the *Rx* locus of potato. The Plant Journal **32,** 195-204.

Bernoux, M., Timmers, T., Jauneau, A., Brière, C., de Wit, P.J.G.M., Marco, Y., and Deslandes, L. (2008). RD19, an *Arabidopsis* Cysteine Protease Required for RRS1-R-Mediated Resistance, Is Relocalized to the Nucleus by the *Ralstonia solanacearum* PopP2 Effector. The Plant Cell Online **20,** 2252-2264.

Bernoux, M., Ve, T., Williams, S., Warren, C., Hatters, D., Valkov, E., Zhang, X., Ellis, Jeffrey G., Kobe, B., and Dodds, Peter N. (2011). Structural and Functional Analysis of a Plant Resistance Protein TIR Domain Reveals Interfaces for Self-Association, Signaling, and Autoregulation. Cell Host & Microbe **9,** 200-211.

Bhattacharjee, S., Halane, M.K., Kim, S.H., and Gassmann, W. (2011). Pathogen Effectors Target *Arabidopsis* EDS1 and Alter Its Interactions with Immune Regulators. Science **334,** 1405-1408.

Bieri, S., Mauch, S., Shen, Q.-H., Peart, J., Devoto, A., Casais, C., Ceron, F., Schulze, S., Steinbiß, H.-H., Shirasu, K., and Schulze-Lefert, P. (2004). RAR1 Positively Controls Steady State Levels of Barley MLA Resistance Proteins and Enables Sufficient MLA6 Accumulation for Effective Resistance. The Plant Cell Online **16,** 3480-3495.

Birkenbihl, R.P., Diezel, C., and Somssich, I.E. (2012). Arabidopsis WRKY33 Is a Key Transcriptional Regulator of Hormonal and Metabolic Responses toward *Botrytis cinerea* Infection. Plant Physiology **159,** 266-285.

Birker, D., Heidrich, K., Takahara, H., Narusaka, M., Deslandes, L., Narusaka, Y., Reymond, M., Parker, J.E., and O'Connell, R. (2009). A locus conferring resistance to *Colletotrichum higginsianum* is shared by four geographically distinct Arabidopsis accessions. The Plant Journal **60,** 602-613.

Boccara, M., Sarazin, A., Thiébeauld, O., Jay, F., Voinnet, O., Navarro, L., and Colot, V. (2014). The Arabidopsis *miR472-RDR6* Silencing Pathway Modulates PAMP- and Effector-Triggered Immunity through the Post-transcriptional Control of Disease Resistance Genes. PLoS Pathog **10,** e1003883.

Bolton, M.D. (2009). Primary Metabolism and Plant Defense—Fuel for the Fire. Molecular Plant-Microbe Interactions **22,** 487-497.

Bonardi, V., Cherkis, K., Nishimura, M.T., and Dangl, J.L. (2012). A new eye on NLR proteins: focused on clarity or diffused by complexity? Current Opinion in Immunology **24,** 41-50.

Botër, M., Amigues, B., Peart, J., Breuer, C., Kadota, Y., Casais, C., Moore, G., Kleanthous, C., Ochsenbein, F., Shirasu, K., and Guerois, R. (2007). Structural and Functional Analysis of SGT1 Reveals That Its Interaction with HSP90 Is Required for the Accumulation of Rx, an R Protein Involved in Plant Immunity. The Plant Cell Online **19,** 3791-3804.

Boyle, P., Le Su, E., Rochon, A., Shearer, H.L., Murmu, J., Chu, J.Y., Fobert, P.R., and Després, C. (2009). The BTB/POZ Domain of the Arabidopsis Disease Resistance Protein NPR1 Interacts with the Repression Domain of TGA2 to Negate Its Function. The Plant Cell Online **21,** 3700-3713.

Brandizzi, F., and Barlowe, C. (2013). Organization of the ER-Golgi interface for membrane traffic control. Nat Rev Mol Cell Biol **14,** 382-392.

Burch-Smith, T.M., Schiff, M., Caplan, J.L., Tsao, J., Czymmek, K., and Dinesh-Kumar, S.P. (2007). A Novel Role for the TIR Domain in Association with Pathogen-Derived Elicitors. PLoS Biol **5,** e68.

Burkinshaw, B.J., and Strynadka, N.C.J. (2014). Assembly and structure of the T3SS. Biochimica et Biophysica Acta (BBA) - Molecular Cell Research **1843,** 1649-1663.

Buscaill, P., and Rivas, S. (2014). Transcriptional control of plant defence responses. Current Opinion in Plant Biology **20,** 35-46.

Caplan, J.L., Mamillapalli, P., Burch-Smith, T.M., Czymmek, K., and Dinesh-Kumar, S.P. (2008). Chloroplastic Protein NRIP1 Mediates Innate Immune Receptor Recognition of a Viral Effector. Cell **132,** 449-462.

Causier, B., Ashworth, M., Guo, W., and Davies, B. (2012). The TOPLESS Interactome: A Framework for Gene Repression in Arabidopsis. Plant Physiology **158,** 423-438.

Cesari, S., Thilliez, G., Ribot, C., Chalvon, V., Michel, C., Jauneau, A., Rivas, S., Alaux, L., Kanzaki, H., Okuyama, Y., Morel, J.-B., Fournier, E., Tharreau, D., Terauchi, R., and Kroj, T. (2013). The Rice Resistance Protein Pair RGA4/RGA5 Recognizes the *Magnaporthe oryzae* Effectors AVR-Pia and AVR1-CO39 by Direct Binding. The Plant Cell Online **25,** 1463-1481.

Césari, S., Kanzaki, H., Fujiwara, T., Bernoux, M., Chalvon, V., Kawano, Y., Shimamoto, K., Dodds, P., Terauchi, R., and Kroj, T. (2014). The NB‐LRR proteins RGA4 and RGA5 interact functionally and physically to confer disease resistance.

Chan, S.L., Mukasa, T., Santelli, E., Low, L.Y., and Pascual, J. (2010). The crystal structure of a TIR domain from *Arabidopsis thaliana* reveals a conserved helical region unique to plants. Protein Science **19,** 155-161.

Chang, C., Yu, D., Jiao, J., Jing, S., Schulze-Lefert, P., and Shen, Q.-H. (2013). Barley MLA Immune Receptors Directly Interfere with Antagonistically Acting Transcription Factors to Initiate Disease Resistance Signaling. The Plant Cell Online **25,** 1158-1173.

Chen, Y.-Q., Yu, H., Li, Y.-X., and Li, Y.-Y. (2010). Sorting out inherent features of head-to-head gene pairs by evolutionary conservation. BMC Bioinformatics **11,** S16.

Chen, Y., Li, Y., Wei, J., and Li, Y.-Y. (2014). Transcriptional regulation and spatial interactions of head-to-head genes. BMC Genomics **15,** 519.

Chen, Z., Zheng, Z., Huang, J., Lai, Z., and Fan, B. (2009). Biosynthesis of salicylic acid in plants. Plant Signaling & Behavior **4,** 493-496.

Cheng, C., Gao, X., Feng, B., Sheen, J., Shan, L., and He, P. (2013). Plant immune response to pathogens differs with changing temperatures. Nat Commun **4**.

Cheng, Y.T., Li, Y., Huang, S., Huang, Y., Dong, X., Zhang, Y., and Li, X. (2011). Stability of plant immune-receptor resistance proteins is controlled by SKP1-CULLIN1-F-box (SCF)-mediated protein degradation. Proceedings of the National Academy of Sciences **108,** 14694-14699.

Cheng, Y.T., Germain, H., Wiermer, M., Bi, D., Xu, F., García, A.V., Wirthmueller, L., Després, C., Parker, J.E., Zhang, Y., and Li, X. (2009). Nuclear Pore Complex Component MOS7/Nup88 Is Required for Innate Immunity and Nuclear Accumulation of Defense Regulators in Arabidopsis. The Plant Cell Online **21,** 2503-2516.

Coemans, B., Takahashi, Y., Berberich, T., Ito, A., Kanzaki, H., Matsumura, H., Saitoh, H., Tsuda, S., Kamoun, S., SÁGi, L., Swennen, R., and Terauchi, R. (2008). High-throughput *in planta* expression screening identifies an ADP-ribosylation factor (ARF1) involved in non-host resistance and R gene-mediated resistance. Molecular Plant Pathology **9,** 25-36.

Collier, S.M., and Moffett, P. (2009). NB-LRRs work a "bait and switch" on pathogens. Trends in Plant Science **14,** 521-529.

Copeland, C., Xu, S., Qi, Y., and Li, X. (2013). MOS2 has redundant function with its homolog MOS2H and is required for proper splicing of *SNC1*. Plant Signaling & Behavior **8,** e25372.

Dangl, J.L., and Jones, J.D.G. (2001). Plant pathogens and integrated defence responses to infection. Nature **411,** 826-833.

Daxinger, L., Hunter, B., Sheikh, M., Jauvion, V., Gasciolli, V., Vaucheret, H., Matzke, M., and Furner, I. (2008). Unexpected silencing effects from T-DNA tags in Arabidopsis. Trends in Plant Science **13,** 4-6.

de Jong, C.F., Takken, F.L.W., Cai, X., de Wit, P.J.G.M., and Joosten, M.H.A.J. (2002). Attenuation of Cf-Mediated Defense Responses at Elevated Temperatures Correlates With a Decrease in Elicitor-Binding Sites. Molecular Plant-Microbe Interactions **15,** 1040-1049.

Deslandes, L., and Rivas, S. (2012). Catch me if you can: bacterial effectors and plant targets. Trends in Plant Science **17,** 644-655.

Deslandes, L., Olivier, J., Theulières, F., Hirsch, J., Feng, D.X., Bittner-Eddy, P., Beynon, J., and Marco, Y. (2002). Resistance to *Ralstonia solanacearum* in *Arabidopsis thaliana* is conferred by the recessive *RRS1-R* gene, a member of a novel family of resistance genes. Proceedings of the National Academy of Sciences **99,** 2404-2409.

Deslandes, L., Olivier, J., Peeters, N., Feng, D.X., Khounlotham, M., Boucher, C., Somssich, I., Genin, S., and Marco, Y. (2003). Physical interaction between RRS1-R, a protein conferring resistance to bacterial wilt, and PopP2, a type III effector targeted to the plant nucleus. Proceedings of the National Academy of Sciences **100,** 8024-8029.

Deslandes, L., Pileur, F., Liaubet, L., Camut, S., Can, C., Williams, K., Holub, E., Beynon, J., Arlat, M., and Marco, Y. (1998). Genetic Characterization of *RRS1*, a Recessive Locus in *Arabidopsis thaliana* that Confers Resistance to the Bacterial Soilborne Pathogen *Ralstonia solanacearum*. Molecular Plant-Microbe Interactions **11,** 659-667.

Després, C., DeLong, C., Glaze, S., Liu, E., and Fobert, P.R. (2000). The Arabidopsis NPR1/NIM1 Protein Enhances the DNA Binding Activity of a Subgroup of the TGA Family of bZIP Transcription Factors. The Plant Cell Online **12,** 279-290.

Dinesh-Kumar, S.P., Tham, W.-H., and Baker, B.J. (2000). Structure–function analysis of the tobacco mosaic virus resistance gene *N*. Proceedings of the National Academy of Sciences **97,** 14789-14794.

Dodds, P.N., and Rathjen, J.P. (2010). Plant immunity: towards an integrated view of plant–pathogen interactions. Nat Rev Genet **11,** 539-548.

Dodds, P.N., Lawrence, G.J., Catanzariti, A.-M., Teh, T., Wang, C.-I.A., Ayliffe, M.A., Kobe, B., and Ellis, J.G. (2006). Direct protein interaction underlies gene-for-gene specificity and coevolution of the flax resistance genes and flax rust avirulence genes. Proceedings of the National Academy of Sciences **103,** 8888-8893.

Duplan, V., and Rivas, S. (2014). E3 ubiquitin-ligases and their target proteins during the regulation of plant innate immunity. Frontiers in Plant Science **5**.

Eitas, T.K., and Dangl, J.L. (2010). NB-LRR proteins: pairs, pieces, perception, partners, and pathways. Current Opinion in Plant Biology **13,** 472-477.

Ellis, J.G., Lawrence, G.J., Luck, J.E., and Dodds, P.N. (1999). Identification of Regions in Alleles of the Flax Rust Resistance Gene *L* That Determine Differences in Gene-for-Gene Specificity. The Plant Cell Online **11,** 495-506.

Engelhardt, S., Boevink, P.C., Armstrong, M.R., Ramos, M.B., Hein, I., and Birch, P.R.J. (2012). Relocalization of Late Blight Resistance Protein R3a to Endosomal Compartments Is Associated with Effector Recognition and Required for the Immune Response. The Plant Cell Online **24,** 5142-5158.

Enkhbayar, P., Kamiya, M., Osaki, M., Matsumoto, T., and Matsushima, N. (2004). Structural principles of leucine-rich repeat (LRR) proteins. Proteins: Structure, Function, and Bioinformatics **54,** 394-403.

Ferrer, J.L., Austin, M.B., Stewart Jr, C., and Noel, J.P. (2008). Structure and function of enzymes involved in the biosynthesis of phenylpropanoids. Plant Physiology and Biochemistry **46,** 356-370.

Feys, B.J., Moisan, L.J., Newman, M.-A., and Parker, J.E. (2001). Direct interaction between the Arabidopsis disease resistance signaling proteins, EDS1 and PAD4. EMBO J **20,** 5400-5411.

Flor, H.H. (1971). Current Status of the Gene-For-Gene Concept. Annual Review of Phytopathology **9,** 275-296.

Frost, D., Way, H., Howles, P., Luck, J., Manners, J., Hardham, A., Finnegan, J., and Ellis, J. (2004). Tobacco Transgenic for the Flax Rust Resistance Gene *L* Expresses Allele-Specific Activation of Defense Responses. Molecular Plant-Microbe Interactions **17,** 224-232.

Furlan, G., Klinkenberg, J., and Trujillo, M. (2012). Regulation of plant immune receptors by ubiquitination. Frontiers in Plant Science **3**.

Gao, Z., Chung, E.-H., Eitas, T.K., and Dangl, J.L. (2011). Plant intracellular innate immune receptor Resistance to *Pseudomonas syringae* pv. *maculicola* 1 (RPM1) is activated at, and functions on, the plasma membrane. Proceedings of the National Academy of Sciences **108,** 7619-7624.

García, A.V., Blanvillain-Baufumé, S., Huibers, R.P., Wiermer, M., Li, G., Gobbato, E., Rietz, S., and Parker, J.E. (2010). Balanced Nuclear and Cytoplasmic Activities of EDS1 Are Required for a Complete Plant Innate Immune Response. PLoS Pathog **6,** e1000970.

Gassmann, W. (2005). Natural Variation in the Arabidopsis Response to the Avirulence Gene hopPsyA Uncouples the Hypersensitive Response from Disease Resistance. Molecular Plant-Microbe Interactions **18,** 1054-1060.

Gassmann, W., Hinsch, M.E., and Staskawicz, B.J. (1999). The Arabidopsis *RPS4* bacterial-resistance gene is a member of the TIR-NBS-LRR family of disease-resistance genes. The Plant Journal **20,** 265-277.

Gendrel, A.-V., Lippman, Z., Martienssen, R., and Colot, V. (2005). Profiling histone modification patterns in plants using genomic tiling microarrays. Nat Meth **2,** 213-218.

Germann, S., Juul-Jensen, T., Letarnec, B., and Gaudin, V. (2006). DamID, a new tool for studying plant chromatin profiling in vivo, and its use to identify putative *LHP1* target loci. The Plant Journal **48,** 153-163.

Gloggnitzer, J., Akimcheva, S., Srinivasan, A., Kusenda, B., Riehs, N., Stampfl, H., Bautor, J., Dekrout, B., Jonak, C., Jiménez-Gómez, José M., Parker, Jane E., and Riha, K. (2014). Nonsense-Mediated mRNA Decay Modulates Immune Receptor Levels to Regulate Plant Antibacterial Defense. Cell Host & Microbe **16,** 376-390.

Goritschnig, S., Zhang, Y., and Li, X. (2007). The ubiquitin pathway is required for innate immunity in Arabidopsis. The Plant Journal **49,** 540-551.

Gou, M., Shi, Z., Zhu, Y., Bao, Z., Wang, G., and Hua, J. (2012). The F-box protein CPR1/CPR30 negatively regulates R protein SNC1 accumulation. The Plant Journal **69,** 411-420.

Gou, M., Su, N., Zheng, J., Huai, J., Wu, G., Zhao, J., He, J., Tang, D., Yang, S., and Wang, G. (2009). An F-box gene, CPR30, functions as a negative regulator of the defense response in Arabidopsis. The Plant Journal **60,** 757-770.

Guo, M., Tian, F., Wamboldt, Y., and Alfano, J.R. (2009). The Majority of the Type III Effector Inventory of *Pseudomonas syringae* pv. *tomato* DC3000 Can Suppress Plant Immunity. Molecular Plant-Microbe Interactions **22,** 1069-1080.

Heidrich, K., Wirthmueller, L., Tasset, C., Pouzet, C., Deslandes, L., and Parker, J.E. (2011). Arabidopsis *EDS1* Connects Pathogen Effector Recognition to Cell Compartment-Specific Immune Responses. Science **334,** 1401-1404.

Heidrich, K., Tsuda, K., Blanvillain-Baufumé, S., Wirthmueller, L., Bautor, J., and Parker, J.E. (2013). Arabidopsis TNL-WRKY domain receptor RRS1 contributes to temperature-conditioned RPS4 auto-immunity. Frontiers in Plant Science **4**.

Hinsch, M., and Staskawicz, B. (1996). Identification of a New Arabidopsis Disease Resistance Locus, *RPS4*, and Cloning of the Corresponding Avirulence Gene, avrRps4, from *Pseudomonas syringae* pv. *pisi*. . MPMI **9,** 55-61.

Holt, B.F., Belkhadir, Y., and Dangl, J.L. (2005). Antagonistic Control of Disease Resistance Protein Stability in the Plant Immune System. Science **309,** 929-932.

Howles, P., Lawrence, G., Finnegan, J., McFadden, H., Ayliffe, M., Dodds, P., and Ellis, J. (2005). Autoactive Alleles of the Flax *L6* Rust Resistance Gene Induce Non-Race-Specific Rust Resistance Associated with the Hypersensitive Response. Molecular Plant-Microbe Interactions **18,** 570-582.

Hu, Z., Yan, C., Liu, P., Huang, Z., Ma, R., Zhang, C., Wang, R., Zhang, Y., Martinon, F., Miao, D., Deng, H., Wang, J., Chang, J., and Chai, J. (2013). Crystal Structure of NLRC4 Reveals Its Autoinhibition Mechanism. Science **341,** 172-175.

Hua, J. (2013). Modulation of plant immunity by light, circadian rhythm, and temperature. Current Opinion in Plant Biology **16,** 406-413.

Huang, J., Gu, M., Lai, Z., Fan, B., Shi, K., Zhou, Y.-H., Yu, J.-Q., and Chen, Z. (2010). Functional Analysis of the Arabidopsis *PAL* Gene Family in Plant Growth, Development, and Response to Environmental Stress. Plant Physiology **153,** 1526-1538.

Huang, S., Monaghan, J., Zhong, X., Lin, L., Sun, T., Dong, O.X., and Li, X. (2014a). HSP90s are required for NLR immune receptor accumulation in Arabidopsis. The Plant Journal **79,** 427-439.

Huang, Y., Minaker, S., Roth, C., Huang, S., Hieter, P., Lipka, V., Wiermer, M., and Li, X. (2014b). An E4 Ligase Facilitates Polyubiquitination of Plant Immune Receptor Resistance Proteins in Arabidopsis. The Plant Cell Online **26,** 485-496.

Hubert, D.A., He, Y., McNulty, B.C., Tornero, P., and Dangl, J.L. (2009). Specific Arabidopsis HSP90.2 alleles recapitulate RAR1 cochaperone function in plant NB-LRR disease resistance protein regulation. Proceedings of the National Academy of Sciences **106,** 9556-9563.

Hubert, D.A., Tornero, P., Belkhadir, Y., Krishna, P., Takahashi, A., Shirasu, K., and Dangl, J.L. (2003). Cytosolic HSP90 associates with and modulates the Arabidopsis RPM1 disease resistance protein. The EMBO Journal **22,** 5679-5689.

Hwang, C.-F., Bhakta, A.V., Truesdell, G.M., Pudlo, W.M., and Williamson, V.M. (2000). Evidence for a Role of the N Terminus and Leucine-Rich Repeat Region of the Mi Gene Product in Regulation of Localized Cell Death. The Plant Cell Online **12,** 1319-1329.

Hyodo, K., Kaido, M., and Okuno, T. (2014). Traffic jam on the cellular secretory pathway generated by a replication protein from a plant RNA virus. Plant Signaling & Behavior **9,** e28644.

Hyodo, K., Mine, A., Taniguchi, T., Kaido, M., Mise, K., Taniguchi, H., and Okuno, T. (2013). ADP Ribosylation Factor 1 Plays an Essential Role in the Replication of a Plant RNA Virus. Journal of Virology **87,** 163-176.

Inoue, H., Hayashi, N., Matsushita, A., Xinqiong, L., Nakayama, A., Sugano, S., Jiang, C.-J., and Takatsuji, H. (2013). Blast resistance of CC-NB-LRR protein Pb1 is mediated by WRKY45 through protein–protein interaction. Proceedings of the National Academy of Sciences **110,** 9577-9582.

Jacob, F., Vernaldi, S., and Maekawa, T. (2013). Evolution and conservation of plant NLR functions. Frontiers in Immunology **4**.

Jelenska, J., van Hal, J.A., and Greenberg, J.T. (2010). *Pseudomonas syringae* hijacks plant stress chaperone machinery for virulence. Proceedings of the National Academy of Sciences **107,** 13177-13182.

Jelenska, J., Yao, N., Vinatzer, B.A., Wright, C.M., Brodsky, J.L., and Greenberg, J.T. (2007). A J Domain Virulence Effector of *Pseudomonas syringae* Remodels Host Chloroplasts and Suppresses Defenses. Current Biology **17,** 499-508.

Jia, Y., McAdams, S.A., Bryan, G.T., Hershey, H.P., and Valent, B. (2000). Direct interaction of resistance gene and avirulence gene products confers rice blast resistance.

Jirage, D., Tootle, T.L., Reuber, T.L., Frost, L.N., Feys, B.J., Parker, J.E., Ausubel, F.M., and Glazebrook, J. (1999). *Arabidopsis thaliana PAD4* encodes a lipase-like gene that is important for salicylic acid signaling. Proceedings of the National Academy of Sciences **96,** 13583-13588.

Johnson, K.C.M., Dong, O.X., Huang, Y., and Li, X. (2012). A Rolling Stone Gathers No Moss, but Resistant Plants Must Gather Their MOSes. Cold Spring Harbor Symposia on Quantitative Biology **77,** 259-268.

Jones, J.D.G., and Dangl, J.L. (2006). The plant immune system. Nature **444,** 323-329.

Kadota, Y., Shirasu, K., and Guerois, R. (2010). NLR sensors meet at the SGT1–HSP90 crossroad. Trends in Biochemical Sciences **35,** 199-207.

Kadota, Y., Sklenar, J., Derbyshire, P., Stransfeld, L., Asai, S., Ntoukakis, V., Jones, Jonathan D., Shirasu, K., Menke, F., Jones, A., and Zipfel, C. (2014). Direct Regulation of the NADPH Oxidase RBOHD by the PRR-Associated Kinase BIK1 during Plant Immunity. Molecular Cell **54,** 43-55.

Kanzaki, H., Yoshida, K., Saitoh, H., Fujisaki, K., Hirabuchi, A., Alaux, L., Fournier, E., Tharreau, D., and Terauchi, R. (2012). Arms race co-evolution of *Magnaporthe oryzae* AVR-Pik and rice *Pik* genes driven by their physical interactions. The Plant Journal **72,** 894-907.

Kawano, Y., Akamatsu, A., Hayashi, K., Housen, Y., Okuda, J., Yao, A., Nakashima, A., Takahashi, H., Yoshida, H., Wong, H.L., Kawasaki, T., and Shimamoto, K. (2010). Activation of a Rac GTPase by the NLR Family Disease Resistance Protein Pit Plays a Critical Role in Rice Innate Immunity. Cell Host & Microbe **7,** 362-375.

Kim, M.G., da Cunha, L., McFall, A.J., Belkhadir, Y., DebRoy, S., Dangl, J.L., and Mackey, D. (2005). Two *Pseudomonas syringae* Type III Effectors Inhibit RIN4-Regulated Basal Defense in Arabidopsis. Cell **121,** 749-759.

Kim, S.H., Kwon, S.I., Saha, D., Anyanwu, N.C., and Gassmann, W. (2009). Resistance to the *Pseudomonas syringae* Effector HopA1 Is Governed by the TIR-NBS-LRR Protein RPS6 and Is Enhanced by Mutations in SRFR1. Plant Physiology **150,** 1723-1732.

Kim, S.H., Gao, F., Bhattacharjee, S., Adiasor, J.A., Nam, J.C., and Gassmann, W. (2010). The Arabidopsis Resistance-Like Gene *SNC1* Is Activated by Mutations in *SRFR1* and Contributes to Resistance to the Bacterial Effector AvrRps4. PLoS Pathog **6,** e1001172.

Kim, S.H., Son, G.H., Bhattacharjee, S., Kim, H.J., Nam, J.C., Nguyen, P.D.T., Hong, J.C., and Gassmann, W. (2014). The Arabidopsis immune adaptor SRFR1 interacts with TCP transcription factors that redundantly contribute to effector-triggered immunity. The Plant Journal **78,** 978-989.

Kim, T.-H., Kunz, H.-H., Bhattacharjee, S., Hauser, F., Park, J., Engineer, C., Liu, A., Ha, T., Parker, J.E., Gassmann, W., and Schroeder, J.I. (2012). Natural Variation in Small Molecule–Induced TIR-NB-LRR Signaling Induces Root Growth Arrest via EDS1- and PAD4-Complexed R Protein VICTR in Arabidopsis. The Plant Cell Online **24,** 5177-5192.

Kinkema, M., Fan, W., and Dong, X. (2000). Nuclear Localization of NPR1 Is Required for Activation of PR Gene Expression. The Plant Cell Online **12,** 2339-2350.

Knepper, C., Savory, E.A., and Day, B. (2011). The role of NDR1 in pathogen perception and plant defense signaling. Plant Signaling & Behavior **6,** 1114-1116.

Kobe, B., and Kajava, A.V. (2001). The leucine-rich repeat as a protein recognition motif. Current Opinion in Structural Biology **11,** 725-732.

Koncz, C., and Schell, J. (1986). The promoter of *TL-DNA gene 5* controls the tissue-specific expression of chimaeric genes carried by a novel type of Agrobacterium binary vector. Molec Gen Genet **204,** 383-396.

Krasileva, K.V., Dahlbeck, D., and Staskawicz, B.J. (2010). Activation of an Arabidopsis Resistance Protein Is Specified by the in Planta Association of Its Leucine-Rich Repeat Domain with the Cognate Oomycete Effector. The Plant Cell Online **22,** 2444-2458.

Kwon, C., and Yun, H.S. (2014). Plant exocytic secretion of toxic compounds for defense. Toxicol Res **30,** 77-81.

Kwon, S.I., Koczan, J.M., and Gassmann, W. (2004). Two Arabidopsis *srfr* (*suppressor of rps4-RLD*) mutants exhibit avrRps4-specific disease resistance independent of *RPS4*. The Plant Journal **40,** 366-375.

Kwon, S.I., Kim, S.H., Bhattacharjee, S., Noh, J.-J., and Gassmann, W. (2009). SRFR1, a suppressor of effector-triggered immunity, encodes a conserved tetratricopeptide repeat protein with similarity to transcriptional repressors. The Plant Journal **57,** 109-119.

Lamb, C.J., Lawton, M.A., Dron, M., and Dixon, R.A. (1989). Signals and transduction mechanisms for activation of plant defenses against microbial attack. Cell **56,** 215-224.

Langmead, B., Trapnell, C., Pop, M., and Salzberg, S. (2009). Ultrafast and memory-efficient alignment of short DNA sequences to the human genome. Genome Biology **10,** R25.

Lee, S.-K., Song, M.-Y., Seo, Y.-S., Kim, H.-K., Ko, S., Cao, P.-J., Suh, J.-P., Yi, G., Roh, J.-H., Lee, S., An, G., Hahn, T.-R., Wang, G.-L., Ronald, P., and Jeon, J.-S. (2009). Rice Pi5-Mediated Resistance to Magnaporthe oryzae Requires the Presence of Two Coiled-Coil–Nucleotide-Binding–Leucine-Rich Repeat Genes. Genetics **181,** 1627-1638.

Leister, R.T., Dahlbeck, D., Day, B., Li, Y., Chesnokova, O., and Staskawicz, B.J. (2005). Molecular Genetic Evidence for the Role of SGT1 in the Intramolecular Complementation of Bs2 Protein Activity in Nicotiana benthamiana. The Plant Cell Online **17,** 1268-1278.

Lewis, J.D., Lee, A.M.Y., Ma, W., Zhou, H., Guttman, D.S., and Desveaux, D. (2011). The YopJ superfamily in plant-associated bacteria. Molecular Plant Pathology **12,** 928-937.

Li, G., Froehlich, J.E., Elowsky, C., Msanne, J., Ostosh, A.C., Zhang, C., Awada, T., and Alfano, J.R. (2014a). Distinct Pseudomonas type-III effectors use a cleavable transit peptide to target chloroplasts. The Plant Journal **77,** 310-321.

Li, L., Li, M., Yu, L., Zhou, Z., Liang, X., Liu, Z., Cai, G., Gao, L., Zhang, X., Wang, Y., Chen, S., and Zhou, J.-M. (2014b). The FLS2-Associated Kinase BIK1 Directly Phosphorylates the NADPH Oxidase RbohD to Control Plant Immunity. Cell Host & Microbe **15,** 329-338.

Li, X., Clarke, J.D., Zhang, Y., and Dong, X. (2001). Activation of an *EDS1*-Mediated *R*-Gene Pathway in the *snc1* Mutant Leads to Constitutive, *NPR1*-Independent Pathogen Resistance. Molecular Plant-Microbe Interactions **14,** 1131-1139.

Li, Y.-Y., Yu, H., Guo, Z.-M., Guo, T.-Q., Tu, K., and Li, Y.-X. (2006). Systematic Analysis of Head-to-Head Gene Organization: Evolutionary Conservation and Potential Biological Relevance. PLoS Comput Biol **2,** e74.

Li, Y., Li, S., Bi, D., Cheng, Y.T., Li, X., and Zhang, Y. (2010). SRFR1 Negatively Regulates Plant NB-LRR Resistance Protein Accumulation to Prevent Autoimmunity. PLoS Pathog **6,** e1001111.

Liu, J.-Z., and Whitham, S.A. (2013). Overexpression of a soybean nuclear localized type–III DnaJ domain-containing HSP40 reveals its roles in cell death and disease resistance. The Plant Journal **74,** 110-121.

Liu, J., Elmore, J.M., Fuglsang, A.T., Palmgren, M.G., Staskawicz, B.J., and Coaker, G. (2009). RIN4 Functions with Plasma Membrane H^+-ATPases to Regulate Stomatal Apertures during Pathogen Attack. PLoS Biol **7,** e1000139.

Liu, Y., and Li, J. (2014). Endoplasmic Reticulum-Mediated Protein Quality Control in Arabidopsis. Frontiers in Plant Science **5**.

Liu, Y., Schiff, M., Serino, G., Deng, X.-W., and Dinesh-Kumar, S.P. (2002). Role of SCF Ubiquitin-Ligase and the COP9 Signalosome in the *N* Gene–Mediated Resistance Response to Tobacco mosaic virus. The Plant Cell Online **14,** 1483-1496.

Liu, Y., Burch-Smith, T., Schiff, M., Feng, S., and Dinesh-Kumar, S.P. (2004). Molecular Chaperone Hsp90 Associates with Resistance Protein N and Its Signaling Proteins SGT1 and Rar1 to Modulate an Innate Immune Response in Plants. Journal of Biological Chemistry **279,** 2101-2108.

Lorković, Z.J., and Barta, A. (2002). Genome analysis: RNA recognition motif (RRM) and K homology (KH) domain RNA-binding proteins from the flowering plant Arabidopsis thaliana. Nucleic Acids Research **30,** 623-635.

Lorković, Z.J., Wieczorek Kirk, D.A., Klahre, U., Hemmings-Mieszczak, M., and Filipowicz, W. (2000). RBP45 and RBP47, two oligouridylate-specific hnRNP-like proteins interacting with poly(A)+ RNA in nuclei of plant cells. RNA **6,** 1610-1624.

Lukasik, E., and Takken, F.L.W. (2009). STANDing strong, resistance proteins instigators of plant defence. Current Opinion in Plant Biology **12,** 427-436.

Mackey, D., Belkhadir, Y., Alonso, J.M., Ecker, J.R., and Dangl, J.L. (2003). Arabidopsis RIN4 Is a Target of the Type III Virulence Effector AvrRpt2 and Modulates RPS2-Mediated Resistance. Cell **112,** 379-389.

Maekawa, T., Kracher, B., Vernaldi, S., Ver Loren van Themaat, E., and Schulze-Lefert, P. (2012). Conservation of NLR-triggered immunity across plant lineages. Proceedings of the National Academy of Sciences **109,** 20119-20123.

Mang, H.-G., Qian, W., Zhu, Y., Qian, J., Kang, H.-G., Klessig, D.F., and Hua, J. (2012). Abscisic Acid Deficiency Antagonizes High-Temperature Inhibition of Disease Resistance through Enhancing Nuclear Accumulation of Resistance Proteins SNC1 and RPS4 in Arabidopsis. The Plant Cell Online.

Marco Llorca, C., Potschin, M., and Zentgraf, U. (2014). bZIPs and WRKYs: two large transcription factor families executing two different functional strategies. Frontiers in Plant Science **5**.

Martin, M. (2011). Cutadapt removes adapter sequences from high-throughput sequencing reads. 2011 **17**.

Mauch-Mani, B., and Slusarenko, A.J. (1996). Production of Salicylic Acid Precursors Is a Major Function of Phenylalanine Ammonia-Lyase in the Resistance of Arabidopsis to Peronospora parasitica. The Plant Cell Online **8,** 203-212.

McClung, C.R., and Davis, S.J. (2010). Ambient Thermometers in Plants: From Physiological Outputs towards Mechanisms of Thermal Sensing. Current Biology **20,** R1086-R1092.

Meyer, Y., Belin, C., Delorme-Hinoux, V., Reichheld, J.-P., and Riondet, C. (2012). Thioredoxin and Glutaredoxin Systems in Plants: Molecular Mechanisms, Crosstalks, and Functional Significance. Antioxidants & Redox Signaling. **Volume: 17,** 1124-1160.

Meyers, B.C., Kozik, A., Griego, A., Kuang, H., and Michelmore, R.W. (2003). Genome-Wide Analysis of NBS-LRR–Encoding Genes in Arabidopsis. The Plant Cell Online **15,** 809-834.

Michael Weaver, L., Swiderski, M.R., Li, Y., and Jones, J.D.G. (2006). The Arabidopsis thaliana TIR-NB-LRR R-protein, RPP1A; protein localization and constitutive activation of defence by truncated alleles in tobacco and Arabidopsis. The Plant Journal **47,** 829-840.

Min, M.K., Jang, M., Lee, M., Lee, J., Song, K., Lee, Y., Choi, K.Y., Robinson, D.G., and Hwang, I. (2013). Recruitment of Arf1-GDP to Golgi by Glo3p-Type ArfGAPs Is Crucial for Golgi Maintenance and Plant Growth. Plant Physiology **161,** 676-691.

Motomura, K., Le, Q.T.N., Kumakura, N., Fukaya, T., Takeda, A., and Watanabe, Y. (2012). The role of decapping proteins in the miRNA accumulation in *Arabidopsis thaliana*. RNA Biology **9,** 644-652.

Mou, Z., Fan, W., and Dong, X. (2003). Inducers of Plant Systemic Acquired Resistance Regulate NPR1 Function through Redox Changes. Cell **113,** 935-944.

Muskett, P.R., Kahn, K., Austin, M.J., Moisan, L.J., Sadanandom, A., Shirasu, K., Jones, J.D.G., and Parker, J.E. (2002). Arabidopsis RAR1 Exerts Rate-Limiting Control of *R* Gene–Mediated Defenses against Multiple Pathogens. The Plant Cell Online **14,** 979-992.

Narusaka, M., Hatakeyama, K., Shirasu, K., and Narusaka, Y. (2014). *Arabidopsis* dual resistance proteins, both RPS4 and RRS1, are required for resistance to bacterial wilt in transgenic *Brassica* crops. Plant Signaling & Behavior **9,** e29130.

Narusaka, M., Kubo, Y., Shiraishi, T., Iwabuchi, M., and Narusaka, Y. (2009a). A dual resistance gene system prevents infection by three distinct pathogens. Plant Signaling & Behavior **4,** 954-955.

Narusaka, M., Shirasu, K., Noutoshi, Y., Kubo, Y., Shiraishi, T., Iwabuchi, M., and Narusaka, Y. (2009b). *RRS1* and *RPS4* provide a dual *Resistance*-gene system against fungal and bacterial pathogens. The Plant Journal **60,** 218-226.

Narusaka, M., Kubo, Y., Hatakeyama, K., Imamura, J., Ezura, H., Nanasato, Y., Tabei, Y., Takano, Y., Shirasu, K., and Narusaka, Y. (2013a). Breaking restricted taxonomic functionality by dual *resistance* genes. Plant Signaling & Behavior **8,** e24244.

Narusaka, M., Kubo, Y., Hatakeyama, K., Imamura, J., Ezura, H., Nanasato, Y., Tabei, Y., Takano, Y., Shirasu, K., and Narusaka, Y. (2013b). Interfamily Transfer of Dual NB-LRR Genes Confers Resistance to Multiple Pathogens. PLoS ONE **8,** e55954.

Nishimura, M.T., and Dangl, J.L. (2014). Paired Plant Immune Receptors. Science **344,** 267-268.

Noël, L.D., Cagna, G., Stuttmann, J., Wirthmüller, L., Betsuyaku, S., Witte, C.-P., Bhat, R., Pochon, N., Colby, T., and Parker, J.E. (2007). Interaction between SGT1 and Cytosolic/Nuclear HSC70 Chaperones Regulates Arabidopsis Immune Responses. The Plant Cell Online **19,** 4061-4076.

Nomura, K., DebRoy, S., Lee, Y.H., Pumplin, N., Jones, J., and He, S.Y. (2006). A Bacterial Virulence Protein Suppresses Host Innate Immunity to Cause Plant Disease. Science **313,** 220-223.

Nomura, K., Mecey, C., Lee, Y.-N., Imboden, L.A., Chang, J.H., and He, S.Y. (2011). Effector-triggered immunity blocks pathogen degradation of an immunity-associated vesicle traffic regulator in Arabidopsis. Proceedings of the National Academy of Sciences **108,** 10774-10779.

Noutoshi, Y., Ito, T., Seki, M., Nakashita, H., Yoshida, S., Marco, Y., Shirasu, K., and Shinozaki, K. (2005). A single amino acid insertion in the WRKY domain of the Arabidopsis TIR–NBS–LRR–WRKY-type disease resistance protein SLH1 (sensitive to low humidity 1) causes activation of defense responses and hypersensitive cell death. The Plant Journal **43,** 873-888.

Okuyama, Y., Kanzaki, H., Abe, A., Yoshida, K., Tamiru, M., Saitoh, H., Fujibe, T., Matsumura, H., Shenton, M., Galam, D.C., Undan, J., Ito, A., Sone, T., and Terauchi, R. (2011). A multifaceted genomics approach allows the isolation of the rice *Pia*-blast resistance gene consisting of two adjacent NBS-LRR protein genes. The Plant Journal **66,** 467-479.

Orian, A. (2006). Chromatin profiling, DamID and the emerging landscape of gene expression. Current Opinion in Genetics & Development **16,** 157-164.

Padmanabhan, M., Cournoyer, P., and Dinesh-Kumar, S.P. (2009). The leucine-rich repeat domain in plant innate immunity: a wealth of possibilities. Cellular Microbiology **11,** 191-198.

Padmanabhan, M.S., and Dinesh-Kumar, S.P. (2010). All Hands on Deck—The Role of Chloroplasts, Endoplasmic Reticulum, and the Nucleus in Driving Plant Innate Immunity. Molecular Plant-Microbe Interactions **23,** 1368-1380.

Padmanabhan, M.S., Ma, S., Burch-Smith, T.M., Czymmek, K., Huijser, P., and Dinesh-Kumar, S.P. (2013). Novel Positive Regulatory Role for the SPL6 Transcription Factor in the N TIR-NB-LRR Receptor-Mediated Plant Innate Immunity. PLoS Pathog **9,** e1003235.

Palma, K., Thorgrimsen, S., Malinovsky, F.G., Fiil, B.K., Nielsen, H.B., Brodersen, P., Hofius, D., Petersen, M., and Mundy, J. (2010). Autoimmunity in Arabidopsis *acd11* Is Mediated by Epigenetic Regulation of an Immune Receptor. PLoS Pathog **6,** e1001137.

Park, C.-J., and Ronald, P.C. (2012). Cleavage and nuclear localization of the rice XA21 immune receptor. Nat Commun **3,** 920.

Park, S.K., Jung, Y.J., Lee, J.R., Lee, Y.M., Jang, H.H., Lee, S.S., Park, J.H., Kim, S.Y., Moon, J.C., Lee, S.Y., Chae, H.B., Shin, M.R., Jung, J.H., Kim, M.G., Kim, W.Y., Yun, D.-J., Lee, K.O., and Lee, S.Y. (2009). Heat-Shock and Redox-Dependent Functional Switching of an h-Type Arabidopsis Thioredoxin from a Disulfide Reductase to a Molecular Chaperone. Plant Physiology **150,** 552-561.

Peart, J.R., Lu, R., Sadanandom, A., Malcuit, I., Moffett, P., Brice, D.C., Schauser, L., Jaggard, D.A.W., Xiao, S., Coleman, M.J., Dow, M., Jones, J.D.G., Shirasu, K., and Baulcombe, D.C. (2002). Ubiquitin ligase-associated protein SGT1 is required for host and nonhost disease resistance in plants. Proceedings of the National Academy of Sciences **99,** 10865-10869.

Peine, N.A. (2013). Impact of Nuclear EDS1 on Arabidopsis Immunity. Doctoral dissertation. University of Cologne, Germany.

Penfield, S. (2008). Temperature perception and signal transduction in plants. New Phytologist **179,** 615-628.

Petersen, N.H.T., Joensen, J., McKinney, L.V., Brodersen, P., Petersen, M., Hofius, D., and Mundy, J. (2009). Identification of proteins interacting with Arabidopsis ACD11. Journal of Plant Physiology **166,** 661-666.

Qi, D., and Innes, R.W. (2013). Recent advances in plant NLR structure, function, localization and signaling. Frontiers in Immunology **4**.

Qin, X.F., Holuigue, L., Horvath, D.M., and Chua, N.H. (1994). Immediate early transcription activation by salicylic acid via the cauliflower mosaic virus *as-1* element. The Plant Cell Online **6,** 863-874.

Rairdan, G.J., and Moffett, P. (2006). Distinct Domains in the ARC Region of the Potato Resistance Protein Rx Mediate LRR Binding and Inhibition of Activation. The Plant Cell Online **18,** 2082-2093.

Ravensdale, M., Bernoux, M., Ve, T., Kobe, B., Thrall, P.H., Ellis, J.G., and Dodds, P.N. (2012). Intramolecular Interaction Influences Binding of the Flax L5 and L6 Resistance Proteins to their AvrL567 Ligands. PLoS Pathog **8,** e1003004.

Redman, J., Whitcraft, J., Johnson, C., and Arias, J. (2002). Abiotic and biotic stress differentially stimulate as-1 element activity in Arabidopsis. Plant Cell Rep **21,** 180-185.

Riehs-Kearnan, N., Gloggnitzer, J., Dekrout, B., Jonak, C., and Riha, K. (2012). Aberrant growth and lethality of Arabidopsis deficient in nonsense-mediated RNA decay factors is caused by autoimmune-like response. Nucleic Acids Research **40,** 5615-5624.

Rietz, S., Stamm, A., Malonek, S., Wagner, S., Becker, D., Medina-Escobar, N., Vlot, A., Feys, B., Niefind, K., and Parker, J. (2011). Different roles of Enhanced Disease Susceptibility1 (EDS1) bound to and dissociated from Phytoalexin Deficient4 (PAD4) in Arabidopsis immunity. New Phytol. **191,** 107-119.

Rochon, A., Boyle, P., Wignes, T., Fobert, P.R., and Després, C. (2006). The Coactivator Function of Arabidopsis NPR1 Requires the Core of Its BTB/POZ Domain and the Oxidation of C-Terminal Cysteines. The Plant Cell Online **18,** 3670-3685.

Rodríguez-Herva, J.J., González-Melendi, P., Cuartas-Lanza, R., Antúnez-Lamas, M., Río-Alvarez, I., Li, Z., López-Torrejón, G., Díaz, I., del Pozo, J.C., Chakravarthy, S., Collmer, A., Rodríguez-Palenzuela, P., and López-Solanilla, E. (2012). A bacterial cysteine protease effector protein interferes with photosynthesis to suppress plant innate immune responses. Cellular Microbiology **14,** 669-681.

Rohde, A., Morreel, K., Ralph, J., Goeminne, G., Hostyn, V., De Rycke, R., Kushnir, S., Van Doorsselaere, J., Joseleau, J.-P., Vuylsteke, M., Van Driessche, G., Van Beeumen, J., Messens, E., and Boerjan, W. (2004). Molecular Phenotyping of the *pal1* and *pal2* Mutants of *Arabidopsis thaliana* Reveals Far-Reaching Consequences on Phenylpropanoid, Amino Acid, and Carbohydrate Metabolism. The Plant Cell Online **16,** 2749-2771.

Rojas, C.M., Senthil-Kumar, M., Tzin, V., and Mysore, K. (2014). Regulation of primary plant metabolism during plant-pathogen interactions and its contribution to plant defense. Frontiers in Plant Science **5**.

Samuel, G. (1931). Some experiments on inoculating methods with plant viruses, and on local lesions. Ann. Appl. Biol. **18,** 494-507.

Saucet, S.B. (2013). Toward the understanding of TIR-NB-LRR-mediated immunity; study of the AvrRps4 recognition model in Arabidopsis. Doctoral dissertation. University of East Anglia, UK.

Schmieder, R., and Edwards, R. (2011). Quality control and preprocessing of metagenomic datasets. Bioinformatics **27,** 863-864.

Schornack, S., Ballvora, A., Gürlebeck, D., Peart, J., Ganal, M., Baker, B., Bonas, U., and Lahaye, T. (2004). The tomato resistance protein Bs4 is a predicted non-nuclear TIR-NB-LRR protein that mediates defense responses to severely truncated derivatives of AvrBs4 and overexpressed AvrBs3. The Plant Journal **37,** 46-60.

Shankaranarayanan, P., Mendoza-Parra, M.-A., van Gool, W., Trindade, L.M., and Gronemeyer, H. (2012). Single-tube linear DNA amplification for genome-wide studies using a few thousand cells. Nat. Protocols **7,** 328-338.

Shen, Q.-H., Saijo, Y., Mauch, S., Biskup, C., Bieri, S., Keller, B., Seki, H., Ülker, B., Somssich, I.E., and Schulze-Lefert, P. (2007). Nuclear Activity of MLA Immune Receptors Links Isolate-Specific and Basal Disease-Resistance Responses. Science **315,** 1098-1103.

Shivaprasad, P.V., Chen, H.-M., Patel, K., Bond, D.M., Santos, B.A.C.M., and Baulcombe, D.C. (2012). A MicroRNA Superfamily Regulates Nucleotide Binding Site–Leucine-Rich Repeats and Other mRNAs. The Plant Cell Online **24,** 859-874.

Sinapidou, E., Williams, K., Nott, L., Bahkt, S., Tör, M., Crute, I., Bittner-Eddy, P., and Beynon, J. (2004). Two *TIR:NB:LRR* genes are required to specify resistance to *Peronospora parasitica* isolate Cala2 in Arabidopsis. The Plant Journal **38,** 898-909.

Slootweg, E.J., Spiridon, L.N., Roosien, J., Butterbach, P., Pomp, R., Westerhof, L., Wilbers, R., Bakker, E., Bakker, J., Petrescu, A.-J., Smant, G., and Goverse, A. (2013). Structural Determinants at the Interface of the ARC2 and Leucine-Rich Repeat Domains Control the Activation of the Plant Immune Receptors Rx1 and Gpa2. Plant Physiology **162,** 1510-1528.

Smirnova, A., Li, H., Weingart, H., Aufhammer, S., Burse, A., Finis, K., Schenk, A., and Ullrich, M. (2001). Thermoregulated expression of virulence factors in plant-associated bacteria. Arch Microbiol **176,** 393-399.

Sohn, K.H., Zhang, Y., and Jones, J.D.G. (2009). The *Pseudomonas syringae* effector protein, AvrRPS4, requires *in planta* processing and the KRVY domain to function. The Plant Journal **57,** 1079-1091.

Spoel, S.H., Mou, Z., Tada, Y., Spivey, N.W., Genschik, P., and Dong, X. (2009). Proteasome-Mediated Turnover of the Transcription Coactivator NPR1 Plays Dual Roles in Regulating Plant Immunity. Cell **137,** 860-872.

Staiger, D., Korneli, C., Lummer, M., and Navarro, L. (2013). Emerging role for RNA-based regulation in plant immunity. New Phytologist **197,** 394-404.

Swiderski, M.R., Birker, D., and Jones, J.D.G. (2009). The TIR Domain of TIR-NB-LRR Resistance Proteins Is a Signaling Domain Involved in Cell Death Induction. Molecular Plant-Microbe Interactions **22,** 157-165.

Tada, Y., Spoel, S.H., Pajerowska-Mukhtar, K., Mou, Z., Song, J., Wang, C., Zuo, J., and Dong, X. (2008). Plant Immunity Requires Conformational Charges of NPR1 via S-Nitrosylation and Thioredoxins. Science **321,** 952-956.

Tahir, J., Watanabe, M., Jing, H.-C., Hunter, D.A., Tohge, T., Nunes-Nesi, A., Brotman, Y., Fernie, A.R., Hoefgen, R., and Dijkwel, P.P. (2013). Activation of R-mediated innate immunity and disease susceptibility is affected by mutations in a cytosolic O-acetylserine (thiol) lyase in Arabidopsis. The Plant Journal **73,** 118-130.

Takahashi, A., Casais, C., Ichimura, K., and Shirasu, K. (2003). HSP90 interacts with RAR1 and SGT1 and is essential for *RPS2*-mediated disease resistance in Arabidopsis. Proceedings of the National Academy of Sciences **100,** 11777-11782.

Takken, F.L.W., and Goverse, A. (2012). How to build a pathogen detector: structural basis of NB-LRR function. Current Opinion in Plant Biology **15,** 375-384.

Takken, F.L.W., Albrecht, M., and Tameling, W.I.L. (2006). Resistance proteins: molecular switches of plant defence. Current Opinion in Plant Biology **9,** 383-390.

Tameling, W.I.L., Elzinga, S.D.J., Darmin, P.S., Vossen, J.H., Takken, F.L.W., Haring, M.A., and Cornelissen, B.J.C. (2002). The Tomato R Gene Products I-2 and Mi-1 Are Functional ATP Binding Proteins with ATPase Activity. The Plant Cell Online **14,** 2929-2939.

Tameling, W.I.L., Vossen, J.H., Albrecht, M., Lengauer, T., Berden, J.A., Haring, M.A., Cornelissen, B.J.C., and Takken, F.L.W. (2006). Mutations in the NB-ARC Domain of I-2 That Impair ATP Hydrolysis Cause Autoactivation. Plant Physiology **140,** 1233-1245.

Tao, Y., Yuan, F., Leister, R.T., Ausubel, F.M., and Katagiri, F. (2000). Mutational Analysis of the Arabidopsis Nucleotide Binding Site–Leucine-Rich Repeat Resistance Gene *RPS2*. The Plant Cell Online **12,** 2541-2554.

Tasset, C., Bernoux, M., Jauneau, A., Pouzet, C., Brière, C., Kieffer-Jacquinod, S., Rivas, S., Marco, Y., and Deslandes, L. (2010). Autoacetylation of the *Ralstonia solanacearum* Effector PopP2 Targets a Lysine Residue Essential for *RRS1-R*-Mediated Immunity in Arabidopsis. PLoS Pathog **6,** e1001202.

Tian, D., Traw, M.B., Chen, J.Q., Kreitman, M., and Bergelson, J. (2003). Fitness costs of *R*-gene-mediated resistance in *Arabidopsis thaliana*. Nature **423,** 74-77.

Tornero, P., and Dangl, J.L. (2001). A high-throughput method for quantifying growth of phytopathogenic bacteria in Arabidopsis thaliana. The Plant Journal **28,** 475-481.

Tornero, P., Merritt, P., Sadanandom, A., Shirasu, K., Innes, R.W., and Dangl, J.L. (2002). RAR1 and NDR1 Contribute Quantitatively to Disease Resistance in Arabidopsis, and Their Relative Contributions Are Dependent on the *R* Gene Assayed. The Plant Cell Online **14,** 1005-1015.

Trujillo, M., and Shirasu, K. (2010). Ubiquitination in plant immunity. Current Opinion in Plant Biology **13,** 402-408.

Valouev, A., Johnson, D.S., Sundquist, A., Medina, C., Anton, E., Batzoglou, S., Myers, R.M., and Sidow, A. (2008). Genome-wide analysis of transcription factor binding sites based on ChIP-Seq data. Nat Meth **5,** 829-834.

van der Hoorn, R.A.L., and Kamoun, S. (2008). From Guard to Decoy: A New Model for Perception of Plant Pathogen Effectors. The Plant Cell Online **20,** 2009-2017.

van Dijk, K., Fouts, D.E., Rehm, A.H., Hill, A.R., Collmer, A., and Alfano, J.R. (1999). The Avr (Effector) Proteins HrmA (HopPsyA) and AvrPto Are Secreted in Culture from *Pseudomonas syringae* Pathovars via the Hrp (Type III) Protein Secretion System in a Temperature- and pH-Sensitive Manner. Journal of Bacteriology **181,** 4790-4797.

van Ooijen, G., van den Burg, H.A., Cornelissen, B.J.C., and Takken, F.L.W. (2007). Structure and Function of Resistance Proteins in Solanaceous Plants. Annual Review of Phytopathology **45,** 43-72.

van Ooijen, G., Mayr, G., Kasiem, M.M.A., Albrecht, M., Cornelissen, B.J.C., and Takken, F.L.W. (2008). Structure–function analysis of the NB-ARC domain of plant disease resistance proteins. Journal of Experimental Botany **59,** 1383-1397.

Venugopal, S.C., Jeong, R.-D., Mandal, M.K., Zhu, S., Chandra-Shekara, A.C., Xia, Y., Hersh, M., Stromberg, A.J., Navarre, D., Kachroo, A., and Kachroo, P. (2009). Enhanced Disease Susceptibility 1 and Salicylic Acid Act Redundantly to Regulate *Resistance* Gene-Mediated Signaling. PLoS Genet **5,** e1000545.

Wagner, S., Stuttmann, J., Rietz, S., Guerois, R., Brunstein, E., Bautor, J., Niefind, K., and Parker, Jane E. (2013). Structural Basis for Signaling by Exclusive EDS1 Heteromeric Complexes with SAG101 or PAD4 in Plant Innate Immunity. Cell Host & Microbe **14,** 619-630.

Wang, D., and Dong, X. (2011). A Highway for War and Peace: The Secretory Pathway in Plant–Microbe Interactions. Molecular Plant **4,** 581-587.

Wang, Y., Bao, Z., Zhu, Y., and Hua, J. (2009). Analysis of Temperature Modulation of Plant Defense Against Biotrophic Microbes. Molecular Plant-Microbe Interactions **22,** 498-506.

Weber, C., Nover, L., and Fauth, M. (2008). Plant stress granules and mRNA processing bodies are distinct from heat stress granules. The Plant Journal **56,** 517-530.

Whitham, S., McCormick, S., and Baker, B. (1996). The *N* gene of tobacco confers resistance to tobacco mosaic virus in transgenic tomato. Proceedings of the National Academy of Sciences **93,** 8776-8781.

Wiermer, M., Feys, B.J., and Parker, J.E. (2005). Plant immunity: the *EDS1* regulatory node. Current Opinion in Plant Biology **8,** 383-389.

Wigge, P.A. (2013). Ambient temperature signalling in plants. Current Opinion in Plant Biology **16,** 661-666.

Williams, S.J., Sornaraj, P., deCourcy-Ireland, E., Menz, R.I., Kobe, B., Ellis, J.G., Dodds, P.N., and Anderson, P.A. (2011). An Autoactive Mutant of the M Flax Rust Resistance Protein Has a Preference for Binding ATP, Whereas Wild-Type M Protein Binds ADP. Molecular Plant-Microbe Interactions **24,** 897-906.

Williams, S.J., Sohn, K.H., Wan, L., Bernoux, M., Sarris, P.F., Segonzac, C., Ve, T., Ma, Y., Saucet, S.B., Ericsson, D.J., Casey, L.W., Lonhienne, T., Winzor, D.J., Zhang, X., Coerdt, A., Parker, J.E., Dodds, P.N., Kobe, B., and Jones, J.D.G. (2014). Structural Basis for Assembly and Function of a Heterodimeric Plant Immune Receptor. Science **344,** 299-303.

Wirthmueller, L., Zhang, Y., Jones, J.D.G., and Parker, J.E. (2007). Nuclear Accumulation of the Arabidopsis Immune Receptor RPS4 Is Necessary for Triggering *EDS1*-Dependent Defense. Current Biology **17,** 2023-2029.

Xia, S., Cheng, Y.T., Huang, S., Win, J., Soards, A., Jinn, T.-L., Jones, J.D.G., Kamoun, S., Chen, S., Zhang, Y., and Li, X. (2013). Regulation of Transcription of Nucleotide-Binding Leucine-Rich Repeat-Encoding Genes *SNC1* and *RPP4* via H3K4 Trimethylation. Plant Physiology **162,** 1694-1705.

Xiao, S., Brown, S., Patrick, E., Brearley, C., and Turner, J.G. (2003). Enhanced Transcription of the Arabidopsis Disease Resistance Genes *RPW8.1* and *RPW8.2* via a Salicylic Acid–Dependent Amplification Circuit Is Required for Hypersensitive Cell Death. The Plant Cell Online **15,** 33-45.

Xu, F., Cheng, Y.T., Kapos, P., Huang, Y., and Li, X. (2014a). P-loop-dependent NLR SNC1 can oligomerize and activate immunity in the nucleus. Molecular Plant.

Xu, F., Kapos, P., Cheng, Y.T., Li, M., Zhang, Y., and Li, X. (2014b). NLR-Associating Transcription Factor bHLH84 and Its Paralogs Function Redundantly in Plant Immunity. PLoS Pathog **10,** e1004312.

Xu, J., and Chua, N.-H. (2009). Arabidopsis Decapping 5 Is Required for mRNA Decapping, P-Body Formation, and Translational Repression during Postembryonic Development. The Plant Cell Online **21,** 3270-3279.

Xu, J., and Chua, N.H. (2012). Dehydration stress activates Arabidopsis MPK6 to signal DCP1 phosphorylation.

Yamasaki, K., Kigawa, T., Seki, M., Shinozaki, K., and Yokoyama, S. (2013). DNA-binding domains of plant-specific transcription factors: structure, function, and evolution. Trends in Plant Science **18,** 267-276.

Yamasaki, K., Kigawa, T., Watanabe, S., Inoue, M., Yamasaki, T., Seki, M., Shinozaki, K., and Yokoyama, S. (2012). Structural Basis for Sequence-specific DNA Recognition by an Arabidopsis WRKY Transcription Factor. Journal of Biological Chemistry **287,** 7683-7691.

Yan, N., Chai, J., Lee, E.S., Gu, L., Liu, Q., He, J., Wu, J.-W., Kokel, D., Li, H., Hao, Q., Xue, D., and Shi, Y. (2005). Structure of the CED-4-CED-9 complex provides insights into programmed cell death in Caenorhabditis elegans. Nature **437,** 831-837.

Yang, S., and Hua, J. (2004). A Haplotype-Specific *Resistance* Gene Regulated by BONZAI1 Mediates Temperature-Dependent Growth Control in Arabidopsis. The Plant Cell Online **16,** 1060-1071.

Yao, C., Wu, Y., Nie, H., and Tang, D. (2012). RPN1a, a 26S proteasome subunit, is required for innate immunity in Arabidopsis. The Plant Journal **71,** 1015-1028.

Yao, N., and Greenberg, J.T. (2006). Arabidopsis ACCELERATED CELL DEATH2 Modulates Programmed Cell Death. The Plant Cell Online **18,** 397-411.

Yi, H., and Richards, E.J. (2007). A Cluster of Disease Resistance Genes in Arabidopsis Is Coordinately Regulated by Transcriptional Activation and RNA Silencing. The Plant Cell Online **19,** 2929-2939.

Zhai, C., Lin, F., Dong, Z., He, X., Yuan, B., Zeng, X., Wang, L., and Pan, Q. (2011). The isolation and characterization of *Pik*, a rice blast resistance gene which emerged after rice domestication. New Phytologist **189,** 321-334.

Zhai, C., Zhang, Y., Yao, N., Lin, F., Liu, Z., Dong, Z., Wang, L., and Pan, Q. (2014). Function and Interaction of the Coupled Genes Responsible for *Pik-h* Encoded Rice Blast Resistance. PLoS ONE **9,** e98067.

Zhang, J., Li, W., Xiang, T., Liu, Z., Laluk, K., Ding, X., Zou, Y., Gao, M., Zhang, X., Chen, S., Mengiste, T., Zhang, Y., and Zhou, J.-M. (2010a). Receptor-like Cytoplasmic Kinases Integrate Signaling from Multiple Plant Immune Receptors and Are Targeted by a *Pseudomonas syringae* Effector. Cell Host & Microbe **7,** 290-301.

Zhang, X.-C., and Gassmann, W. (2003). *RPS4*-Mediated Disease Resistance Requires the Combined Presence of *RPS4* Transcripts with Full-Length and Truncated Open Reading Frames. The Plant Cell Online **15,** 2333-2342.

Zhang, X.-C., and Gassmann, W. (2007). Alternative Splicing and mRNA Levels of the Disease Resistance Gene *RPS4* Are Induced during Defense Responses. Plant Physiology **145,** 1577-1587.

Zhang, X., Chen, S., and Mou, Z. (2010b). Nuclear localization of NPR1 is required for regulation of salicylate tolerance, isochorismate synthase 1 expression and salicylate accumulation in Arabidopsis. Journal of Plant Physiology **167,** 144-148.

Zhang, Y., Goritschnig, S., Dong, X., and Li, X. (2003). A Gain-of-Function Mutation in a Plant Disease Resistance Gene Leads to Constitutive Activation of Downstream Signal Transduction Pathways in *suppressor of npr1-1, constitutive 1*. The Plant Cell Online **15,** 2636-2646.

Zhang, Y., Dorey, S., Swiderski, M., and Jones, J.D.G. (2004). Expression of *RPS4* in tobacco induces an AvrRps4-independent HR that requires EDS1, SGT1 and HSP90. The Plant Journal **40,** 213-224.

Zhang, Y., Fan, W., Kinkema, M., Li, X., and Dong, X. (1999). Interaction of NPR1 with basic leucine zipper protein transcription factors that bind sequences required for salicylic acid induction of the *PR-1* gene. Proceedings of the National Academy of Sciences **96,** 6523-6528.

Zhang, Y., Liu, T., Meyer, C., Eeckhoute, J., Johnson, D., Bernstein, B., Nusbaum, C., Myers, R., Brown, M., Li, W., and Liu, X.S. (2008). Model-based Analysis of ChIP-Seq (MACS). Genome Biology **9,** R137.

Zhang, Z., Shrestha, J., Tateda, C., and Greenberg, J.T. (2014). Salicylic Acid Signaling Controls the Maturation and Localization of the Arabidopsis Defense Protein ACCELERATED CELL DEATH6. Molecular Plant **7,** 1365-1383.

Zhu, Y., Qian, W., and Hua, J. (2010a). Temperature Modulates Plant Defense Responses through NB-LRR Proteins. PLoS Pathog **6,** e1000844.

Zhu, Z., Xu, F., Zhang, Y., Cheng, Y.T., Wiermer, M., Li, X., and Zhang, Y. (2010b). Arabidopsis resistance protein SNC1 activates immune responses through association with a transcriptional corepressor. Proceedings of the National Academy of Sciences **107,** 13960-13965.

6. Supplementary

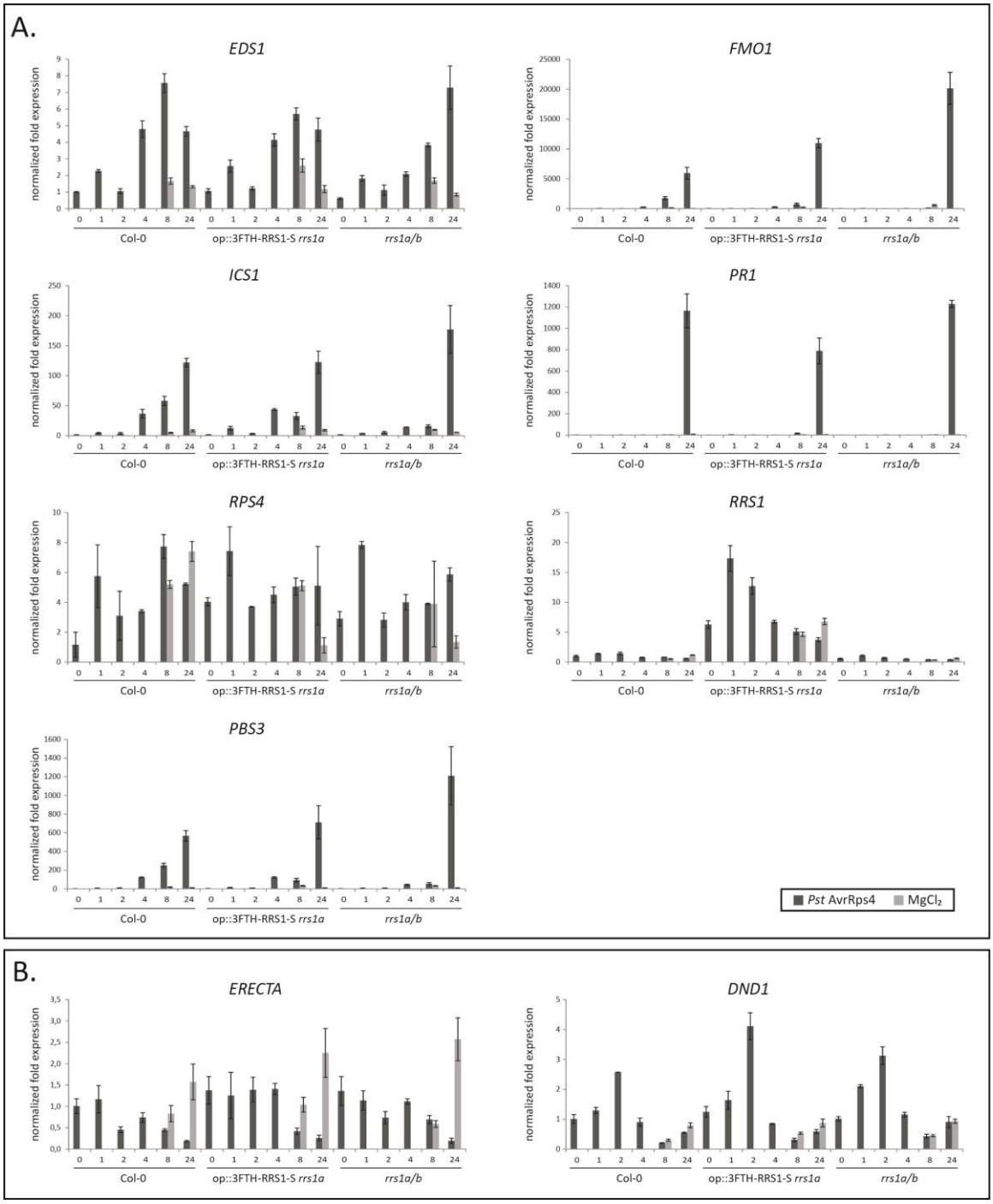

Figure S 1: Regulation of defense-related genes upon *Pst* AvrRps4 infection is wt-like in *3FTH-RRS1* plants.

Transcriptional reprogramming in 4.5-week-old *3FTH-RRS1*, Col-0 and *rrs1a/b* syringe-infiltrated with *Pst* AvrRps4 was analysed by qPCR. Normalized fold expression was calculated by relating sample values to the geometric mean of three reference genes (*actin*, *GAPDH* and *expressed protein*) and normalizing to the Col-0 untreated sample. Experiment was repeated twice with similar results. (**A**) Regulation of defense-induced genes. (**B**) Regulation of defense-repressed genes.

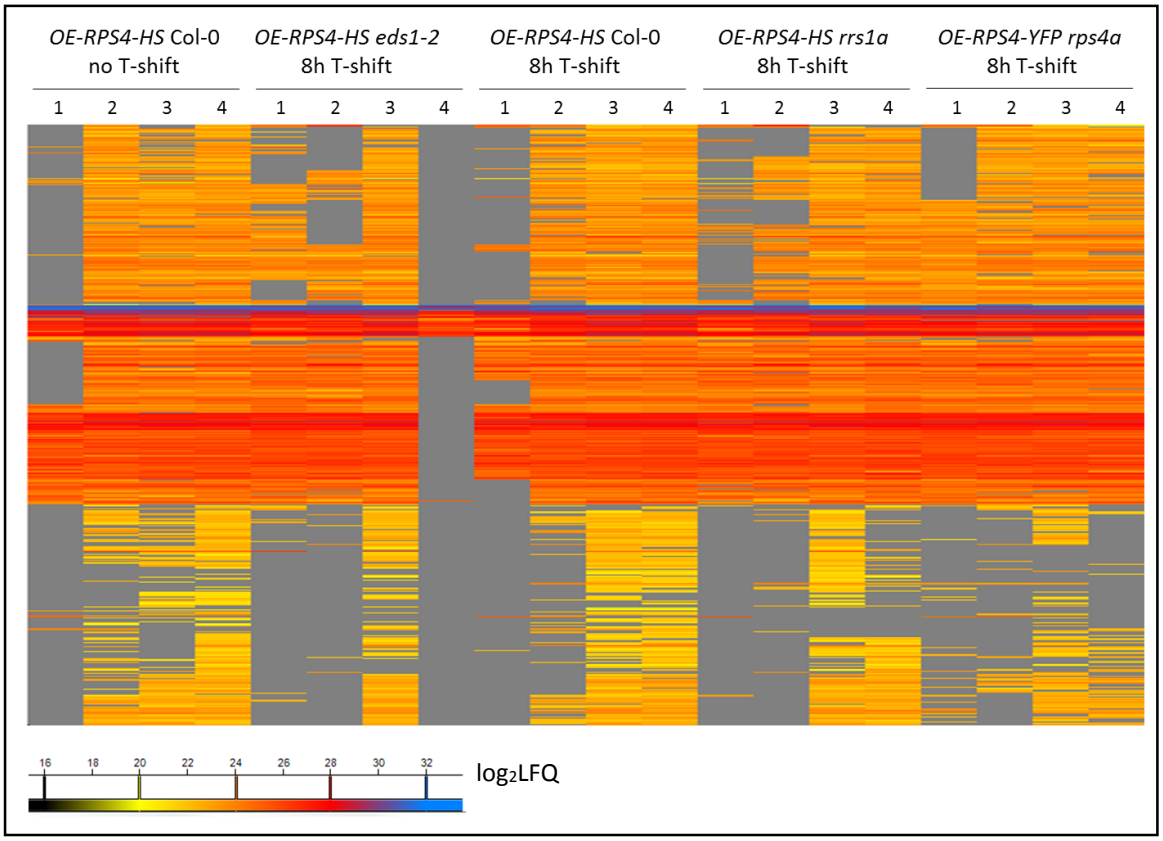

Figure S 2: Pulldown replicates show high consistency of a core set of detected proteins.

Strep-tag-mediated RPS4-pulldown was performed in four replicates. Heatmap allows comparison of LFQ values of proteins detected among different replicates and samples (compare figure legend; gray – not detected). As protein detection in several single replicates was very low, the threshold for consideration of RPS4 co-identified proteins was set to two instead of three replicates.

Table S 1: RPS4-HS interactors in pre- and post-activation complexes and genotype dependency of post-activation protein hits

A. Pre-activation protein hits		**unique peptides**	**in post-activation *OE-RPS4-HS…***		
Protein ID	**Fasta header**		**Col-0**	***rrs1a***	***eds1-2***
AT1G20200	EMB2719, HAP15 | PAM domain (PCI/PINT associated module) protein	5			
AT1G45201	ATTLL1, TLL1 | triacylglycerol lipase-like 1	3			
AT2G14880	SWIB/MDM2 domain superfamily protein	2			
AT4G33030	SQD1 | sulfoquinovosyldiacylglycerol 1	5			
AT1G79930	HSP91 | heat shock protein 91	9			
AT2G47390	Prolyl oligopeptidase family protein	4			
AT4G34200	EDA9 | D-3-phosphoglycerate dehydrogenase	3			
AT5G38430	Ribulose bisphosphate carboxylase (small chain) family protein	3			

B. Shared protein hits		**unique peptides**	**in post-activation *OE-RPS4-HS…***		
Protein ID	**Fasta header**		**Col-0**	***rrs1a***	***eds1-2***
AT5G45250	RPS4 | Disease resistance protein (TIR-NBS-LRR class)	31			
AT3G62410	CP12-2, CP12 | CP12 domain-containing protein 2	2			
AT1G49600	ATRBP47A, RBP47A | RNA-binding protein 47A	8			
AT3G04790	Ribose 5-phosphate isomerase, type A protein	2			
AT1G03600	PSB27 | photosystem II family protein	2			
AT1G16080	unknown protein	7			
AT2G26080	AtGLDP2, GLDP2 | glycine decarboxylase P-protein 2	6			
AT5G45390	CLPP4, NCLPP4 | CLP protease P4	4			
AT3G63190	RRF, HFP108, cpRRF, AtcpRRF | ribosome recycling factor, chloroplast precursor	6			
AT5G42020	BIP, BIP2 | Heat shock protein 70 (Hsp 70) family protein	11			
AT5G27700	Ribosomal protein S21e	3			
AT2G32730	26S proteasome regulatory complex, non-ATPase subcomplex, Rpn2/Psmd1 subunit	4			
AT5G24490	30S ribosomal protein, putative	2			
AT4G14880	OASA1 | O-acetylserine (thiol) lyase (OAS-TL) isoform A1	9			
AT3G02520	GRF7, GF14 NU | general regulatory factor 7	4			
AT3G57610	ADSS | adenylosuccinate synthase	4			
AT3G29360	UDP-glucose 6-dehydrogenase family protein	4			
AT2G40490	HEME2 | Uroporphyrinogen decarboxylase	3			
AT1G59359	Ribosomal protein S5 family protein	1			
AT3G09500	Ribosomal L29 family protein	4			
AT1G70310	SPDS2 | spermidine synthase 2	2			
AT3G26450	Polyketide cyclase/dehydrase and lipid transport superfamily protein	4			
AT3G48990	AMP-dependent synthetase and ligase family protein	2			
AT5G64130	cAMP-regulated phosphoprotein 19-related protein	3			

Table S 1: continued

B. Shared protein hits		unique peptides	in post-activation *OE-RPS4-HS…*		
Protein ID	**Fasta header**		**Col-0**	***rrs1a***	***eds1-2***
AT3G53260	PAL2, ATPAL2 | phenylalanine ammonia-lyase 2	5			
AT1G26110	DCP5 | decapping 5	2			
AT2G42530	COR15B | cold regulated 15b	7			
AT2G20420	ATP citrate lyase (ACL) family protein	4			
AT1G08520	ALB1, ALB-1V, V157, PDE166, CHLD | ALBINA1	4			
AT3G24430	HCF101 | ATP binding	2			
AT3G25530	GHBDH, ATGHBDH, GLYR1, GR1 | glyoxylate reductase 1	2			
AT5G16840	BPA1 | binding partner of acd11 1	3			
AT2G03420	unknown protein	2			
AT5G42980	ATTRX3, ATH3, ATTRXH3, TRXH3, TRX3 | thioredoxin 3	2			
AT3G01480	CYP38, ATCYP38 | cyclophilin 38	6			
AT3G08740	elongation factor P (EF-P) family protein	3			
AT4G10340	LHCB5 | light harvesting complex of photosystem II 5	2			
AT4G31990	ASP5 | aspartate aminotransferase 5	4			
AT4G39960	Molecular chaperone Hsp40/DnaJ family protein	5			
AT5G63310	NDPK2, NDPK1A, NDPK IA IA, NDPK IA, ATNDPK2 | nucleoside diphosphate kinase 2	4			

C. Post-activation protein hits		unique peptides	in post-activation *OE-RPS4-HS…*		
Protein ID	**Fasta header**		**Col-0**	***rrs1a***	***eds1-2***
AT5G60670	Ribosomal protein L11 family protein	2			
AT5G16050	GRF5, GF14 UPSILON | general regulatory factor 5	3			
AT3G25230	ROF1, ATFKBP62, FKBP62 | rotamase FKBP 1	5			
AT2G24850	TAT3, TAT | tyrosine aminotransferase 3	3			
AT1G65960	GAD2 | glutamate decarboxylase 2	5			
AT2G41530	ATSFGH, SFGH | S-formylglutathione hydrolase	2			
AT2G37690	phosphoribosylaminoimidazole carboxylase, putative / AIR carboxylase, putative	4			
AT3G48000	ALDH2B4, ALDH2, ALDH2A | aldehyde dehydrogenase 2B4	3			
AT5G02490	Heat shock protein 70 (Hsp 70) family protein	3			
AT5G46750	AGD9 | ARF-GAP domain 9	5			

Table S 1: continued

D. Post-activation protein hits enriched in *rrs1a*		**unique peptides**	**in post-activation *OE-RPS4-HS…***		
Protein ID	**Fasta header**		**Col-0**	***rrs1a***	***eds1-2***
AT4G15545	unknown protein	2			
AT4G24820	26S proteasome, regulatory subunit Rpn7;Proteasome component (PCI) domain	3			
AT3G47370	Ribosomal protein S10p/S20e family protein	2			
AT3G61440	ATCYSC1, ARATH;BSAS3;1, CYSC1 | cysteine synthase C1	5			
AT3G60240	EIF4G, CUM2 | eukaryotic translation initiation factor 4G	7			

(**A**) Pre-activation protein hits = significantly enriched before shift (**B**) Shared protein hits = proteins identified in both samples (**C**) Post-activation protein hits = significantly enriched after shift. (**D**) Post-activation protein hits enriched in *rrs1a*. Protein ID colored green – detected in 3 or 4 replicates.

Acknowledgements …oder einfach: Danke!

Jane, many thanks for supervising my PhD in your lab, providing scientific freedom and teaching me the meaning of scientific independence. Thanks to you, Paul, for the opportunity to work in your department and your encouraging feedback. Many thanks also to the amiable members of my thesis committee: Prof. Aska Goverse and Prof. Flügge for the thesis evaluation and indulgence with extended deadlines, and Prof. Ute Höcker for taking the chair of my defense. Thanks to Simon Saucet for sharing information and *rrs1a/b* and *rps4a/b* seeds and to Laurent Deslandes for interesting discussions and sharing 3FTH-RRS1-S seeds and unpublished data. Thanks go to the MPIPZ proteomics facility for sample analysis and data management support.

Liebe Jaqueline, ohne deinen allzeit liebenswert-geduldigen Rat und deine Unterstützung hätte ich es nicht geschafft. Ich danke dir von Herzen für all deine Anleitung und Hilfe! A biiiig THANKS goes to all JP groupees for a "good working atmosphere" in every respect! Thomas, deine Unterstützung (sowohl fachlich als auch moralisch) hat mir durch so manche schwere Stunde geholfen, mich motiviert und aufgebaut – danke dafür! Marcel, Deepak, Jindge – it was a pleasure working with you, and there's scarcely anything better to deal with just another failed experiment than hanging out with you guys! Dmitry[2] and Haitao, your valuable feedback and comments (both positive and critical) were and are always highly appreciated! My precious thesis-writing-company! Shachi, thanks for sharing this experience and reducing the burden by joint panic attacks as well as tea breaks… and yes: We could!

Wie langweilig wäre es hier am MPIPZ gewesen ohne dich! Gemeinsam lachen, weinen, fluchen – und manchmal alles gleichzeitig! Ich kenne nur wenige Menschen mit so viel Herz und Verstand wie dich… Ich freue mich schon auf unsere Ü80-WG, liebste Caro! Für schlechte Witze und hochgeschätzten Sarkasmus zu jeder Zeit: Danke, Jonas! To all my colleagues from the department – and especially those who grew to become friends along the way: Thanks! Big special thanks go to all of you who were available for some last minute proofreading… :D

Der letzte Dank gebührt meiner Familie: Danke für eure Unterstützung, Aufmunterung und Ablenkung – und dafür, dass ihr immer an mich geglaubt habt!

XXX

Erklärung

Ich versichere, dass ich die von mir vorgelegte Dissertation selbständig angefertigt, die benutzten Quellen und Hilfsmittel vollständig angegeben und die Stellen der Arbeit – einschließlich Tabellen, Karten und Abbildungen –, die anderen Werken im Wortlaut oder dem Sinn nach entnommen sind, in jedem Einzelfall als Entlehnung kenntlich gemacht habe; dass diese Dissertation noch keiner anderen Fakultät oder Universität zur Prüfung vorgelegen hat; dass sie – abgesehen von auf Seite I angegebenen Teilpublikationen – noch nicht veröffentlicht worden ist sowie, dass ich eine solche Veröffentlichung vor Abschluss des Promotionsverfahrens nicht vornehmen werde. Die Bestimmungen dieser Promotionsordnung sind mir bekannt. Die von mir vorgelegte Dissertation ist von Prof. Dr. Paul Schulze-Lefert betreut worden.

Köln, 14. Oktober 2014 _____

Anne Coerdt